



Instituto Politécnico de Coimbra
Escola Superior de Tecnologia da Saúde Coimbra

The effects of weight and injected dose in the liver's Signal-to-Noise Ratio in patients submitted to PET/CT scans

Diogo Teixeira da Silva Duarte

Mestrado em Ciências Nucleares Aplicadas na Saúde
2011/2013



Instituto Politécnico de Coimbra
Escola Superior de Tecnologia da Saúde Coimbra

Mestrado em Ciências Nucleares Aplicadas na Saúde
Projecto/Estágio/Dissertação

The effects of weight and injected dose in the liver's Signal-to-Noise Ratio in patients submitted to PET/CT scans

Diogo Teixeira da Silva Duarte

Orientador:

Prof. Dr. Francisco José Cerqueira Alves

Prof. Dr. Wim van den Broek

Coimbra, Dezembro, 2013

Acknowledgments

The making of this Masters' Dissertation was only possible thanks to the collaboration and the contribution, directly or indirectly, of a lot of people and institutions, which I would like to send my deepest thanks and appreciation, in particular:

To my professor and supervisor in Portugal Francisco Alves, for the opportunity he gave me to do an international internship, for the willingness to guide me in this adventure and his precious help on making this an experience to help me open new doors in the future;

To the responsible at the International Office at College of Health Technology of Coimbra, Rui Branco Lopes, for all the precious help he gave me in contacting Nijmegen and for all the willingness and information he showed and gave in making this possible;

To my supervisor in Nijmegen and superintendent technologist Wim van den Broek for welcoming me in the Nuclear Medicine Department in Radboud University MC, for giving me the chance to gain more knowledge and experience in this area, for all the guidance he gave me throughout the whole internship, for all the help he always demonstrated, for the valuable tips and indications to make this dissertation, for reviewing every work I made in order to get even better and for making me feel part of the staff;

To the Nuclear Medicine Technologist Merijn Janssen for all the guidance and help he gave me in order to complete my project but also for helping me in my internship, on dealing with all the protocols involved in scanning patients, on giving me hints and help on interacting with patients and for all the support he gave me;

To the Nuclear Medicine Technologists Jurrian Butter, Marie-Claire Attard, Michel de Groot, Peter Kok, Eddy Mijnheere, Diana Valks, Martin Engels, Marga Ouwens, Marjo van de Ven and Bernadette Bosveld for all the help and support they gave me on my internship;

To the Nuclear Medicine physician Dennis Vriens for helping me in all the mathematics theory and calculations and for pointing me in the right direction on how to perform my study and reach new insights;

To all the Nuclear Medicine physicians for all their help and willingness on explaining me procedures and analysing scans;

To all the Nuclear Medicine department staff for all their kindness and help on making me feel integrated during this internship;

To my friends for their support, friendship and help;

Last but not least, to my parents, Lúcia Duarte and Guilherme Duarte, for all their support and efforts to make this internship possible; to my brother and his mate, Nuno Duarte and Magda Oliveira for all their support; to my god parents, Teresa Teixeira and Augusto, for all their support and effort; and to my girlfriend, Sara Raimundo, for all her support, companionship, patience, help and comprehension during this five months of internship.

To everyone, my deepest appreciation and eternal gratitude.

Index

Illustrations, graphs and tables index	4
Abbreviations.....	5
Resumo	6
Summary	7
Introduction.....	8
Material and Methods.....	9
PET/CT.....	9
18F-Fluorodeoxyglucose.....	12
Pathophysiology of Glucose and FDG's Biodistribution	12
FDG "Trapping"	13
Physiological and Para-Physiological Distribution of FDG	14
Normal FDG uptake in the liver	16
Body Mass Index.....	17
Procedure.....	19
Results and Discussion	25
Conclusion.....	46
References	47
Appendix	49

Illustrations, graphs and tables index

Illustration 1 - Example of CT image (left), FDG-PET image (middle) and FDG-PET/CT image (right)	8
Illustration 2 - Example of PET/CT scanner	11
Illustration 3 - Examples of normal FDG uptake	15
Illustration 4 - Normal liver uptake (left) and abnormal liver uptake (right)	16
Illustration 5 - Positioning of the point in the CT scan	21
Illustration 6 - Positioning of the point in the PET WB scan	21
Illustration 7 - Positioning of the point in the PET WB EANM scan	21
Illustration 8 - First ROI on CT (left), PET WB (middle) and PET WB EANM (right)	22
Illustration 9 - Second ROI on CT (left), PET WB (middle) and PET WB EANM (right)	22
Illustration 10 - Third ROI on CT (left), PET WB (middle) and PET WB EANM (right)	22
Illustration 11 - Fourth ROI on CT (left), PET WB (middle) and PET WB EANM (right)	22
Illustration 12 - Fifth ROI on CT (left), PET WB (middle) and PET WB EANM (right)	22
Illustration 13 - Values of the ROI's in the PET WB	23
Illustration 14 - Values of the ROI's in the PET WB	23
Illustration 15 - Table of every value of every patient of PET WB	24
Illustration 16 - Relation between weight and SNR_{liver} in Clinical and EANM reconstructions	35
Illustration 17 - The highest SNR	42
Illustration 18 - SNR of a 70 Kg Patient	42
Illustration 19 - SNR of an 86 Kg Patient	42
Illustration 20 - SNR of an 86 Kg Patient	43
Illustration 21 - The lowest SNR	43
Graphs 1 - Relation between Weight and Dose Injected on the PET WB (left) and PET WB EANM (right)	25
Graphs 2 - Relation between BMI and Dose Injected on the PET WB (left) and PET WB EANM (right)	25
Graphs 3 - Relation between Dose Injected and SNR on the PET WB (left) and PET WB EANM (right)	26
Graphs 4 - Relation between BMI and SNR on the PET WB (left) and PET WB EANM (right)	26
Graphs 5 - Relation between Weight and SNR on the PET WB (left) and PET WB EANM (right)	27
Graphic 6 - Linear line for weight and dose injected	28
Graphs 7 - Relation between SNR and AC_{liver} from 5 to 3600s and 30 to 900s respectively	34
Graphs 8 - Relation between weight and New SNR_{liver} based on Power and Exponential Formula	37
Graphs 9 - Relation between Weight and New Dose based on Power and Exponential Formula	38
Graphs 10 - Relation between new Dose and New SNR_{liver} based on Power and Exponential Formula	38
Graphic 11 - Relation between the dose injected and the new dose based on Power Formula	39
Graphic 12 - Relation between the dose injected and the new dose based on Exponential Formula	39
Graphic 13 - Equations for dosing schemes according to different references	41
Table 1 - BMI Categories	17
Table 2 - Relation between liver's AC and SNR based on measurements on a Ga-86/Ge-68 phantom	34
Table 3 - Regressors (r_1 and r_2) and fit quality (R^2) between SNR^*_{liver} and different measures of body size (W and BMI)	35
Table 4 - Difference between injected doses, new doses and total effective doses	40
Table 5 - Equations for non-linear dosing according to several references	40

Abbreviations

PET – Positron Emission Tomography

CT – Computed Tomography

LOR – Line of Response

¹⁸F-FDG – ¹⁸F-Fluorodeoxyglucose

SNR – Signal-to-Noise Ratio

ROI – Region of Interest

BMI – Body Mass Index

MBq – Megabecquerel

WB – Whole Body

EANM – European Association of Nuclear Medicine

MRI – Magnetic Resonance Imaging

NHS – National Health Service

SD – Standard Deviation

CT-LD – Computed Tomography Low Dose

FWHM – Full width at half maximum

Resumo

A qualidade da imagem em exames de PET/CT 18F-FDG em pacientes obesos encontra-se, geralmente, diminuída. Este estudo pretende avaliar, retrospectivamente, a relação entre a SNR, peso e dose injectada em 65 pacientes, com uma variação de peso entre 35 a 120 kg, com exames efectuados utilizando o modelo Biograph mCT num protocolo standard no departamento de Medicina Nuclear do Centro Médico Universitário de Radboud em Nijmegen, Holanda.

Foram efectuados cinco ROI's no fígado, órgão que na teoria tem um metabolismo homogéneo, no mesmo local, em cinco cortes consecutivos nos exames PET/CT para obter os valores da média de captação (sinal) e o seu desvio-padrão (ruído). A relação de ambos dá-nos a relação Sinal-Ruído no fígado. Com o auxílio de uma folha de cálculo, o peso, a altura, a SNR e o Índice de Massa Corporal foram calculados e os gráficos foram realizados de maneira a obter a relação entre estes factores. Os gráficos demonstraram que a SNR diminuía assim que o peso e/ou o IMC aumentava, assim como também demonstrou que a SNR também diminuía com o aumento da dose injectada. Isto é devido ao facto de pacientes mais pesados receberem uma dose mais elevada e, como já foi referido, pacientes mais pesados têm menor SNR. Estas descobertas sugerem que a qualidade das imagens, medidas pela SNR, que foram adquiridas em pacientes pesados, são inferiores do que em pacientes magros, apesar das doses mais elevadas.

Tendo isto em consideração, foi necessário conceber uma nova fórmula para calcular a nova dose a injectar em pacientes, conseguindo uma SNR boa e constante em todos. Através de cálculos matemáticos, foi possível alcançar duas novas equações que davam uma imagem com uma SNR de um exame feito com um peso de referência específico (86 kg foi o considerado) que era independente do peso do paciente. Este estudo implica que, com estas novas fórmulas, os pacientes mais pesados que o peso de referencia, irão receber uma dose mais elevada e os pacientes mais magros irão receber uma dose mais baixa. A mediana sendo de 86 kg, a nova dose e o novo SNR foram calculados e concluiu-se que a qualidade das imagens mantém-se praticamente constante à medida que o peso aumenta e a quantidade necessária de FDG mantém-se quase a mesma, sem aumentar os custos da quantidade total necessária de FDG utilizada nestes pacientes.

Summary

The quality of the image of 18F-FDG PET/CT scans in overweight patients is commonly degraded. This study evaluates, retrospectively, the relation between SNR, weight and dose injected in 65 patients, with a range of weights from 35 to 120 kg, with scans performed using the Biograph mCT using a standardized protocol in the Nuclear Medicine Department at Radboud University Medical Centre in Nijmegen, The Netherlands.

Five ROI's were made in the liver, assumed to be an organ of homogenous metabolism, at the same location, in five consecutive slices of the PET/CT scans to obtain the mean uptake (signal) values and its standard deviation (noise). The ratio of both gave us the Signal-to-Noise Ratio in the liver. With the help of a spreadsheet, weight, height, SNR and Body Mass Index were calculated and graphs were designed in order to obtain the relation between these factors. The graphs showed that SNR decreases as the body weight and/or BMI increased and also showed that, even though the dose injected increased, the SNR also decreased. This is due to the fact that heavier patients receive higher dose and, as reported, heavier patients have less SNR. These findings suggest that the quality of the images, measured by SNR, that were acquired in heavier patients are worst than thinner patients, even though higher FDG doses are given.

With all this taken in consideration, it was necessary to make a new formula to calculate a new dose to give to patients and having a good and constant SNR in every patient. Through mathematic calculations, it was possible to reach to two new equations (power and exponential), which would lead to a SNR from a scan made with a specific reference weight (86 kg was the considered one) which was independent of body mass. The study implies that with these new formulas, patients heavier than the reference weight will receive higher doses and lighter patients will receive less doses. With the median being 86 kg, the new dose and new SNR was calculated and concluded that the quality of the image remains almost constant as the weight increases and the quantity of the necessary FDG remains almost the same, without increasing the costs for the total amount of FDG used in all these patients.

Introduction

PET/CT with ^{18}F -Fluorodeoxyglucose has been one of the most widely used imaging modality to diagnose a variety of pathologies. The image quality of this kind of procedure is crucial in order to make a correct diagnosis. This is dependent on having a high sensitivity and having a good detection due to fast scintillation rate and low dead times by scintillation crystals which result in a better count rate performance [1–5]. Over the years, there have been lots of advances in this technology, which led to better image quality thanks to less-noisy CT-based attenuation correction and better performance of scintillator crystals as detectors [6].

Although there have been remarkable advances, the quality of PET/CT images on overweight patients is often degraded [7–9]. This can turn into a situation where the physician can't separate pathology from noise, leading to false scan results. There have been studies, where some suggested optimizing acquisition times, while others suggest optimizing the injected dose of the radiopharmaceuticals in order to improve the image quality [5,7,8]. However, recommended doses of ^{18}F -Fluorodeoxyglucose per kilogram of body weight are different from each country, leading to uncertainty whether a high injected dose is really necessary or if a longer scan time is the best solution [5,7,10].

The aim of this master's dissertation is to study, retrospectively, the relation between Signal-to-Noise Ratio, the injected dose and the weight on a number of patients with a wide range of weights on scans performed in the Nuclear Medicine Department of the Radboud University Medical Centre in Nijmegen, The Netherlands. The purpose is to see if there is a direct relation between these factors and if the image quality can be improved in heavy patients with a different approach.

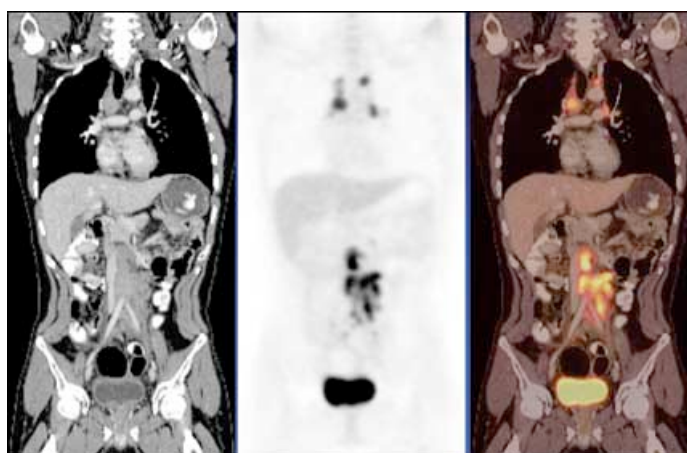


Illustration 1 - Example of CT image (left), FDG-PET image (middle) and FDG-PET/CT image (right)

Material and Methods

PET/CT

Nuclear medicine nowadays has gone through a lot of technological evolution. One of the most known techniques is positron emission tomography, also called PET. This type of scan is one of the most frequently used molecular imaging procedures. Molecular imaging is a type of medical imaging that provides detailed images of what is happening inside the body at a molecular and cellular level [2,4]. Other diagnostic imaging procedures, like x-rays, computed tomography (CT), and ultrasound predominantly offer anatomical pictures but molecular imaging allows physicians to see how the body is functioning and to measure its chemical and biological processes [6]. Molecular imaging offers unique insights into the human body that enable physicians to personalize patient care. In terms of diagnosis, molecular imaging is able to:

- Give information that is unattainable with other imaging technologies or that would require more invasive procedures such as biopsy or surgery [2,3];
- Identify disease in its earliest stages and determine the exact location of the disease, often before symptoms occur or abnormalities can be detected with other diagnostic tests (i.e. detection sensitivity) [2–4].

It is also a tool for evaluating and managing the care of patients, since molecular imaging studies help physicians to:

- Determine the extent or severity of the disease, including whether it has spread elsewhere in the body;
- Select the most effective therapy based on the unique biologic characteristics of the patient and the molecular properties of a disease;
- Determine a patient's response to specific drugs;
- Accurately assess the effectiveness of a treatment regimen;
- Adapt treatment plans quickly in response to changes in cellular activity;
- Assess disease progression;
- Identify recurrence of disease and help manage on-going care.

When disease occurs, the biochemical activity of cells begins to change. For example, cancer cells multiply at a much faster rate and use more glucose than normal cells. Brain cells affected by dementia consume less energy than normal brain cells. Heart cells deprived of adequate blood flow are dysfunctional (hibernating), although they can still be viable. As disease progresses, this abnormal cellular activity begins to affect body tissue and structures, causing anatomical changes that may be seen on CT or magnetic resonance imaging (MRI) scans [1,4]. For example, cancer cells may form a mass or tumour. With the loss of brain cells, overall brain volume may decrease or affected parts of the brain may appear different in density than the normal areas. Similarly, the heart muscle cells that are affected stop contracting and the overall heart function deteriorates. Molecular imaging excels at detecting the cellular changes that occur early in the course of a disease, often well before structural changes can be seen with other diagnostic imaging resources such as CT and MRI. Most molecular imaging procedures involve an imaging device and an imaging agent. A variety of imaging agents are used to visualize cellular activity, such as the chemical processes involved in metabolism, oxygen use or blood flow. In nuclear medicine, which is a branch of molecular imaging, the imaging agent is a radiotracer, a compound that includes a radioactive atom and a specific imaging agent. Other molecular imaging modalities, such as optical imaging and molecular ultrasound use a variety of different agents. Once the imaging agent is introduced into the body, it accumulates in a target organ or attaches to specific cells depending on the substance injected. The imaging device detects the radiation (and thus the amount and localization) of the radiotracer and creates images that show how it is distributed in the body. Depending on the process, different images are created. This distribution pattern helps physicians discern how well organs and tissues are functioning [2–4].

Nowadays, PET is always fused with the CT technique. The Radboud University MC uses Low Dose CT for fusing images. It is the fusion of functional (PET) and anatomic information (CT) acquired almost simultaneously that lets us see the body and disease in a way that is diagnostically more powerful than both imaging techniques separately. An understanding of the normal and benign as well as the pitfalls and artifacts is essential to accurate interpretation.

The PET/CT scanners are essentially full ring coincidence detectors, the P.E.T. portion, physically mounted together with CT systems of various types. There are various PET crystals (BGO, LSO, GSO) used to detect the emission photons and convert them to light signals. This scintillation event is converted to an electric signal, matched with another coincidence signal, within the selected time window, and a line of response (LOR) is made. All LOR's can be reconstructed to an image that can be displayed on a monitor.

Photons that originate from structures deeper in the body are more highly attenuated by the intervening soft tissue than those originating closer to the surface. This effect of attenuation is not accounted for in the non-attenuation corrected images, which appear to have high activity towards the surface of the patient and relatively low activity toward the centre.

In addition to providing anatomic data, the low dose CT is scaled down and used as a transmission scan to generate an attenuation map that can be used to correct this attenuation effect. Because of the lower photon energy of the CT x-rays (polychromatic 100-140 keV), the CT attenuation coefficients are rescaled to reflect the attenuation of the high-energy monochromatic 511keV emission photons. Then, the energy-scaled CT is scaled down in resolution (matrix) to correct for the high spatial resolution of the CT in comparison to the PET. Once fully scaled, the CT can be applied to the emission (uncorrected) data to obtain the attenuation corrected PET image.

This correction process is essential for quantitative assessment (S.U.V. standardized uptake values) as well as improved image quality. Since artifacts can be introduced during this process, any suspected findings can be verified by seeing if the abnormality was present on the uncorrected emission image [2,3,6]. If it is present on the uncorrected image, then it is likely an increased uptake took place. For example, a patient with a high density hip prosthesis will overcorrect the PET scan in that area. Similar artifacts occur when the patient moves between CT acquisition and PET acquisition (e.g. breathing).

Usually the CT transmission scan is acquired followed by the PET scan. Because the scanners are in the same gantry the patient remains in the same position on a single scanning table scans. Therefore they are intrinsically registered as seen on the fusion image.

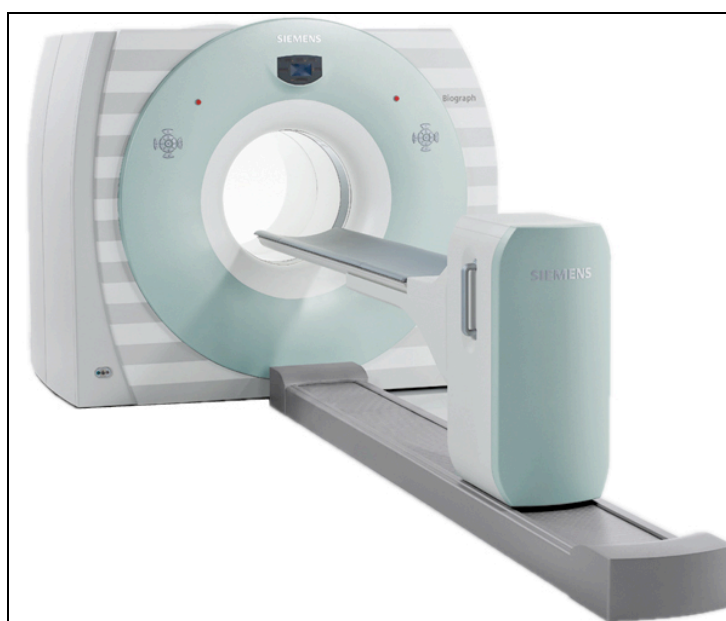


Illustration 2 - Example of PET/CT scanner

18F-Fluorodeoxyglucose

Since the patients went through PET/CT scans with this specific radiopharmaceutical, it is important to know the main principles behind it.

PET/CT radiopharmaceuticals are different from the ones used in gamma cameras as they have radionuclides that are positron emitters and the majority of them have very short half-lives. Today, more than 95% of PET procedures worldwide are performed with F-18 fluoro-deoxyglucose (FDG) [11,12]. This situation is due to practical reasons: Fluorine 18 is easily produced by cyclotrons, with the capability to radiolabel relevant biological molecules. Because of the relatively long half-life (110 minutes) with respect to other positron emitters such as shorter lived C-11 (20.4 minutes), N-13 (10 minutes) and O-15 (2 minutes), Fluorine-18 is the only one in this series that can be distributed also to PET/CT centres without cyclotrons. Therefore it can be used in a wider geographic area [11]. From a chemical point of view, Fluorine is part of a group in the periodic table called halogen, allowing a very stable binding that does not affect the functional part of the molecule. But the real “absolute” value of F-18 is derived by its capability to radiolabel deoxy-glucose producing FDG; i. e., the glucose analogue.

Glucose is an essential compound for living organisms, being the most important carbon supplier with most metabolic processes depending largely on its availability. The slightly adapted version called deoxyglucose has the property that it is taken up by cells like normal glucose, but cells are not capable of metabolizing it further, therefore (fluor)deoxyglucose accumulates in the cells and is not exhaled as H₂O and CO₂ as normal glucose would be.

Pathophysiology of Glucose and FDG's Biodistribution

To correctly interpret PET/CT images, based on the interpretation of all molecular involved events, first we need to analyse the normal glucose distribution, starting from the knowledge of its pathophysiological behaviour. A more extensive and/or specialized publications based on a deeper analysis of FDG as a “molecular tracer” of glucose transporters, suggests that glucose uptake in human cells can take place through two mechanisms: facilitated diffusion and active transport [11,12]. The first one is a carrier-mediated transport, therefore characterized by saturation (and influenced by insulin, increasing its rate up to 20-fold). This means that a competitive inhibition of transport can occur in the presence of a second ligand that binds to the same carrier. This also explains the strong interference on FDG uptake determined by variations in glucose and insulin levels in the blood and by diabetes. High levels of insulin will force FDG, along with glucose, into skeletal muscle, myocardium and

liver, increasing the image background and decreasing the availability of the tracer for uptake by the lesions not influenced by insulin. For these reasons, it is crucial to define a fasting time (at least 4–6 hours), a serum glucose range (3-7 mmol/L, below 10 mmol/L) and, in diabetes, the timing after insulin injection (4 hours prior to the scan). High glucose values or when there's presence of insulin, reduces diagnostic accuracy because of their strong interference with the biodistribution [11].

FDG “Trapping”

After glucose has been taken up in the cells by the membrane-bound sodium dependent glucose transporters (GLUTs), the biochemical destinations of glucose start with phosphorylation. The phosphorylation, both for glucose and FDG, is promoted by hexokinase in the large majority of cells, being dependent on glucokinase in the liver [11]. After this first step, glucose-6-phosphate progresses in its metabolic destination, undergoing further glycolysis with as ultimate products: energy, H₂O and CO₂. Glucose-6-phosphate can also be dephosphorylated mediated by glucose-6-phosphatase (gluconeogenesis) used for the storage of glycogen. FDG-6-phosphate can't be further metabolized in the glycolytic pathway, as this molecule will not fit in the hexokinase enzyme. Therefore, it remains “intracellularly trapped”, because of the lack of significant amounts of FDG-6-phosphatase to reverse the phosphorylation. This is a major advantage for PET/CT imaging: the “trapped” FDG can reliably “in vivo” trace glucose's fate, reflecting the glucose metabolism in the whole organism. Healthy individuals do not excrete glucose through the urinary system but an intense FDG uptake is observed in the urinary system. In fact, whereas normal glucose is freely filtered by glomeruli and rapidly reabsorbed by the nephron, FDG is poorly reabsorbed after filtration, being excreted in a large amount in the urine. In individuals with normal renal function, 50% of the radioactivity reaches the bladder in two hours [11]. A way to reduce the dose to the urinary system is maintaining a good hydration and frequent toilet use, under the influence of forced diuresis by furosemide.

A major contraindication, which has to be remembered, is that FDG crosses the placenta, being distributed mainly in fetal brains and excreted by fetal kidneys. However, the 511 keV radiation occurring from positron annihilation in the mother would contribute to the major radiation burden of the developing fetus.

Physiological and Para-Physiological Distribution of FDG

After fasting for at least 4-6 hours but well hydrated, the patient is injected i.v. with FDG before the PET/CT scan. During the injection and the following uptake phase of one hour preceding the scan, the individual has to rest in a quiet room, comfortable, warm and relaxed. The patient must try to avoid muscular or regional cerebral activity because this will increase FDG uptake in those areas. Since it is impossible to avoid breathing and/or swallowing, the glucose uptake can't be controlled in this case. Patients undergoing a PET/CT scan for head and neck tumours have FDG uptake in the vocal cords when talking. Under standard conditions the highest FDG activity is seen at the cerebral level (mainly in grey matter), since the brain is the only organ exclusively using glucose as a metabolic agent. When fasting, cardiac uptake is variable, but most commonly has a mild and homogeneous uptake but this can be very heterogeneous as parts of the myocardium can use fatty acids for fuel as well. Sometimes it can be hard to analyse the heart due to high blood pool activity at the level of the great vessels, mainly in the mediastinum. While liver and spleen show high and low-grade diffuse activity respectively, variable uptake is seen in the gastrointestinal system, creating difficulties in the analysis and problems in differential diagnosis in the guts. Low and/or absent concentration of FDG is observed at the level of bone marrow. No activity is also seen at the level of normal lymph nodes, but after FDG's extravasation at the injection site, high uptake in the draining regional glands can be seen. Moderate activity can be seen in tonsils, salivary glands, myelohyoid muscles and, in young patients, in the thymus, adenoidal tissue and testicles. No uptake is normally seen at the level of lungs. The skeletal muscle's uptake increases as a specific response to stress and/or exercise in the involved muscular cells. An increased uptake can be determined by many conditions such as hyperventilation, hiccupping, torticollis and intense eye movement, as a result of (in)voluntary tensions. The muscular uptake is generally bilateral and symmetric. An apparent unilateral pathological concentration can be observed contra laterally to a nerve palsy. The urinary excretion, determining a high normal background at the renal and vesicle level, can create difficulties in evaluating FDG's pathological uptake in the pelvic area. Small areas of ureteric stasis may simulate lymphadenopathy. The presence of different locations of kidneys and ureters has to be known to avoid mistakes in PET/CT images interpretation. Diffuse thyroid uptake can be occasionally observed in clinically normal patients, being frequently caused by thyroiditis or hyperthyroidism. In premenopausal women (and/or in women taking estrogens) breast tissue often demonstrates moderate symmetrical FDG concentration. Breastfeeding mothers present intense uptake. A faint-to moderate uterine uptake can be observed during menstruation. In adipose tissue a typical symmetric intense uptake can be determined by active brown fat, mainly in winter months in young patients with

a lower body mass index. Since the lesion's detectability in nuclear medicine is dependent on lesion/background ratio, it is evident that major difficulties in PET/CT are present at the cerebral level and/or in the abdominal-pelvic territory. Nevertheless, many physiological and para-physiological uptakes can be distinguished by the morphostructural information obtained by CT.

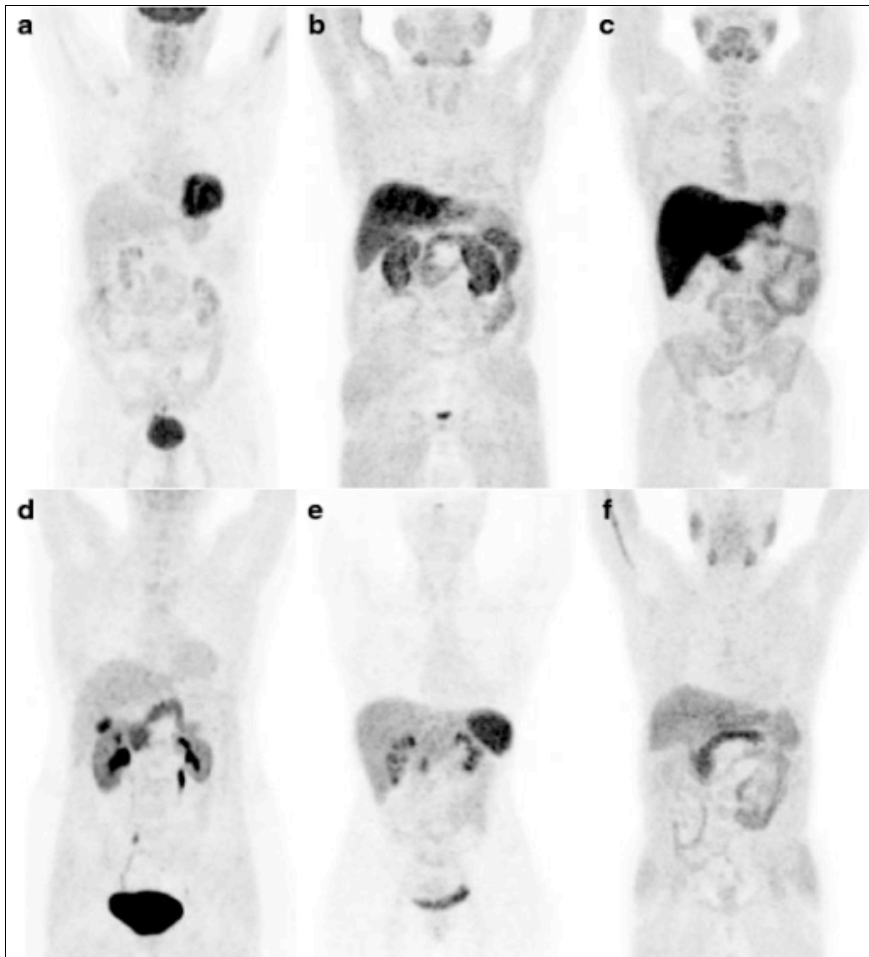


Illustration 3 - Examples of normal FDG uptake

Normal FDG uptake in the liver

At the time of imaging, (approximately 1 hour after injection) moderate uptake can be seen throughout the liver in almost all patients [5,7,13]. The level of uptake is usually slightly higher than blood pool activity. The distribution sometimes can be somewhat heterogeneous and difficult to interpret but generally the liver shows a homogenous distribution [5,7]. This problem is further affected by artifacts as a result of attenuation correction methods and movement during breathing. For example, the positioning of the arms can influence the quality of the image in the liver area. Sensitivity for the detection of small benign hepatic lesions is low in the liver due to small FDG uptake in a moderate FDG uptake organ. This can make diagnosis difficult for physicians. However, there is an increased FDG uptake in tumour cells due to increased expression of glucose transporter (GLUT) molecules on the cell surface, increased activity of hexokinase and reduced levels of glucose-6-phosphatase.

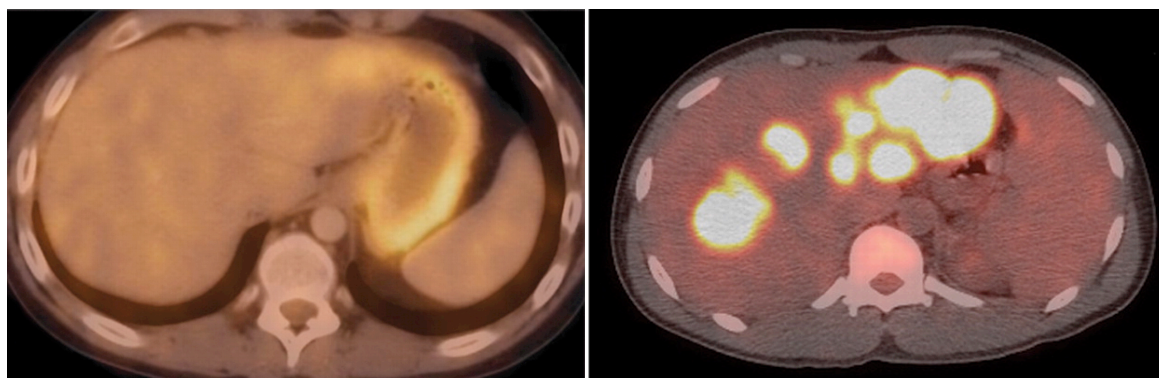


Illustration 4 - Normal liver uptake (left) and abnormal liver uptake (right)

The liver is a major organ for carbohydrate metabolism and storage. It is particularly involved in glycolysis and glycogen storage. Hepatocytes have high levels of glucose-6-phosphatase, which allow for intracellular FDG clearance from the liver. This decreasing activity is beyond what is expected simply due to decay of the radionuclide but under usual circumstances is very small (phosphorylation rates are 100 to 1000x higher than dephosphorylation rates).

Body Mass Index

In order to relate the Signal-to-Noise Ratio of the liver with the patient's weight, it's important to have a measurement tool that relates the weight with the height. By only using weight, we don't take in consideration the height, which means the patient can be heavy and theoretically is considered obese but the real weight category might not be the same. Among every tool available for this calculation, Body Mass Index (BMI) seems to be the most appropriate one. Body Mass Index is a number calculated mainly from a person's weight and height, although age and gender can also be considered. BMI is a fairly reliable indicator of body fatness. BMI can be considered as an alternative for measuring body fat. Additionally, BMI is an inexpensive and easy-to-perform method of screening for weight categories [14–16].

However, it is important to remember, that BMI is not a direct measure of body fatness and that BMI is calculated from an individual's weight, which includes both muscle and fat. As a result, some individuals may have a high BMI but not have a high percentage of body fat. For example, highly trained athletes may have a high BMI because of increased muscularity rather than increased body fatness. Although some people with a BMI in the overweight range (from 25.0 to 29.9) may not have excess body fatness, most people with a BMI in the obese range (equal to or greater than 30) will have increased levels of body fatness. The standard weight status categories associated with BMI ranges for adults are shown in the following table [14].

BMI	Weight Status
Below 18.5	Underweight
18.5 – 24.9	Normal
25.0 – 29.9	Overweight
30.0 and Above	Obese

Table 1 - BMI Categories

Although it has its limitations, most patients that were collected are considered to be “normal” relatively to their weight, making this tool the best one to make the calculations. BMI is used as a screening tool to identify possible weight problems for adults but is not considered a diagnostic tool [14].

BMI is calculated the same way for both adults and children. The calculation is based on the following formula:

$$\frac{\text{Weight (Kg)}}{[\text{Height (m)}]^2}$$

The correlation between the BMI number and body fatness is fairly strong; however the correlation varies by sex, race, and age. These variations include the following examples:

- At the same BMI, women tend to have more body fat than men.
- At the same BMI, older people, on average, tend to have more body fat than younger adults.
- Highly trained athletes may have a high BMI because of increased muscularity rather than increased body fatness

Procedure

The purpose of this project is to study and analyse the effects of the patient's weight on the Signal-to-Noise Ratio (SNR) in the liver. The first objective is to see if there is any relation between the dose injected, the SNR and the weight. The Body Mass Index was also calculated for each patient, taking in consideration his or her age, height, weight and gender, according to the National Health Service from the United Kingdom. This calculator was used because it takes in consideration a lot of variables and the study must be as precise as possible. This variable was also used to also see if there is a relation with the dose injected and the SNR but it became clear that BMI isn't useful in clinical practice. The second objective of this project is to try to get to a new formula to calculate the new FDG dose and get a better and constant SNR without being affected by the patient's bodyweight.

The project started by selecting patients with different weights from the department's database. 65 patients (39 males and 26 females) with weight ranging from 39 Kg to 125 Kg and BMI ranging from 14,5 to 39,45 were gathered, retrospectively. All the selected patients were scans performed in the department in several different periods of time, in a standard protocol (4 minutes per bed position) on the specific model Siemens Biograph mCT. The dose given to these patients was calculated with the following formula, based on the Netherlands protocol for standardization of FDG whole body PET studies (NEDPAS Protocol) [17] and on scanner properties:

$$\frac{(6,4 \times \text{Weight in Kg})}{\text{Minutes per bed position}} \text{ MBq}$$

Several exclusion criteria were used for the selection of the patients:

- If the patient had diabetes, it couldn't be selected because it would affect the FDG uptake and would affect the outcome results;
- Any kind of liver disease (including metastases) that would affect the assumption of homogeneous distribution of FDG uptake;
- Any kind of breathing artifacts that would affect the liver and if another portion of the organ couldn't be selected;
- Any kind of disease that would affect the FDG normal distribution on the body;
- Any surgical history on the liver that might affect the SNR;
- Any changes performed in the scanning protocol, like arms down;

After the selection of the patients, the SNR was going to be calculated in every person. The SNR was used as a measure of the quality of the PET/CT images and was analysed as a function of the patient's body mass. This measure was calculated for each patient in the liver, because it is the only large organ in the human body that has a relatively homogeneous distribution of FDG uptake. In the software "Hermes", with the help of a crosshair, five slices were selected and the SNR was determined on each one of them, using the same sized Region of Interest (ROI). The selected slices were chosen at a position where the cross-section area of the liver was at maximum. The mean signal (MBq/Kg liver tissue) and the standard deviation (SD, MBq/Kg liver tissue) [18] were measured in the selected area of the liver. As we assume the liver is an organ with homogenous glucose metabolism [5,7,19], the mean uptake reflects the image signal and standard deviation reflects the image noise. This took in consideration possible artifacts like partial volume effect, so the slices were selected away from the boundaries of the liver or other intrahepatic structures like vessels or gall bladder. With both of these values, the SNR was calculated by dividing the mean signal with the standard deviation. For each patient the mean SNR was determined five times to make sure that a reliable value was obtained.

There are two different PET images: PET Whole Body (WB) and PET WB European Association of Nuclear Medicine (EANM). The main differences between these two are in the parameters of Image Size and the Full Width at Half Maximum (FWHM). In the PET WB, image size is 200 and the FWHM is 3.0 mm whilst in the EANM is 256 and 8.0 mm respectively. The FWHM is a parameter used to describe the point spread function of a source measured at half of its maximum shown on a curve or function. The lower this value is, the greater the spatial resolution will be. In other words, the PET WB has higher spatial resolution but therefore is noisier (less counts per pixel); the PET EANM has lower spatial resolution (i.e. is "smoothed") and is therefore less noisy. Higher SNRs are therefore expected in the PET EANM than in the PET WB, but the relation with bodyweight is not expected to be different.

After choosing the patient and the corresponding Computed Tomography Low Dose (CT-LD), the PET WB and the PET, taking in consideration every view (transaxial, sagittal and coronal), an optimal position was chosen in the liver. This was done on the CT image since it has a better image for localization and confirmed in the other images. By doing so, the position was automatically chosen in the other two PET images.

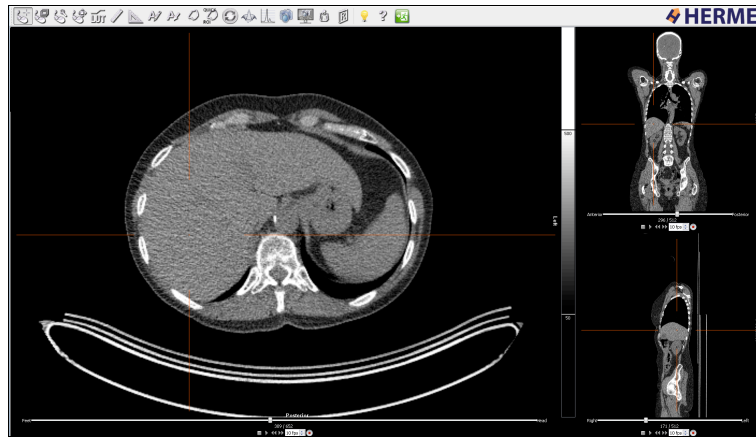


Illustration 5 - Positioning of the point in the CT scan

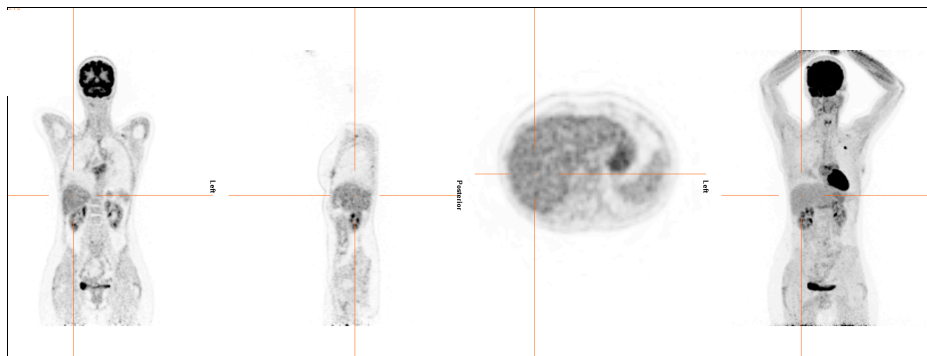


Illustration 6 - Positioning of the point in the PET WB scan

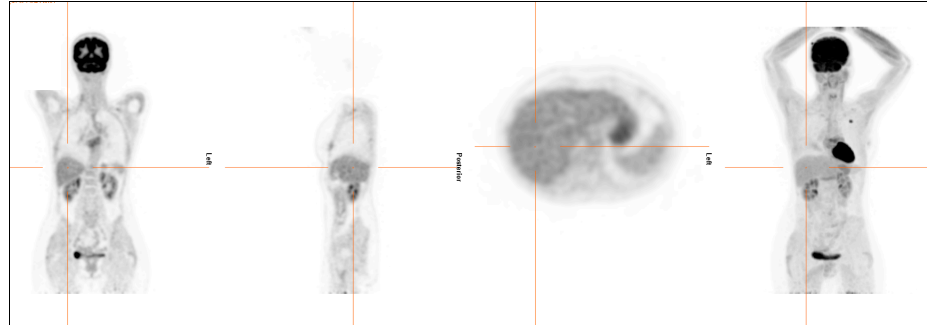


Illustration 7 - Positioning of the point in the PET WB EANM scan

After choosing one point in the liver, a ROI would be made in five consecutive slices in the PET images. Every ROI was a circle with a diameter of exactly 50 mm. Since the CT was acquired with more slices than the PET, the slices made weren't consecutive in the CT but intercalated. On the CT will appear that way but in the PET's they are consecutive.

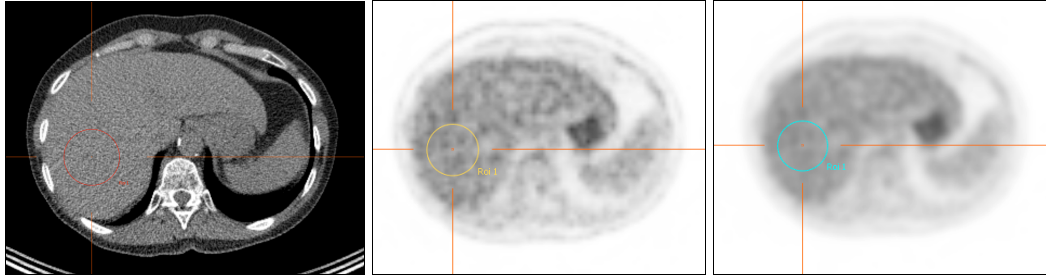


Illustration 8 - First ROI on CT (left), PET WB (middle) and PET WB EANM (right)

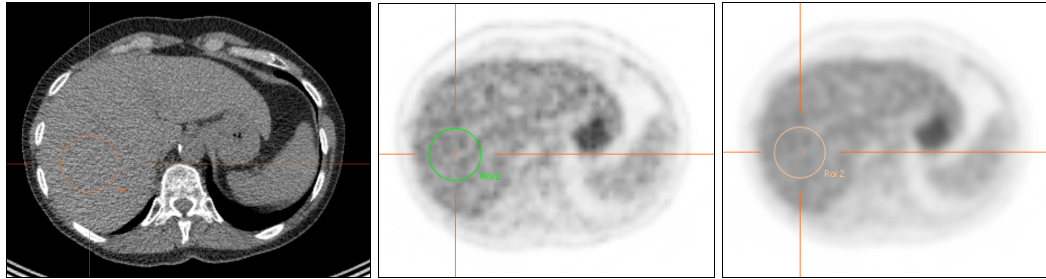


Illustration 9 - Second ROI on CT (left), PET WB (middle) and PET WB EANM (right)

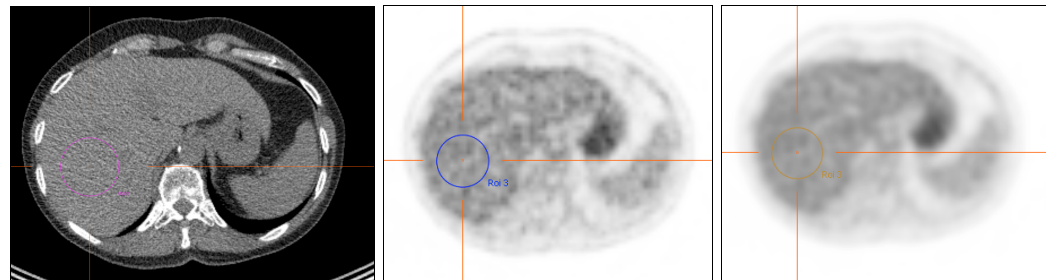


Illustration 10 - Third ROI on CT (left), PET WB (middle) and PET WB EANM (right)

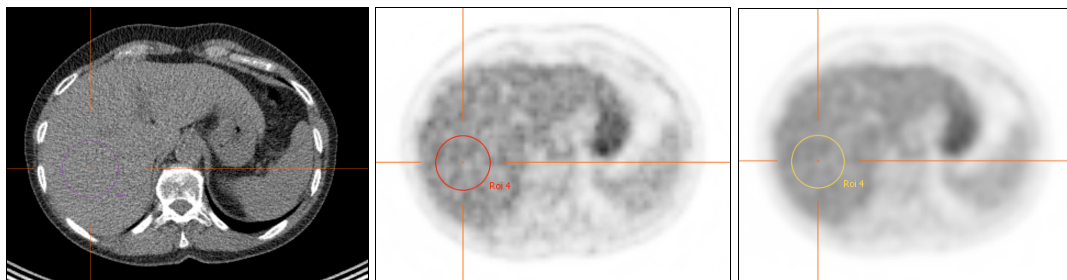


Illustration 11 - Fourth ROI on CT (left), PET WB (middle) and PET WB EANM (right)

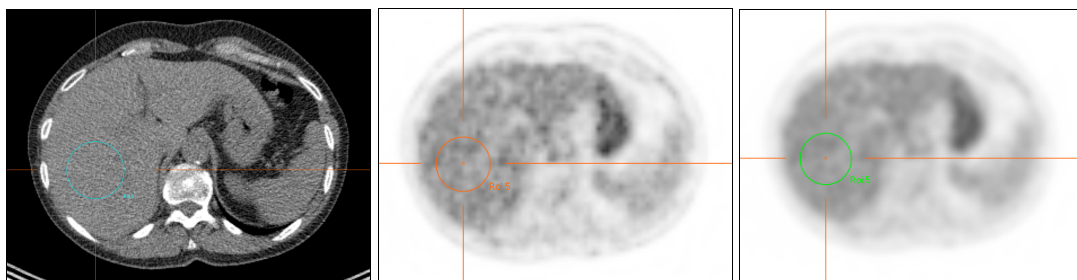


Illustration 12 - Fifth ROI on CT (left), PET WB (middle) and PET WB EANM (right)

The effects of weight and injected dose in the liver's Signal-to-Noise Ratio in patients submitted to PET/CT scans

After making five ROI's, we would get several values from that area of the five slices and three images. The values that are important for us are the "Mean" and the "Deviation". Like reported earlier, the division between the mean and deviation would give the SNR. With the help of a table in Microsoft Excel, it was possible to automatically calculate the SNR of each slice and the mean SNR of every patient, by summing the five means and the five deviations and then dividing by five. This would give the mean of each value, which afterwards was used to calculate the SNR. This was done in both PET images.

ROI/VOI	Image Number	Cells	Total	Mean	Min	Max	Median	Deviation	Suv Peak	Diameter mm	Area cm ²	Volume cm ³
ROI												
Transverse												
ROI 1	156	118	330.55	2.78	2.05	3.62	2.78	0.92		50	19.57	
ROI 2	155	114	321.42	2.82	2.13	3.66	2.83	0.94		50	19.91	
ROI 3	154	118	329.75	2.77	2.02	3.68	2.74	0.93		50	19.57	
ROI 4	153	118	328.40	2.76	1.95	3.62	2.77	0.96		50	19.57	
ROI 5	152	112	313.22	2.75	1.98	3.67	2.73	0.99		50	19.58	
Coronal												
Sagittal												
VOI												
Transverse												
Coronal												
Sagittal												

Illustration 13 - Values of the ROI's in the PET WB

ROI/VOI	Image Number	Cells	Total	Mean	Min	Max	Median	Deviation	Suv Peak	Diameter mm	Area cm ²	Volume cm ³
ROI												
Transverse												
ROI 1	156	193	550.98	2.75	2.35	3.18	2.78	0.17		50	19.54	
ROI 2	155	189	534.94	2.77	2.47	3.15	2.76	0.17		50	19.14	
ROI 3	154	193	551.64	2.76	2.42	3.16	2.73	0.18		50	19.54	
ROI 4	153	193	546.73	2.73	2.33	3.19	2.71	0.20		50	19.54	
ROI 5	152	186	524.68	2.72	2.27	3.24	2.71	0.22		50	18.83	
Coronal												
Sagittal												
VOI												
Transverse												
Coronal												
Sagittal												

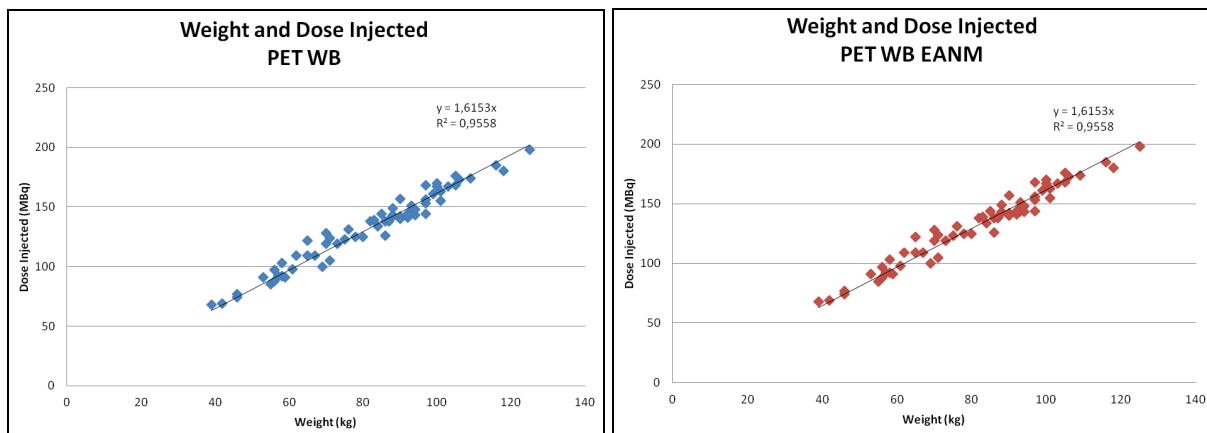
Illustration 14 - Values of the ROI's in the PET WB

The effects of weight and injected dose in the liver's Signal-to-Noise Ratio in patients submitted to PET/CT scans

PET WB																																
ROI 1		ROI 2		ROI 3		ROI 4		ROI 5		Total																						
Mean	Deviation	SNR	Mean	Deviation	SNR	Mean	Deviation	SNR	Mean	Deviation	SNR	Mean	Deviation	SNR	Dose Injected (MBq)	Gender	Weight (Kg)	Height (cm)	BMI													
274	0.4	6.85	2.8	0.59	4.745763	2.68	0.62	4.322581	2.64	0.66	5.73931	2.86	0.47	6.085956	2.744	0.508	5.409575	853	M	87	184	28.65										
276	0.32	6.6875	2.82	0.36	6.24189	2.77	0.23	6.333333	2.76	0.26	7.86687	2.75	0.29	7.65032	2.736	0.246	7.07101	108	F	65	165	23.69										
257	0.47	5.468891	2.65	0.53	5	2.71	0.46	5.891304	2.59	0.4	6.475	2.58	0.45	5.733333	2.62	0.462	5.678996	128	M	86	182	25.96										
153	0.8	8.5	1.53	0.22	6.954545	1.53	0.2	7.85	1.53	0.21	7.28974	1.53	0.21	7.28974	1.53	0.204	7.5	88	F	39	84	14.5										
231	0.3	7.7	2.21	0.35	6.39426	2.16	0.29	7.74362	2.22	0.26	8.50462	2.29	0.26	8.00762	2.228	0.23	7.71241	98	F	61	170	21.01										
358	0.44	6.936336	2.62	0.5	7.24	2.65	0.53	6.88782	2.63	0.52	6.880769	2.63	0.42	6.804762	2.652	0.462	7.473029	123	F	75	174	24.77										
232	0.4	5.9	2.48	0.42	5.804762	2.55	0.5	5.1	2.65	0.52	5.08954	2.7	0.49	5.63204	2.54	0.466	6.450844	144	M	87	178	30.81										
287	0.46	6.239104	2.67	0.41	6.1	2.65	0.41	6.962439	2.6	0.5	5.6	2.64	0.438	6.45051	144	F	87	169	30.49													
223	0.34	6.686625	2.3	0.2	7.686667	2.9	0.21	7.39707	2.92	0.26	6.444444	2.95	0.4	5.975	2.98	0.362	6.783338	105	F	71	161	27.29										
221	0.37	5.972973	2.19	0.37	5.938939	2.19	0.37	5.938939	2.19	0.39	5.65385	2.19	0.47	4.658574	2.194	0.394	5.568238	100	F	69	185	20.16										
252	0.45	5.6	2.58	0.43	5.2	2.67	0.51	5.252924	2.69	0.48	5.804907	2.77	0.49	5.653861	2.646	0.472	5.699232	138	M	82	184	30.49										
269	0.43	6.709392	2.52	0.47	6.212766	2.56	0.5	6.39	2.69	0.48	6.026323	2.81	0.49	5.939776	2.84	0.474	6.487879	138	F	86	188	26.47										
248	0.55	4.958939	2.62	0.57	4.586491	2.81	0.69	4.122353	2.65	0.59	4.492525	2.6	0.56	4.642897	2.632	0.59	4.643007	212	M	100	191	27.41										
235	0.37	5.938939	2.19	0.37	5.938939	2.19	0.37	5.938939	2.19	0.37	5.938939	2.19	0.37	5.938939	2.19	0.37	5.938939	189	F	79	163	28.96										
225	0.5	4.5	2.22	0.47	4.724044	2.36	0.29	5.939462	2.39	0.44	4.954545	2.39	0.44	5.93939	2.39	0.446	4.959993	162	F	87	160	22.27										
333	0.41	6.129852	2.35	0.42	7.97919	3.42	0.45	7.6	3.32	0.46	7.217391	3.25	0.43	7.55814	3.334	0.434	7.682028	119	M	70	173	23.39										
203	0.39	5.209332	2.06	0.35	5.085714	2.14	0.33	6.494349	2.14	0.34	6.249193	2.11	0.37	5.702703	2.096	0.356	5.689764	125	M	79	176	25.93										
288	0.36	5.777778	2	0.23	6.069696	2.08	0.29	5.333333	2.01	0.45	4.844444	2.05	0.4	5.375	2.099	0.386	5.423233	109	M	67	168	23.74										
267	0.38	7.026393	2.71	0.44	6.859091	2.81	0.42	6.630476	2.83	0.36	7.86111	2.79	0.36	7.75	2.782	0.382	7.045918	109	F	62	156	26.14										
234	0.59	4.939593	2.8	0.56	5	2.81	0.62	4.932592	2.81	0.52	5.403846	2.79	0.48	5.8325	2.81	0.504	5.072202	144	F	76	165	31.63										
341	0.36	6.472222	2.43	0.26	6.026316	3.37	0.29	6.804621	3.31	0.43	7.937974	3.3	0.43	7.874489	3.264	0.396	6.448494	128	F	79	168	24.9										
269	0.55	4.890991	2.63	0.49	5.267247	2.63	0.49	5.479857	2.63	0.48	5.479857	2.63	0.52	5.657832	2.642	0.504	5.242063	242	M	90	175	29.39										
246	0.54	4.57037	2.5	0.47	5.339149	2.43	0.44	5.522727	2.39	0.42	5.666667	2.4	0.35	6.897463	2.432	0.444	5.477477	134	M	84	177	26.81										
182	0.34	6.947468	1.93	0.3	6.432333	2.06	0.39	5.439353	2.13	0.29	5.483539	2.03	0.32	6.34375	2.091	0.346	5.620909	125	M	89	186	23.82										
25	0.45	5.555556	2.63	0.49	5.704545	2.52	0.46	5.478261	2.5	0.46	5.434703	2.5	0.44	5.69898	2.506	0.45	5.568889	107	M	100	188	28.23										
362	0.61	5.934332	2.57	0.65	5.452389	3.64	0.72	4.986301	3.79	0.73	5.93781	3.73	0.66	5.659595	3.67	0.676	5.428994	241	F	105	187	46.86										
228	0.52	4.48656	2.63	0.56	4.686428	2.65	0.52	5.039594	2.6	0.59	4.462759	2.73	0.54	5.655556	2.598	0.546	4.752423	100	M	109	186	34.11										
157	0.21	7.478995	1.59	0.22	7.18918	1.53	0.19	8.052632	1.49	0.2	7.45	1.45	0.2	7.25	1.524	0.204	7.470988	161	F	55	162	20.96										
288	0.51	5.647058	2.64	0.51	5.568627	2.88	0.53	5.433962	2.95	0.59	5	2.89	0.54	5.937037	2.909	0.536	5.429373	264	M	114	195	37.22										
321	0.36	6.447384	2.22	0.26	6.47304	2.21	0.47	6.829197	2.05	0.46	6.647628	2.04	0.41	7.685537	2.06	0.42	7.689774	144	M	93	185	27.87										
173	0.27	6.407474	1.84	0.24	4.919795	1.67	0.27	4.519514	1.73	0.23	5.242424	1.82	0.24	5.352941	1.724	0.233	5.224242	284	M	95	173	28.27										
237	0.46	5.923739	2.4	0.45	5.333333	2.45	0.45	5.444444	2.49	0.47	5.278986	2.4	0.51	4.705882	2.42	0.489	5.57094	289	M	100	187	28.6										
2	0.29	6.447384	2.22	0.26	6.47304	2.21	0.47	6.829197	2.05	0.46	6.647628	2.04	0.41	7.685537	2.06	0.42	7.689774	144	M	93	185	27.87										
173	0.27	6.407474	1.84	0.24	4.919795	1.67	0.27	4.519514	1.73	0.23	5.242424	1.82	0.24	5.352941	1.724	0.233	5.224242	284	M	95	173	28.27										
237	0.46	5.923739	2.4	0.45	5.333333	2.45	0.45	5.444444	2.49	0.47	5.278986	2.4	0.51	4.705882	2.42	0.489	5.57094	289	M	100	187	28.6										
2	0.29	6.447384	2.22	0.26	6.47304	2.21	0.47	6.829197	2.05	0.46	6.647628	2.04	0.41	7.685537	2.06	0.42	7.689774	144	M	93	185	27.87										
173	0.27	6.407474	1.84	0.24	4.919795	1.67	0.27	4.519514	1.73	0.23	5.242424	1.82	0.24	5.352941	1.724	0.233	5.224242	284	M	95	173	28.27										
237	0.46	5.923739	2.4	0.45	5.333333	2.45	0.45	5.444444	2.49	0.47	5.278986	2.4	0.51	4.705882	2.42	0.489	5.57094	289	M	100	187	28.6										
2	0.29	6.447384	2.22	0.26	6.47304	2.21	0.47	6.829197	2.05	0.46	6.647628	2.04	0.41	7.685537	2.06	0.42	7.689774	144	M	93	185	27.87										
173	0.27	6.407474	1.84	0.24	4.919795	1.67	0.27	4.519514	1.73	0.23	5.242424	1.82	0.24	5.352941	1.724	0.233	5.224242	284	M	95	173	28.27										
237	0.46	5.923739	2.4	0.45	5.333333	2.45	0.45	5.444444	2.49	0.47	5.278986	2.4	0.51	4.705882	2.42	0.489	5.57094	289	M	100	187	28.6										
2	0.29	6.447384	2.22	0.26	6.47304	2.21	0.47	6.829197	2.05	0.46	6.647628	2.04	0.41	7.685537	2.06	0.42	7.689774	144	M	93	185	27.87										
173	0.27	6.407474	1.84	0.24	4.919795	1.67	0.27	4.519514	1.73	0.23	5.242424	1.82	0.24	5.352941	1.724	0.233	5.224242	284	M	95	173	28.27										
237	0.46	5.923739	2.4	0.45	5.333333	2.45	0.45	5.444444	2.49	0.47	5.278986	2.4	0.51	4.705882	2.42	0.489	5.57094	289	M	100	187	28.6										
2	0.29	6.447384	2.22	0.26	6.47304	2.21	0.47	6.829197	2.05	0.46	6.647628	2.04	0.41	7.685537	2.06	0.42	7.689774	144	M	93	185	27.87										
173	0.27	6.407474	1.84	0.24	4.919795	1.67	0.27	4.519514	1.73	0.23	5.242424	1.82	0.24	5.352941	1.724	0.233	5.224242	284	M	95	173	28.27										
237	0.46	5.923739	2.4	0.45	5.333333	2.45	0.45	5.444444	2.49	0.47	5.278986	2.4	0.51	4.705882	2.42	0.489	5.57094	289	M	100	187	28.6										
2	0.29	6.447384	2.22	0.26	6.47304	2.21	0.47	6.829197	2.05	0.46	6.647628	2.04	0.41	7.685537	2.06	0.42	7.689774	144	M	93	185	27.87										
173	0.27	6.407474	1.84	0.24	4.919795	1.67	0.27	4.519514	1.73	0.23	5.242424	1.82	0.24	5.352941	1.724	0.233	5.224242	284	M	95	173	28.27										
237	0.46	5.923739	2.4	0.45	5.333333	2.45	0.45	5.444444	2.49	0.47	5.278986	2.4	0.51	4.705882	2.42	0.489	5.57094	289	M	100	187	28.6										
2	0.29	6.447384	2.22	0.26	6.47304	2.21	0.47	6.829197	2.05	0.46	6.647628	2.04	0.41	7.685537	2.06	0.42	7.689774	144	M	93	185	27.87										
173	0.27	6.407474	1.84	0.24	4.919795	1.67	0.27	4.519514	1.73																							

Results and Discussion

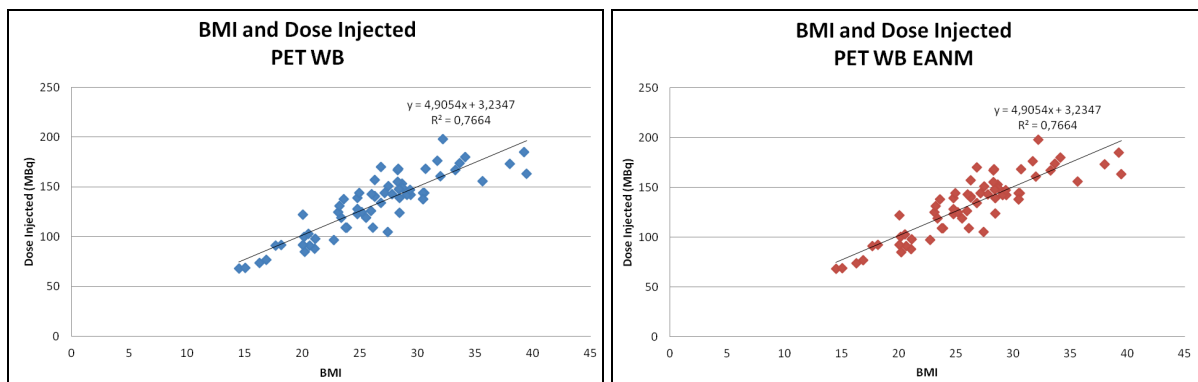
After filling in all the values in the table about mean, deviation, SNR, dose injected (in MBq), gender, weight (in Kg), height (in cm) and BMI, several graphs related to SNR, dose, weight and BMI were made to see which were the results. All the graphs were made with the values of the PET WB and the PET WB EANM to see if there are any significant differences between them.



Graphs 1 - Relation between Weight and Dose Injected on the PET WB (left) and PET WB EANM (right)

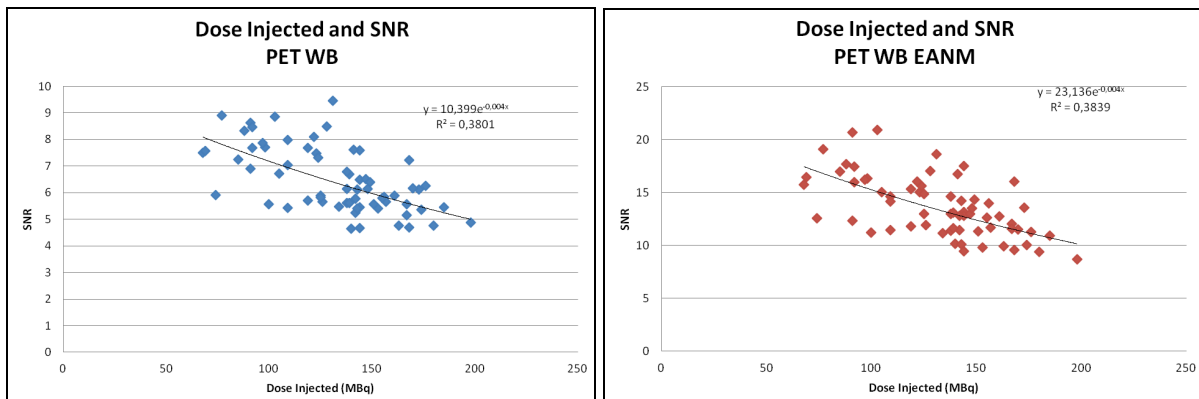
First of all, relating the weight to the dose injected, we can see that both graphs look-a-like. The positioning of the points is quite similar and the behaviour of the graph is the same. So, as we can see, as the weight increases, the injected dose also increases, almost in a straight line. This makes sense, since the dose injected is dependent of the value of the weight in the formula used to calculate the dose. The points create almost an exact growing line. The function of the line is $Dose = 1,62 \times Weight$. Therefore the patients are dosed 1.62MBq/kg

which is exactly what we opt to give ($\frac{6,4}{4} = 1,6$).



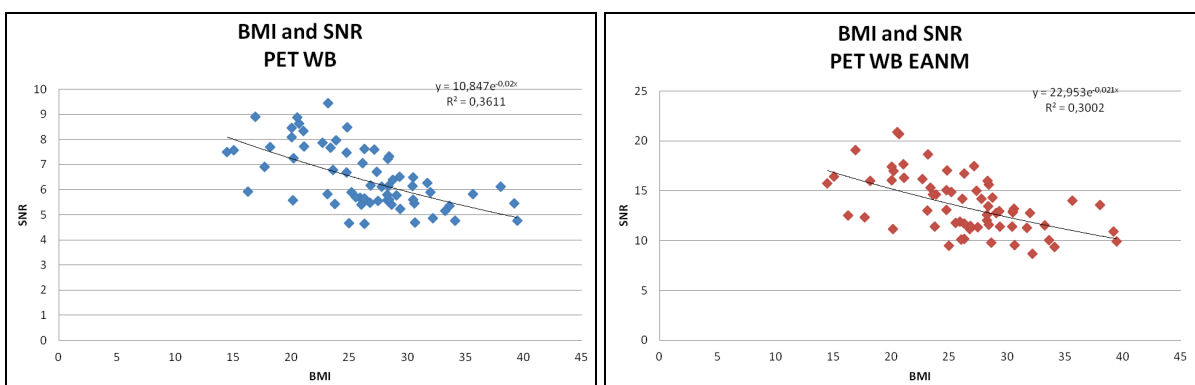
Graphs 2 - Relation between BMI and Dose Injected on the PET WB (left) and PET WB EANM (right)

Next, we have the graphs relating BMI to the dose injected. Like the previous one, both graphs have the same behaviours. And, like the previous graphs, the dose also increases as the BMI increases. However, it's not the same increase as the weight in the previous graphs. This is because the dose is calculated in a formula that includes weight and not BMI. This measurement takes in consideration more values, so it is normal that the increase is not as concentrated as the previous ones.



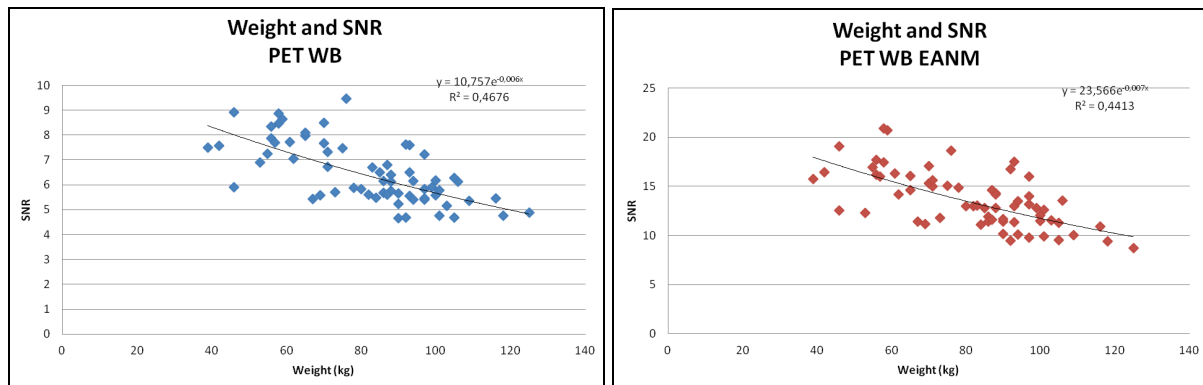
Graphs 3 - Relation between Dose Injected and SNR on the PET WB (left) and PET WB EANM (right)

Comparing the dose injected with the SNR, we can see that both graphs have a similar behaviour. However, the PET WB EANM has higher SNR values due to the parameters reported earlier, which would give a smoother image and consequently increases the SNR values. As the dose injected increases, the SNR decreases. This is because patients who receive higher doses (at least in this study) are heavier and, as it was reported, as the weight increases, the dose would also increase. In other words: even though the dose in heavier patients is higher, the SNR still deteriorates.



Graphs 4 - Relation between BMI and SNR on the PET WB (left) and PET WB EANM (right)

Like the previous graphs, both have a similar behaviour and only differentiate in the SNR values, due to the different parameters. So, comparing the BMI with the SNR, we see that as BMI increases, the SNR decreases. So, as the patient is considered more obese, the less quality the picture will have while patients who are underweight have a higher SNR. However, the quality seems to be best when the patient is considered normal weight (between the BMI values 19 to 24 approximately).



Graphs 5 - Relation between Weight and SNR on the PET WB (left) and PET WB EANM (right)

In these graphs, we can clearly see that as the weight increases, the SNR will decrease (even though higher FDG doses are given) in both PET WB scan and the PET WB EANM scan. When the patient is light, the SNR is higher and so the quality of the image will be better.

There are some interesting findings in these graphs. With these results, it can be said that the weight does interfere with the quality of the image, specifically the SNR. As we can see in Graphs 5, when the patient is heavier, the SNR clearly decreases. Graphs 4 shows that the SNR also decreases with BMI. So, as the patient is considered more obese, the quality of the image is decreased. So, obesity indeed affects image quality due to the photon attenuation and scatter fractions being higher in obese patients than in patients with a normal BMI or weight. The dose injected increases as the weight and BMI increase, as it should according to the formula to obtain the optimal dose, according to the department's protocol. However, according to the findings in Graphs 3, following this formula, the heavier patients don't have the same SNR as thinner patients. The behavior of the Graphs 3 and 5 should be almost an horizontal line because we want a constant SNR in all patients and not a decrease with patients' weight.

So, with these results, it was shown that the formula used to calculate the optimal dose for patients performing PET/CT scans isn't the best one for a constant SNR, regardless of the

The effects of weight and injected dose in the liver's Signal-to-Noise Ratio in patients submitted to PET/CT scans

patients' weight. Taking this in consideration, a new formula was needed in order to get a constant SNR for all patients.

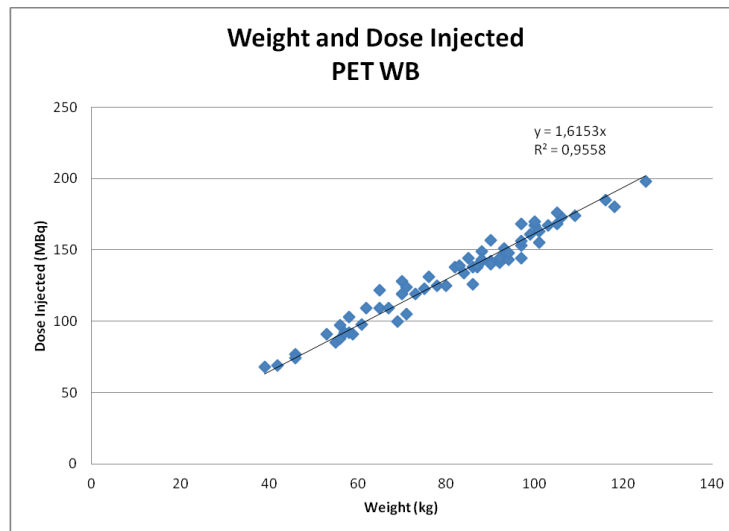
Starting from the beginning, the current FDG dose is calculated with the following formula:

$$D = a \times W$$

Equation 1

The Dose D is a value in MBq, the a is the value used to calculate the quantity of MBq per Kilogram (MBq/Kg) and the W is the weight of the patient. The a value is 1,6MBq/Kg (i.e. $\frac{6,4}{4}$). In order to check if the data collected is correct, we can confirm this value with the

following graphic:



Graphic 6 - Linear line for weight and dose injected

Based on the study of 65 patients (weight ranging between 39 to 125 kg, with the median being 86 kg), the injected dose was, in fact, 1,62MBq/kg ($R^2=0,96$), therefore the patients were indeed injected with the dose according to protocol.

The quality of a PET/CT scan was defined in this project as Signal-to-Noise Ratio and, as reported earlier, it can be calculated by dividing the mean liver activity concentration (μ) by the standard deviation of activity concentration in the liver (σ):

$$SNR_{liver} = \frac{\mu_{liver}}{\sigma_{liver}}$$

Equation 2

We can assume that there is a relation between the number of detected true events (T_{liver} [counts/mL]), μ_{liver} and σ_{liver} . According to Poisson statistics, the following could be expected (n=0,5 if Poisson statistics are considered) [18]:

$$\mu_{liver} \propto T_{liver}$$

Equation 3.1

$$\sigma_{liver} \propto (T_{liver})^n$$

Equation 3.2

There's a relation between T_{liver} and the dose injected (D_A [Bq]) which is dependent on the activity concentration of the radiopharmaceutical in the liver (AC_{liver} [Bq/mL] dependent on biodistribution of the pharmacon and its pharmacokinetics) and on the relation between detected true events and total events (e.g. photon scattering, photo attenuation correction, etc). These factors are supposed to be dependent on the size of the patient [$F(X)$ with X being the variable to describe the patient size (weight or BMI)]:

$$T_{liver} \propto D_A \times F(X)$$

Equation 3.3

From this equation, we can obtain the following:

$$\mu_{liver} \propto D_A \times F(X)$$

Equation 3.4

$$\sigma_{liver} \propto (D_A \times F(X))^n$$

Equation 3.5

$$SNR_{liver} \propto \frac{\mu_{liver}}{\sigma_{liver}} \propto (D_A)^{1-n} \times F(X)^{1-n}$$

Equation 3.6

The measured SNR_{liver} should be normalized for $(D_A)^{1-n}$ to describe the weight dependent quality function $F(X)$. This is defined as the case that every patient of any weight would have received $D_A=I$ Bq and is hereby called the normalized SNR_{liver} denoted by asterix:

$$SNR_{liver}^* \propto \frac{SNR_{liver}}{(D_A)^{1-n}}$$

Equation 4

There's an inverse relation between SNR_{liver}^* and measure for patient size, defined by X (weight or BMI): the lower the SNR_{liver}^* is, the higher the X is.

This kind of relation can be of three kinds: linear, power or exponential. Since the relation is expected to be negative, r_1 is expected to be lower than 0 in any type of regression:

Linear:

$$SNR_{liver}^* = r_1 \times X \times r_2$$

Equation 5a

Power:

$$SNR_{liver}^* = r_2 \times X^\eta$$

Equation 5b

Exponential:

$$SNR_{liver}^* = r_2 \times e^{\eta \times X}$$

Equation 5c

The effects of weight and injected dose in the liver's Signal-to-Noise Ratio in patients submitted to PET/CT scans

Since the current adopted formula has proven to be insufficient (equation 1), we want a new relation between target dose (D_T) and body size (X). This new relation ($D'_T(X)$) would lead to a constant SNR_{liver} whose value is dependent on the needs of the physicians and is called $SNR_{standard}$.

Based on equation 4, we can have derive:

$$SNR_{liver}^* = \frac{SNR_{standard}}{(D'_T(X))^{1-n}}$$

Equation 6a

Therefore:

$$D'_T(X) = \left(\frac{SNR_{standard}}{SNR_{liver}^*} \right)^{\frac{1}{1-n}}$$

Equation 6b

The $SNR_{standard}$ is a value determined by physicians based on what they describe as minimal image quality. This can be expressed as function of body size:

$$SNR_{standard} = SNR_{liver}(X) = (D_A)^{1-n} \times F(X)^{1-n}$$

Equation 7

So, for example, if the physician considers a scan of a 86 kg patient (b) with the current dosing formula the minimum image quality that should be attained in patients of any body size, we can consider the following: $X = W$; $W = b = 86$; $D_A = D_T = a \times W = a \times b$.

In this case, we have: $SNR_{standard} = (a \times b)^{1-n} \times F(X)^{1-n}$.

Replacing equations 1, 5a, 5b and 5c, results in:

Linear:

$$D'_T(X) = a \times b \times \left(\frac{r_{1,W} \times b + r_{2,W}}{r_{1,X} \times X + r_{2,X}} \right)^{\frac{1}{1-n}}$$

Equation 8a

Power:

$$D'_T(X) = a \times b \times (r_{2,W})^{\frac{1}{1-n}} \times b^{\frac{r_1}{1-n}} \times (r_{2,X})^{-\frac{1}{1-n}} \times X^{-\frac{r_1}{1-n}}$$

Equation 8b

Exponential:

$$D'_T(X) = a \times b \times (r_{2,W})^{\frac{1}{1-n}} \times e^{\frac{r_1}{1-n} \times b} \times (r_{2,X})^{-\frac{1}{1-n}} \times e^{-\frac{r_1}{1-n} \times X}$$

Equation 8c

These three equations can be simplified to:

Linear:

$$D'_T(X) = C_1 \times \left(\frac{C_2}{r_{1,X} \times X + r_{2,X}} \right)^{\frac{1}{1-n}}$$

Equation 9a

With $C_1 = a \times b$ \wedge $C_2 = r_{1,W} \times b + r_{2,W}$

Power:

$$D'_T(X) = C_3 \times X^{C_4}$$

Equation 9b

$$\text{With } C_3 = a \times b \times (r_{2,w})^{\frac{1}{1-n}} \times b^{\frac{r_1}{1-n}} \times (r_{2,X})^{\frac{1}{1-n}} \wedge C_4 = -\frac{r_1}{1-n}$$

Exponential:

$$D'_T(X) = C_5 \times e^{C_6 \times X}$$

Equation 9c

$$\text{With } C_5 = a \times b \times (r_{2,w})^{\frac{1}{1-n}} \times e^{\frac{r_1 \times b}{1-n}} \times (r_{2,X})^{\frac{1}{1-n}} \wedge C_6 = -\frac{r_1}{1-n}$$

In order to check if the Poisson assumptions were correct, a Ge-68/Ga-68 cylindrical phantom (V=8407 mL, Activity Concentration = 5,768 Bq/mL at time of acquisition) was scanned for 60 minutes in listmode together with a CT-LD using clinical settings. This data was histogrammed for different time intervals, from 5 seconds up to 3600 seconds, to represent different activity concentrations. Based on the total amount of Ga-68 events (decays/mL) occurring during these timeframes, the corresponding activity concentration of F-18 (Bq/mL) was computed for a hypothetical scan of 4 minutes acquiring the same amount of F-18 events.

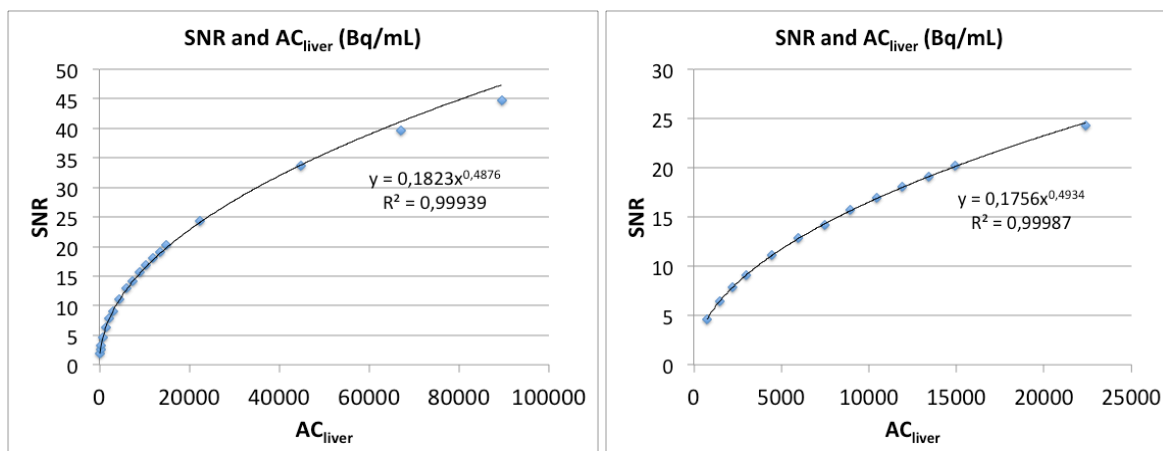
From previous scans, we have acknowledged that the mean liver SUV's vary from 1.4 to 5.6 g/mL (mean 2.6) with an injected dose of 1.6MBq/Kg. This means that a liver has an activity concentration from 2.2 to 9.0KBq/mL (mean 4.1).

For the range of extreme low dosing (around 0.5MBq/Kg) and extreme high dosing (around 4MBq/Kg), this would lead to an activity concentration of the liver between 0.7kBq/mL and 22.5kBq/mL, corresponding to a number of G-68 decays acquired during a time-frame between 30 and 900 seconds. From this, $n \approx 0,488$ (all data, 95%-CI: [0,482-0,494]) and $1-n \approx 0,493$, resulting in $n \approx 0,507$ (within the range of 30-900s, 95%-CI: [0,485-0,501]) so the Poisson relation assumption is nearly correct.

The effects of weight and injected dose in the liver's Signal-to-Noise Ratio in patients submitted to PET/CT scans

Frاملength (s)	Total Ga-68 (decays/mL)	Similar F-18 AC (Bq/mL)	SNR
5	28841	124	1,9
10	57681	249	2,6
15	86522	373	3,2
30	173044	746	4,6
60	346088	1491	6,4
90	519132	2237	7,9
120	692175	2983	9,1
180	1038262	4474	11,1
240	1384348	5965	12,9
300	1730433	7457	14,2
360	2076518	8948	15,7
420	2422602	10439	16,9
480	2768686	11931	18,1
540	3114769	13422	19,1
600	3460851	14913	20,2
900	5191254	22370	24,3
1800	10382369	44739	33,6
2700	15573346	67107	39,7
3600	20764185	89475	44,7

Table 2 - Relation between liver's AC and SNR based on measurements on a Ga-86/Ge-68 phantom



Graphs 7 - Relation between SNR and AC_{liver} from 5 to 3600s and 30 to 900s respectively

Based on the 65 analysed patients (with the median being 86 kg in a range between 39 and 125 kg), the injected dose was 1,62MBq/kg ($R^2=0,96$). The different correlation coefficient for the relation between SNR^*_{liver} and X are:

	Clinical Reconstruction			EANM Reconstruction		
Linear	r_1	r_2	R^2	r_1	r_2	R^2
X=W	-0,008	1,241	0,774	-0,017	2,654	0,724
X=BMI	-0,025	1,264	0,621	-0,053	2,671	0,555
Power	r_1	r_2	R^2	r_1	r_2	R^2
X=W	-0,932	34,126	0,777	-0,967	83,137	0,726
X=BMI	-1,020	15,957	0,639	-1,031	34,587	0,566
Exponential	r_1	r_2	R^2	r_1	r_2	R^2
X=W	-0,013	1,620	0,790	-0,013	3,549	0,749
X=BMI	-0,040	1,669	0,626	-0,041	3,532	0,555

Table 3 - Regressors (r_1 and r_2) and fit quality (R^2) between SNR^*_{liver} and different measures of body size (W and BMI)

From the table above, we can see that $r_1 < 0$ and the highest correlations (R^2) were reached for weight as measure for body size (X=W), therefore BMI was not considered any further. There is only a slight preference for exponential regression over power and linear regression. For X=W we have the following:

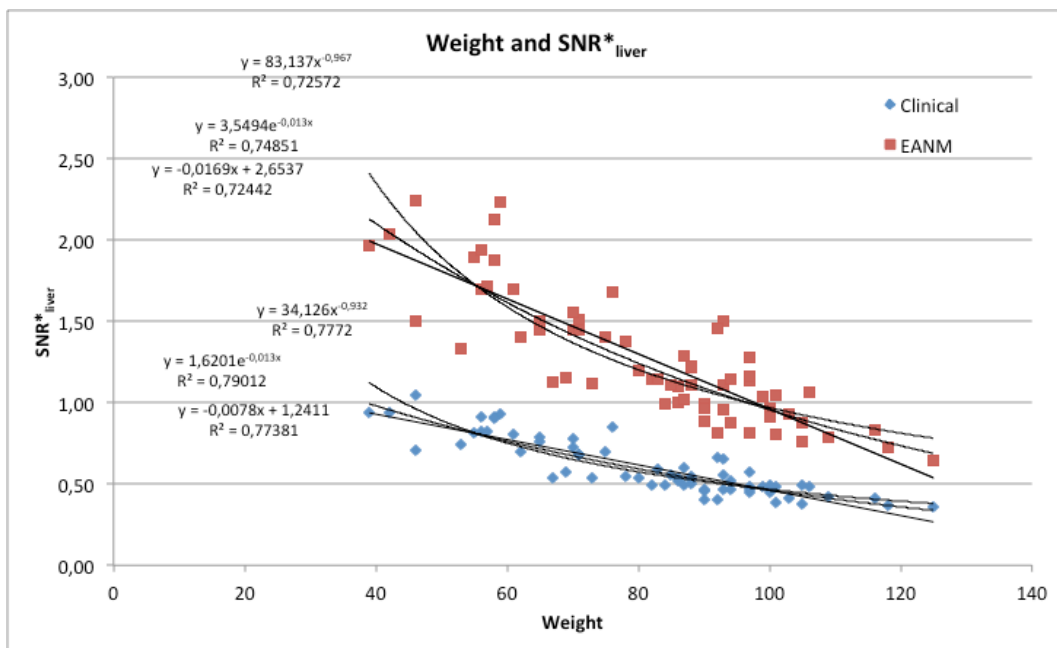


Illustration 16 - Relation between weight and SNR^*_{liver} in Clinical and EANM reconstructions

The SNR is clearly higher in the EANM reconstructions, due to the different parameters resulting in lower noise levels. A linear relationship is unlikely since it will reach negative values, which is not possible. For both the power and exponential regression, negative values will not be reached.

Therefore, linear equation was not considered and equations 9b and 9c, using $X=W$ will take the following form:

$$D'_T(X) = C_3 \times W^{C_4}$$

Equation 10b

$$\text{With } C_3 = a \times b \times \left(\frac{r_1+1}{1-n}\right) \wedge C_4 = -\frac{r_1}{1-n}$$

$$D'_T(X) = C_5 \times e^{C_6 \times W}$$

Equation 10c

$$\text{With } C_5 = a \times b \times e^{\left(\frac{r_1 \times b}{1-n}\right)} \wedge C_6 = -\frac{r_1}{1-n}$$

For the hypothetical case based on clinical image reconstruction with $X=W$, $a=1,6$ MBq/kg and $b=86$ kg (median bodyweight), we can derive the following new dosing formulas:

Power

$$D'_T(W)[MBq] = 0,0305 \times W[kg]^{1,889}$$

$$SNR_{liver}^* = 0,537$$

$$SNR_{standard} = 6,1$$

Equation 11b

Exponential:

$$D'_T(W)[MBq] = 15,41 \times e^{0,02546 \times W[kg]}$$

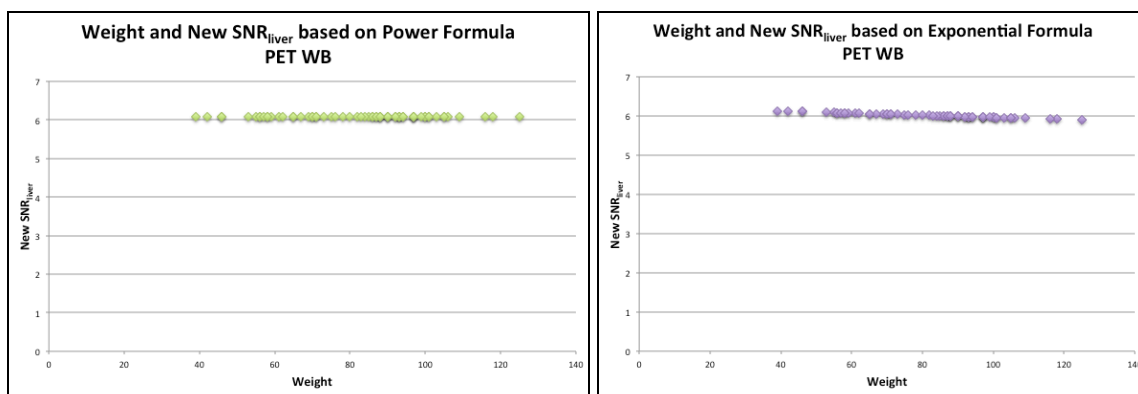
$$SNR_{liver}^* = 0,550$$

$$SNR_{standard} = 6,2$$

Equation 11c

Therefore, in order to have a bodyweight independent SNR_{liver} of 6,1-6,2, corresponding to a scan of a 86 kg with the current dosing formula, the new dose to be administered should be according to equation 11b or 11c.

Now that we have a new formula to calculate the dose of FDG to be injected, we can simulate how this new dose will affect the SNR. Using Equations 4, 6a, 11b and 11c we can obtain these values. After inserting the equations in Excel, we got the results of the new dose ($D'_T(X)$), the SNR_{liver}^* and the new SNR in the liver ($SNR_{standard}$). Now, we can see if there's a different behaviour regarding these new values.

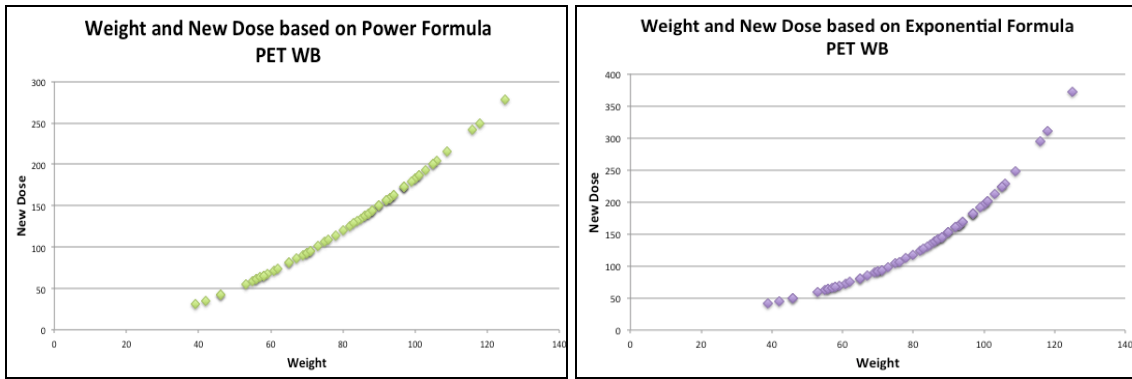


Graphs 8 - Relation between weight and New SNR_{liver} based on Power and Exponential Formula

Comparing these graphs with graphs 5, we can see a big difference now. While on graphs 5, the SNR would decrease as the weight increases, here we have a different behaviour. While with the old dosing formula, there was a big decrease in SNR, here we have a constant value, maintaining an acceptable one (around 6.1 in power formula and 6 in exponential). Between both formulas, the difference is not that big and the SNR is a matter of decimals only, not resulting in a very different image quality.

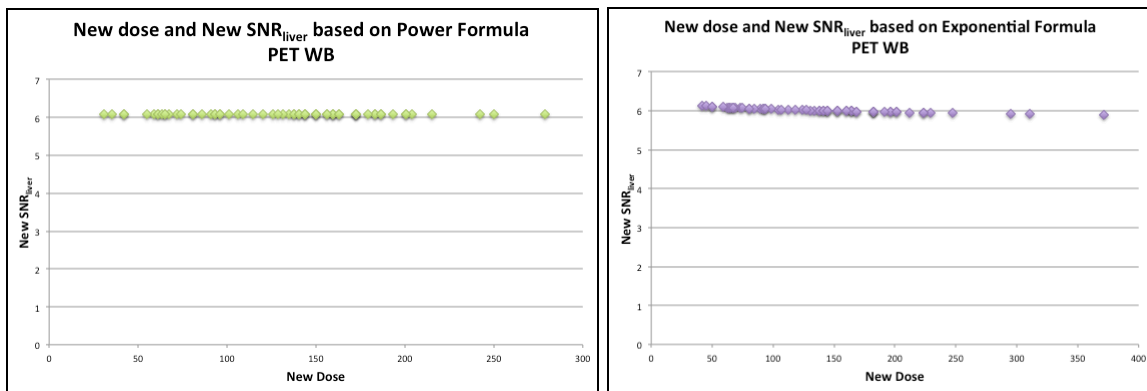
The relation between weight and the SNR based on the new dose is somewhat negative. Analysing the regression lines ($y = -6^{-0,5x} + 6,0927$ for power and $y = -0,0027x + 6,2352$ for exponential), both of them state that there is a decrease in SNR per kg of weight. However, due to both values, this decrease is extremely low and almost irrelevant.

The effects of weight and injected dose in the liver's Signal-to-Noise Ratio in patients submitted to PET/CT scans



Graphs 9 - Relation between Weight and New Dose based on Power and Exponential Formula

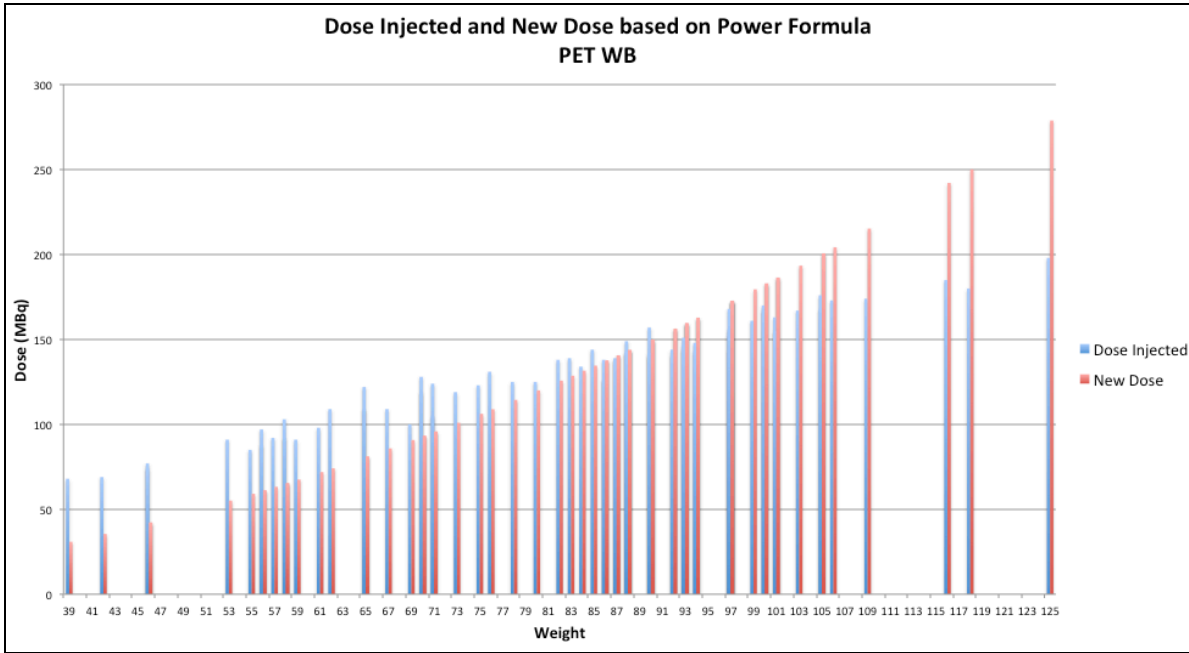
Comparing graphs 9 to graphs 1, we can see now that as the weight increases, the new dose increases exponentially instead of linearly. This means that lighter patients will receive less FDG dose and the heavier patients will receive more dose than with the previous dosage formula. This will achieve a more constant SNR instead of a decreasing one.



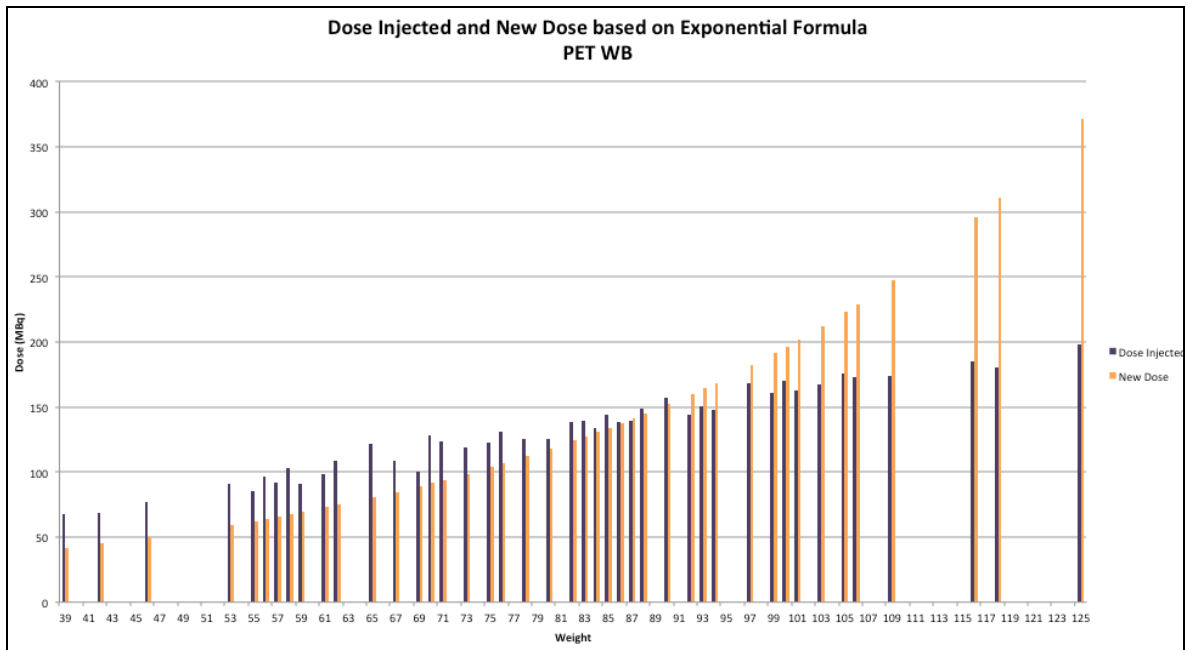
Graphs 10 - Relation between new Dose and New SNR_{liver} based on Power and Exponential Formula

Comparing graphs 10 to graphs 3, there's clearly a difference with this new formula. The SNR now maintains a constant value. Whereas in graphs 3 the SNR would decrease from around 9 to 4, in this case maintains a SNR value of around 6, in both formulas.

We only presented both formulas in clinical reconstructions and not in EANM reconstructions because the behaviour would be exactly the same, only the SNR would be higher due to less noisier values.



Graphic 11 - Relation between the dose injected and the new dose based on Power Formula



Graphic 12 - Relation between the dose injected and the new dose based on Exponential Formula

In these graphs, we can see that as the weight increases, the dose increased, whether was calculated with the current formula or with the new ones. However, for patients lighter than 86 kg, the dose injected is higher than the new dosing regimens with a significant difference. For patients heavier than 86kg (the reference mass b), we can see that the new doses are increasing exponentially. In the following table, we can see the different total quantity of FDG needed in our population using the new dosing formula compared to the current one and the total effective dose in adults (based on the value of 0,019 mSv/MBq):

Type of formula	Total Injected Dose (MBq)	Total New Doses (MBq)	Difference	Total effective doses in adults (mSv/MBq)
Power	8618	8531	-87	162,089
Exponential	8618	9047	429	171,893

Table 4 - Difference between injected doses, new doses and total effective doses

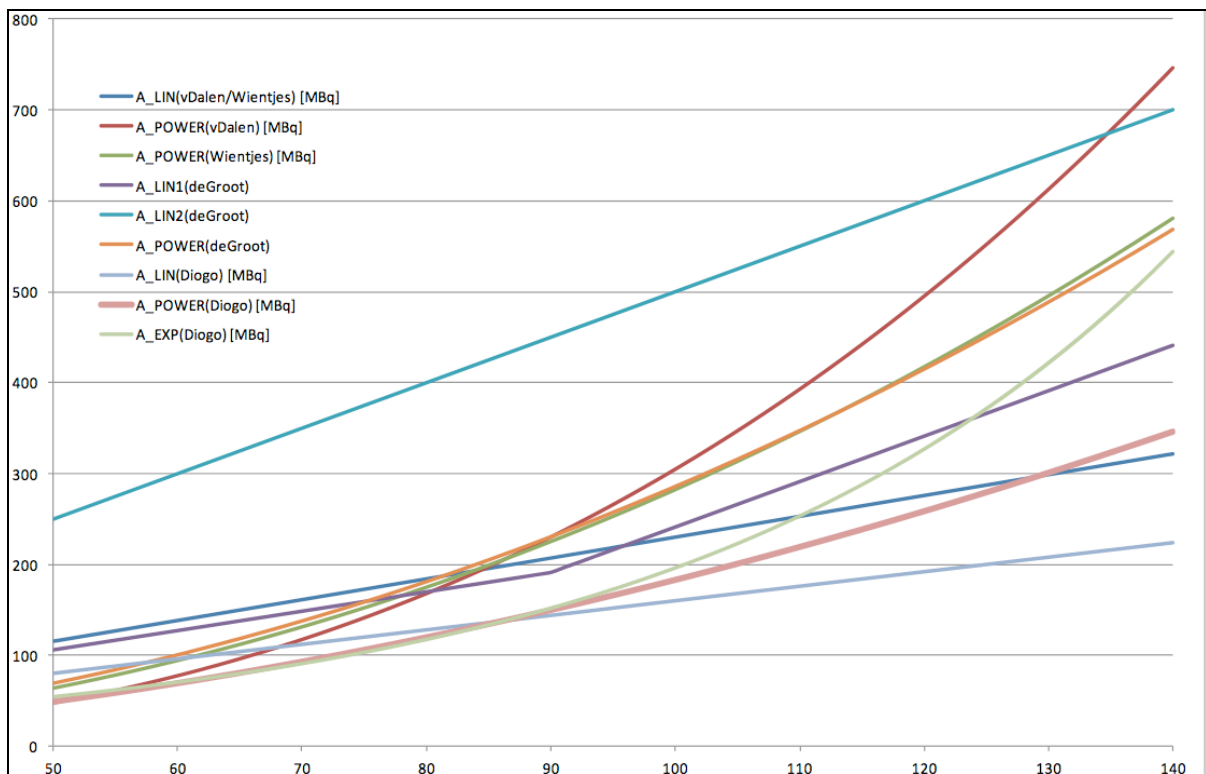
With these results, it's possible to say that using the power formula, we would need less FDG to get a weight-independent SNR. But using the exponential formula, we would use more FDG as it is given with the current formula but still get a weight-independent SNR for all patients. However, the total injected dose is different from the calibrated dose, so this value might be less than it actually is.

Using the same method as we did, vDalen et al [5], Wientjes et al [20] and de Groot et al [21], used a similar research and found the following:

	vDalen et al.	Wientjes et al.	De Groot et al.	This project
Linear dosing:	$D_T = 2,3 \times W$	$D_T = 2,3 \times W$	$D_T = 5 \times W$ $< 90Kg$ $D_T = 2,13 \times W$ $> 90Kg$ $D_T = 191,7 + 5(W - 90)$	$D_T = 1,6 \times W$
Standard SNR:	6	7,8 (75Kg patient, 4 min/bp)	9,58	6,1 (86Kg patient)
New Dose (MBq):	$1,46 \times 10^{-3} \times W^{2,66}$	$\frac{3,6 \times 10^{-3}}{2,5 \times W^{2,146}}$	$0,023 \times W^{2,047}$	$0,0305 \times W[kg]^{1,889}$ $15,41 \times e^{0,02546 \times W[kg]}$

Table 5 - Equations for non-linear dosing according to several references

Graphically, looks like this:



Graphic 13 - Equations for dosing schemes according to different references

With all this considered, we should ask ourselves what is the ideal reference mass. For image quality, the lowest reference mass will be best (as lighter patients give better images). From a radiation point of view, a higher reference mass will be best [as all patients with a weight below the reference mass will get less FDG and all patients heavier will get (exponentially) more FDG] [22,23]. The latter is also the case from a financial point of view. The question therefore should be towards an acceptable SNR. This question can only be answered by nuclear medicine physicians. As an example, the following PET WB reconstructions are presented showing 5 extremes of SNR (highest SNR, 70kg patient, 86kg patient, 100kg patient, lowest SNR):

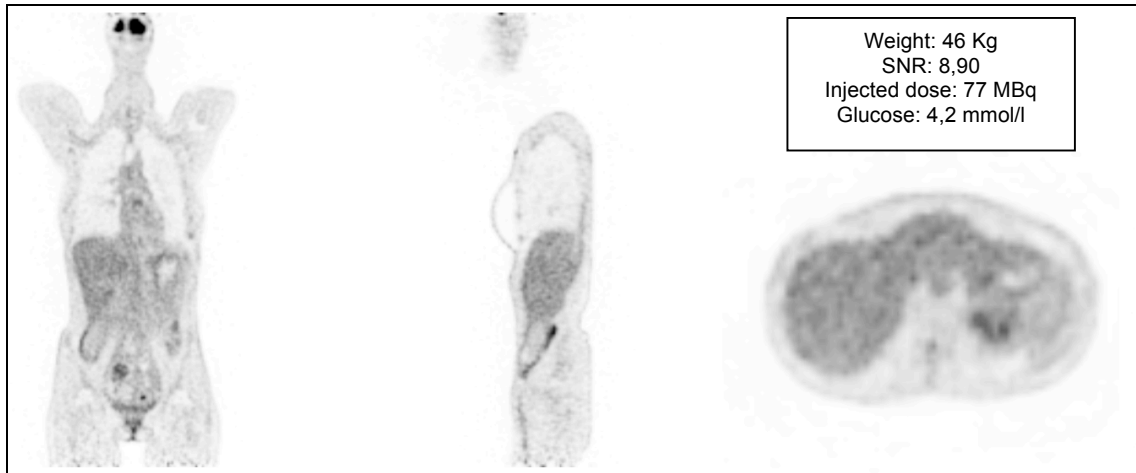


Illustration 17 - The highest SNR

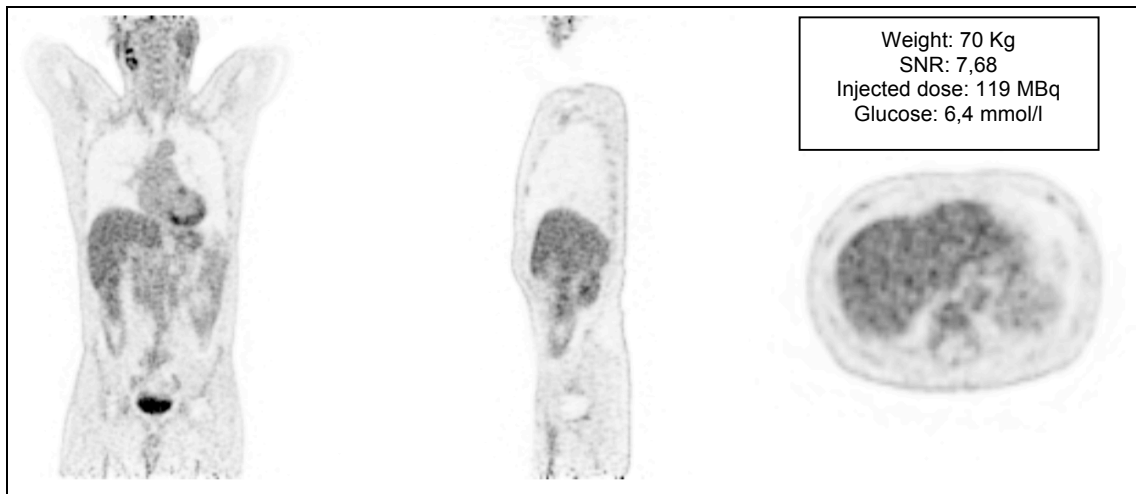


Illustration 18 - SNR of a 70 Kg Patient

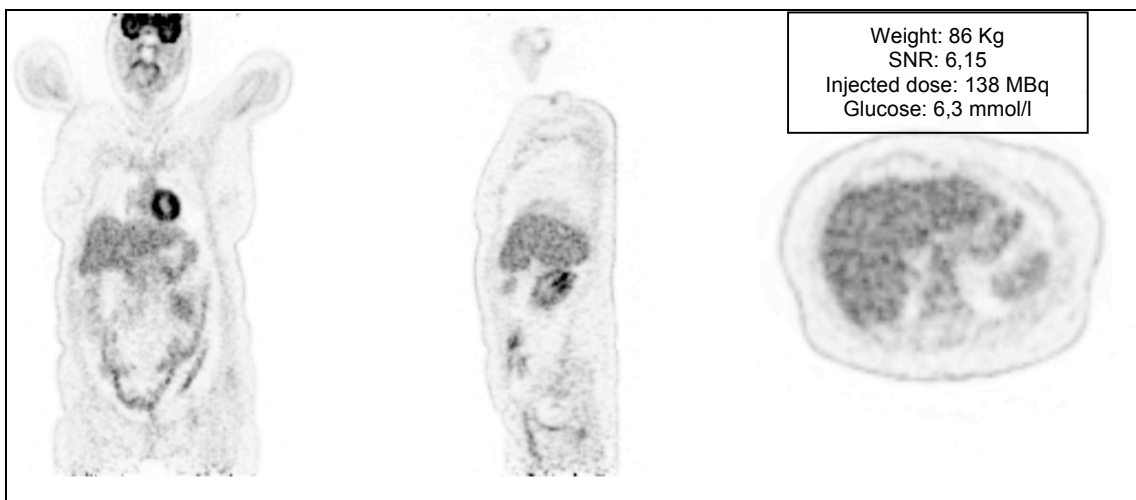


Illustration 19 - SNR of an 86 Kg Patient

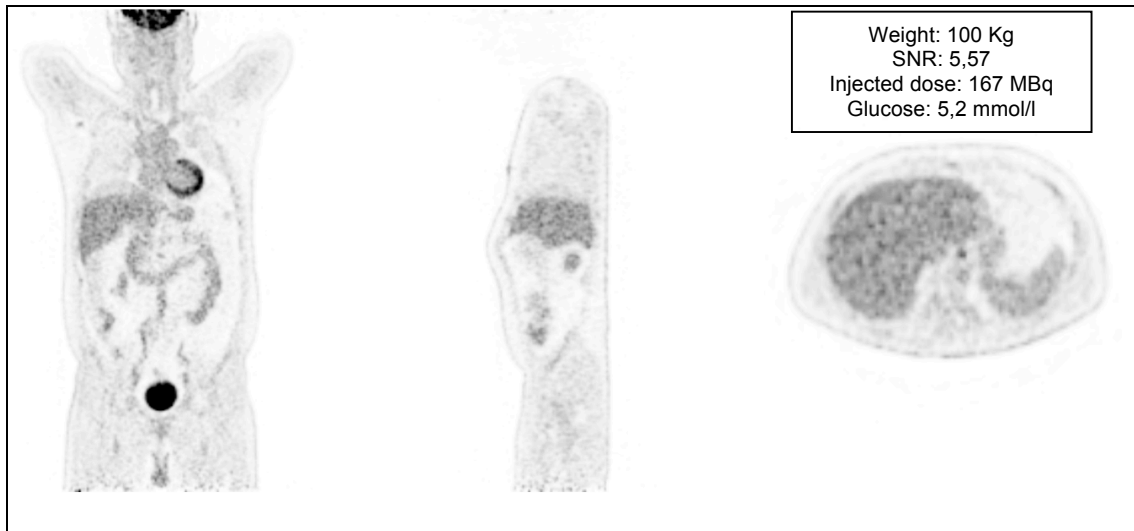


Illustration 20 - SNR of an 86 Kg Patient

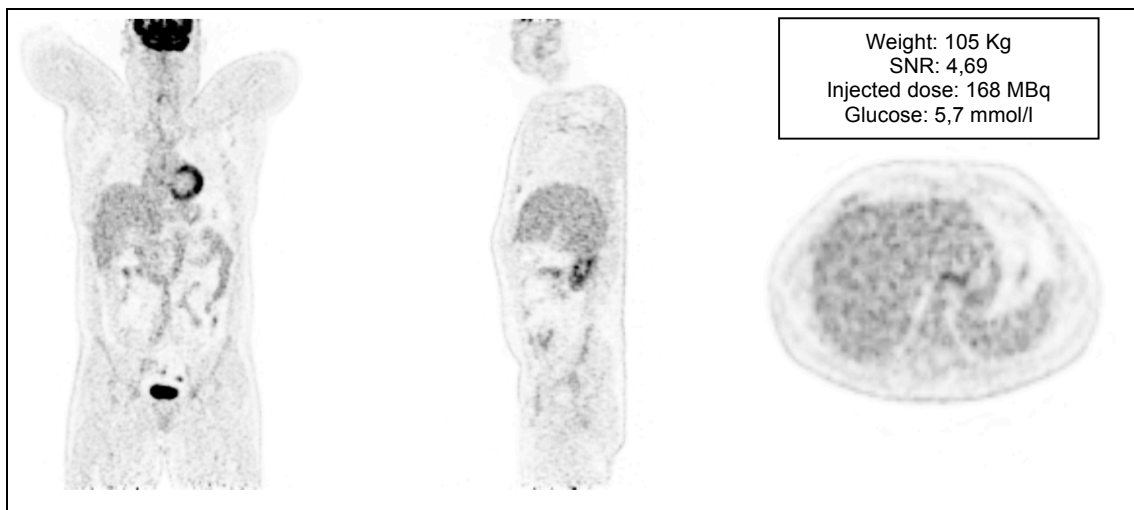


Illustration 21 - The lowest SNR

So, as we can see in these illustrations, between the highest and the lowest SNR, there is a clear difference in image quality, best seen in the liver. With the current formula used to calculate the necessary dose, it's clear that as the weight increases, the SNR decreases and that affects the image. Therefore, we built new formulas to give us a weight-independent SNR of a 86 kg reference patient. We can see here that Illustration 18 gives us the highest SNR of all three references and Illustration 20 gives us the lowest one. However, in order to maintain the SNR of a 70 kg patient (SNR around 7,6) for all patients, a lot more of FDG would have to be ordered and heavier patients would receive even more FDG. Since the median of our population was 86 kg, the SNR of a patient with that weight is acceptable and

better than the one obtained currently in heavier patients. If the median is used, half of the patients would receive less FDG and the other half would receive more.

With all this considered, the SNR of a 86 kg patient seems to be the most possible and acceptable one, taking in consideration new image quality (good quality), new costs (hardly changed), new doses (acceptable even for overweight patients) and new radiation burden.

We found a negative relation between image quality and bodyweight even though heavier patients received more FDG. Based on Poissonian (and confirmed with a phantom) we suggested new dosing schemes that should give a weight-independent SNR with good image quality and with no additional costs or radiation burden to the whole group. However, this should be prospectively validated next.

This study had some limitations. To evaluate the image quality, only the SNR in the liver was used and it didn't take in consideration the soft-tissue contrast. However, the primary objective of this study was to see the effects of the weight in the SNR of the liver and not the image quality as a whole. The use of five consecutive ROI's in a lot of different patients can vary due to the anatomy of each one. For example, the size of the liver might affect the localization of the five ROI's. As a marker of noise, the standard deviation might not be enough, although it's used in several studies related to clinical imaging. Noise is described as the extent of the variation in radioactivity in an image of uniform uptake. But there are several factors that can contribute to the image noise [7]. Another type is the structured noise which is generated from the process of reconstruction. There weren't a lot of patients heavier than 110 kg, which restrained a little bit the results on much heavier patients. All the calculations were based on theory and a few assumptions and weren't put in practice, even though the predictions are very promising since the assumption of Poissonian relation might not be correct in a corrected PET image. However, according to other studies [18], the assumption of Poissonian in this case should be correct, therefore making reliable results. In Table 4, the differences between the doses were based on the injected one and not the calibrated one. This may give us different results, since the total dose that was bought should be higher than those values presented. In the same table, total effective dose was also calculated; however, it was based on the value of 0,019 mSv/MBq (which is for a 70 kg healthy adult) but since the weight increases, the absorbed doses will also increase, therefore the results might be different [10,22]. Giving the FDG dose based on a different formula might not be the only option to obtain a constant SNR. Performing longer scans might increase the SNR of heavier patients compared to now since the PET image is based only on true coincidence detection (random, scattered photons are removed from the image) [5,7,8]. Doubling the dose will double the total counts derived from patients, but the number of randoms will also go up by a factor of 4. So, the net counts used to reconstruct an image

The effects of weight and injected dose in the liver's Signal-to-Noise Ratio in patients submitted to PET/CT scans

will not go up exactly by a factor of 2 and in very high doses of FDG it might even go down. This will not happen if the patient is scanned longer, since scanning twice as long will leave us with twice as much total counts but also with twice as much randoms and scatter, therefore the net counts used to reconstruct an image will double. It might be better to scan longer than to increase FDG dose but it is hard to model since we should know the count rate statistics of each scan [5,7,8]. Also, due to the planning system and logistics, this is not done in the department. Another factor against longer scans is the patient's movement, since adding more time to the scan, the probability of him moving is higher.

Conclusion

With the findings of this study, it's safe to assume that the weight has an important role in the quality of the PET/CT image using the current formula. The more heavy the patient is, the less SNR the image will have even when FDG doses are (linearly) adapted to patient weight. This was also true for BMI, which takes in consideration height as well. Adjusting techniques in some parameters, like attenuation correction or others to reduce random and scatter noise, might be helpful in overweight patients but isn't the solution. It is important to know that adjusting these kind of parameters may give an image which seems smoother and with a bigger SNR but the lesion detection might be reduced. Also, every nuclear medicine department has their own protocols and logistics, so it might not be desirable to make changes in the protocols, like scanning longer for every patient. With this considered, two new formulas to calculate the FDG dose to give to the patient were proposed. These new ways to calculate the dose gives, theoretically, a weight-independent SNR for every patient based on the SNR of a 86 kg reference mass patient. With the given equations, we can replace the values with the ones from a patient with a SNR we want and have that for everyone. But, having the SNR of a 70 kg patient might not be very helpful because, even though the SNR is quite good, the dosage would be very high and that implies more costs and more radiation burden for all patients. So, with the patients of this study with a distribution of weight between 39 and 125 kg, the median was 86 kg. This means that half of the patients will have less dose and the other half will have more and gives us an acceptable SNR for every patient.

So, in conclusion, patient's weight is an important factor in these procedures, since it affects the SNR of the liver. Proceeding with the new given formulas, replacing W with the patient's weight, it will give the new dose to be injected which will give, theoretically, a constant SNR, with the weight not being a factor anymore in patient's SNR.

References

1. Zaidi H. Optimisation of whole-body PET/CT scanning protocols. *Biomedical imaging and intervention journal* [Internet]. 2007 [cited 2013 Mar 6];3:1–9. Available from: <http://www.pubmedcentral.nih.gov/articlerender.fcgi?artid=3097669&tool=pmcentrez&rendertype=abstract>
2. Hogg P, Testanera G. *Principles and Practice of PET/CT Part 1: A Technologist's Guide*. European Association of Nuclear Medicine. 2010;
3. Van den Broek WJM, Testanera G. *Principles and Practice of PET/CT Part 2: A Technologist's Guide*. European Association of Nuclear Medicine. 2010;
4. Imaging S of NM and M. What Is PET ?
5. Van Dalen DJA, Mulder DH, de Bruin DW, Zuidwijk DMD, V. Subramaniam PD. Optimizing administered FDG dose for PET imaging. *Tijdschr Nuclear Geneeskunde*. 2010;32:339–43.
6. Nagaki A, Onoguchi M, Matsutomo N. CT tube current for attenuation map in a combined PET/CT system: obese patient simulated phantom study. *The Japanese Society of Nuclear Medicine - Annals of nuclear medicine* [Internet]. 2012 [cited 2013 Mar 6];26:359–64. Available from: <http://www.ncbi.nlm.nih.gov/pubmed/22359224>
7. Masuda Y, Kondo C, Matsuo Y, Uetani M, Kusakabe K. Comparison of imaging protocols for 18F-FDG PET/CT in overweight patients: optimizing scan duration versus administered dose. *Journal of nuclear medicine : official publication, Society of Nuclear Medicine* [Internet]. 2009 [cited 2013 Mar 6];50:844–8. Available from: <http://www.ncbi.nlm.nih.gov/pubmed/19443586>
8. Halpern BS, Dahlbom M, Auerbach M a, Schiepers C, Fueger BJ, Weber W a, et al. Optimizing imaging protocols for overweight and obese patients: a lutetium orthosilicate PET/CT study. *Journal of nuclear medicine : official publication, Society of Nuclear Medicine* [Internet]. 2005;46:603–7. Available from: <http://www.ncbi.nlm.nih.gov/pubmed/15809482>
9. Nagaki A, Onoguchi M, Matsutomo N. Patient weight-based acquisition protocols to optimize (18)F-FDG PET/CT image quality. *Journal of nuclear medicine technology* [Internet]. 2011 [cited 2013 Mar 6];39:72–6. Available from: <http://www.ncbi.nlm.nih.gov/pubmed/21565951>
10. Boellaard R, O'Doherty MJ, Weber W a, Mottaghy FM, Lonsdale MN, Stroobants SG, et al. FDG PET and PET/CT: EANM procedure guidelines for tumour PET imaging: version 1.0. *European journal of nuclear medicine and molecular imaging* [Internet]. 2010 [cited 2013 Feb 28];37:181–200. Available from: <http://www.pubmedcentral.nih.gov/articlerender.fcgi?artid=2791475&tool=pmcentrez&rendertype=abstract>
11. Fanti S, Farsad M, Mansi L. *Atlas of PET-CT. A Quick Guide to Image Interpretation*. Softcover. Springer, editor. Springer; 2009. page Chapter 1 p. 1–23.

12. Saha GB. Basics of PET Imaging. Springer; 2005.
13. PhD, Dominique Delbeke M, Center VUM. Physiological Variations of FDG Distribution and Pitfalls of Interpretation of PET-CT. VUMC PET Conference. 2009.
14. Centers for Disease Control and Prevention. BMI - Body Mass Index. 2011.
15. Chang T, Chang G, Kohlmyer S, Clark JW, Rohren E, Mawlawi OR. Effects of injected dose, BMI and scanner type on NECR and image noise in PET imaging. *Physics in medicine and biology* [Internet]. 2011 [cited 2013 Mar 6];56:5275–85. Available from: <http://www.ncbi.nlm.nih.gov/pubmed/21791730>
16. Organization WH. Physical Status: The use and interpretation of anthropometry. WHO Technical Report Series. 1995.
17. Boellaard R, Oyen WJG, Hoekstra CJ, Hoekstra OS, Visser EP, Willemsen AT, et al. The Netherlands protocol for standardisation and quantification of FDG whole body PET studies in multi-centre trials. *European journal of nuclear medicine and molecular imaging* [Internet]. 2008 [cited 2013 Mar 6];35:2320–33. Available from: <http://www.ncbi.nlm.nih.gov/pubmed/18704407>
18. PhD MSR. The AAPM/RSNA Physics Tutorial for Residents Counting Statistics. *RadioGraphics*. 1999;19:765–82.
19. Lin C-Y, Ding H-J, Lin C-C, Chen C-C, Sun S-S, Kao C-H. Impact of age on FDG uptake in the liver on PET scan. *Clinical imaging* [Internet]. Elsevier Inc.; 2010 [cited 2013 Mar 6];34:348–50. Available from: <http://www.ncbi.nlm.nih.gov/pubmed/20813297>
20. Wientjes MSc R, Dickerscheid PhD D, Lavalaye PhD J, Habraken MS JBA. Body mass independent 18F-FDG PET image quality; implementation of a power law based dosage regime. *ijdschrift voor nucleaire geneeskunde*. 2013;
21. De Groot EH, Post N, Boellaard R, Wagenaar NR, Willemsen AT, van Dalen J a. Optimized dose regimen for whole-body FDG-PET imaging. *EJNMMI research* [Internet]. 2013 [cited 2013 Sep 16];3:63. Available from: <http://www.pubmedcentral.nih.gov/articlerender.fcgi?artid=3751692&tool=pmcentrez&endertype=abstract>
22. Muller SP, Beyer T, Brix G, Lechel U, Glatting G, Ziegler SI, et al. Radiation Exposure of Patients Undergoing Whole-Body Dual-Modality 18F-FDG PET/CT Examinations. *Journal of nuclear medicine : official publication, Society of Nuclear Medicine*. 2005;46:608–13.
23. ICRP. Radiation Dose to Patients from Radiopharmaceuticals. *Annals of the ICRP, ICRP Publication 106* [Internet]. 2008 [cited 2013 Mar 6];38:1–193. Available from: <http://linkinghub.elsevier.com/retrieve/pii/S0146645308000389>

Appendix

I. Research Plan

What to do:	When is scheduled to be completed:	Status
Collect patients	25 th January, 2013	Done
Collect theory background about PET/CT	22 nd – 23 rd November, 2012	Done
Collect theory background about FDG	22 nd – 23 rd November, 2012	Done
Translation of the PET/CT protocol	29 th November, 2012	Done
Write first sketches in the project with collected information	6 th December, 2012	Done
Collect studied information about FDG uptake on patients with different weights	7 th December, 2012	Done
Collect information about normal liver uptake	13 th December, 2012	Done
Analyse the various measurements tools available	20 th December, 2012	Done
Decide with one measurement tool and describe it	21 st December, 2012	Done
Add more data to the project with new collected information	11 th January, 2013	Done
Review all the information collected in the project	18 th January, 2013	Done
Decide how many patients to use and begin to analyse each one	8 th February, 2013	Done
With the help of Hermes, do a ROI on every patient and get SNR result	12 th February, 2013	Done
Make several graphs regarding the relation between weight, dose and liver's SNR	20 th February, 2013	Done
Analyse results and get to a conclusion	22 nd February, 2013	Done

With collected results, describe my analysis in the project	25 th February, 2013	Done
Analyse result and reflect about if there is a direct relation between dose, SNR and weight	25 th February, 2013	Done
Write about limitations found in the research	26 th February, 2013	Done
Meet with Dennis Vriens and discuss possible ways to calculate a new formula	25 th February to 29 th February, 2013	Done
Calculate new dose, new SNR and analyse graphs	27 th February, 2013	Done
Write and present a first draft of the project	1 st March, 2013	Done
Write and present a second draft of the project	6 th March, 2013	Done
Write and present the final project	14 th March, 2013	Done

II. PET/CT Standard Protocol

Principle:

FDG is accumulated in tissues with a high degree of glycolysis. This mainly concerns neoplastic tissues and from lesions with a high concentration of inflammatory cells, such as activated macrophages and granulocytes. FDG goes to the cell membrane in the same way as glucose and both are phosphorylated in the cell. The remaining molecule (FDG-6-Phosphate) differs from glucose-6-phosphate to a point that the next enzymes used in glycolysis have no more effect. The FDG-6-Phosphate gets trapped intracellularly as it can't enter glycolysis unlike glucose, while this one continues with the glycolysis. The desphosphorylation of FDG is slow and within the acquisition time of a PET/CT scan, it remains present in the cell.

Tumour cells are highly dependent for their energy from glycolysis. Since glycolysis ATP provides less than the normal tumour cycle, this means that tumour cells, in contrast to normal ones, have a bigger uptake, therefore they also need uptake from FDG. FDG uptake in activated white blood cells ((18)F-FDG-WBCs) is increased making infections and acute or chronic inflammations visible.

Indication:

- Suspicion or presence of malignancy or infection.

Contraindications:

- Pregnancy;
- Severe claustrophobia.

Required material:

- Radiopharmaceutical: F-18 fluodeoxyglucose;
- Nuclide: Fluor-18;
- Dosage: $((6.4 \times \text{body weight}) / (\text{number of min} / \text{BP})) \text{ MBq}$;
- Minimum dose in children: 20 MBq;
- Administration: Intravenous.

Material needed for the scan:

- Venflon/butterfly needle with three-way stopcock and 10 ml NaCl 0.9%;
- 10 mg furosemide;
- "Glucocard Memory 2", System 1 for glucose measurement;
- On indication: bladder catheter;
- On indication: diazepam (5 mg/tablet) or oxazepam (10 mg/tablet).

Information needed concerning the patient:

- Indication;
- Possible known tumour localizations;
- Nature of malignancy;
- Relevant patient history;

- Relevant results from other imaging studies (especially CT/MRI);
- Completed contrast checklist;
- Diabetes mellitus requiring medication (insulin/o.a.d.);
- Height and weight;
- Claustrophobia.

Method:

Administered radiopharmaceutical:

A nuclear medicine assistant injects the radiopharmaceutical intravenously.

Patient preparation:

- The patient should be fasting at least 6 hours before the start of the study and must not have had any kind of glucose;
- The patient should not have been administered with insulin or similar medication recently;
- Hydrate the patient prior to the examination with 500 ml of water orally or 500 ml of NaCl 0.9% intravenously;
- On the following cases, give the patient diazepam/oxazepam (with a dose recommended by the physician) 15 minutes prior to the administration of FDG:
 - PET-CT scan focused on head and neck, to prevent harmful accumulation of FDG in the cervical musculature and vocal cord region;
 - Claustrophobia;
 - Tension/anxiety.

Execution:

- Give the patient detailed explanation about the course of the investigation;
- Complete the acquisition form;
- Make an infusion system on the patient;
 - In case of a clinical patient that has an infusion of over 24 hours, a new infusion system should be applied. If the patient is very difficult to puncture than the infusion that he has must be checked with the physician if it's good enough to be used;
- Take blood through the infusion system to determine the glucose value with "Glucocard Memory2";
 - At values > 10 mmol/l consultation should follow with a nuclear medicine physician before proceeding with the investigation;
 - Record the value of the glucose in the acquisition form and the application;
- The nuclear medicine physician in training injects the furosemide and then the FDG (as a slow bolus) intravenously and flushes the entire system with 20 ml NaCl 0.9%;
- The patient should lay down approximately 60 minutes before starting the acquisitions;
 - Instruct the patient to lay as still as possible and avoid talking except when the patient needs to use the bathroom;
- Ask the patient prior to the start of the scan to urinate;
- Tell the patient to remove every metal objects in the FOV;
- Position the patient in the camera;
 - Adjust the table height so that the patient is exactly in the middle;
- Perform the requested scan acquisitions;
 - Standard whole body protocol is from subtrochanter to skull;
 - 6-8 bed positions depending on the length patient;
 - 4 minutes per bed position;

- Possibly adjust according to the indication;
 - 3 min / BP to scan when including legs;
 - 5 min / BP when low on activity;
- Select the right patient with the right investigation in the browser.
- Fill in the required fields:
 - Patient weight;
 - Protocol:
 - Specials → PETCT_LD_WB_UMC;
 - Specials → PETCT_LD_WB_XL_UMCN (for scan including legs).
 - Patient position;
- Choose Exam;
- You will enter the Examination tab;
 - Make sure Match FOV is checked in the box PET Planning;
- Perform an AP Topogram;
- Set the region of interest in the X-ray image;
 - Standard including groin and upper orbital;
- Select the low dose CT scan and check the selected mAs;
 - Ref. mAs: 50;
 - 120kV;
 - Change kV from 120 to 100 if patient weighs less than 70kg;
 - CARE Dose4D on;
- Fill in all the PET data;
 - Radiopharmaceutical dose;
 - Injection time;
- Select Load;
- Move the patient's bed to the PET's bed position;
- Select Start and note the start time on the acquisition form;
- When the investigation is done, choose End Study in the Examination tab;
- Close all tabs before you begin a new study;
 - Protocol → unload study;
- Make additional recordings on indication;
 - See CT protocols;
- Finally, remove the patient from the scan table.

Addition to standard version

Supplement performance scanning with legs:

- Extend ScanBed with additional extension on top of standard bed extension;
- Position the patient with arms down and select "Feet First";
- Select the acquisition protocol: PETCT_LD_WB_XL_UMCN;
 - PET: 1.5 min per bed position for legs and 3 minutes per bed position for the rest of the body;
 - On indication, the time per bed position can be changed.

Supplement head/neck Protocol:

- Position the patient with arms down in the scanner;
 - Use the special headrest and head positioning wedge;
 - Select the acquisition protocol: _PETCT_LD_WB_UMCN;
 - Set in 2 bed positions head to clavicles;
 - PET: 5 min per bed position;

The effects of weight and injected dose in the liver's Signal-to-Noise Ratio in patients submitted to PET/CT scans

- Scan the rest of the body according to PETCT_LD_WB_UMCN protocol;
 - From clavicles to the groin;
 - Patient's arms up.

Supplement performance in suspected presence of a malignancy in the pelvic area:

- Cervical carcinoma, endometrial carcinoma, chorionic carcinoma, bladder/ureters/renal pelvis carcinoma, among others;

Supplement execution with proven/suspected infection in heart/mediastinum, unexplained high fever or metastases infection research:

- High fever, metastases infections, endocarditis, pericarditis and cardiac sarcoidosis, among others;

Scanner and computer

Scanner:

- Siemens MCT PET;
 - UltraHD and TrueV (extended FOV);
 - 40 Spiral CT Adaptive 4D slices;

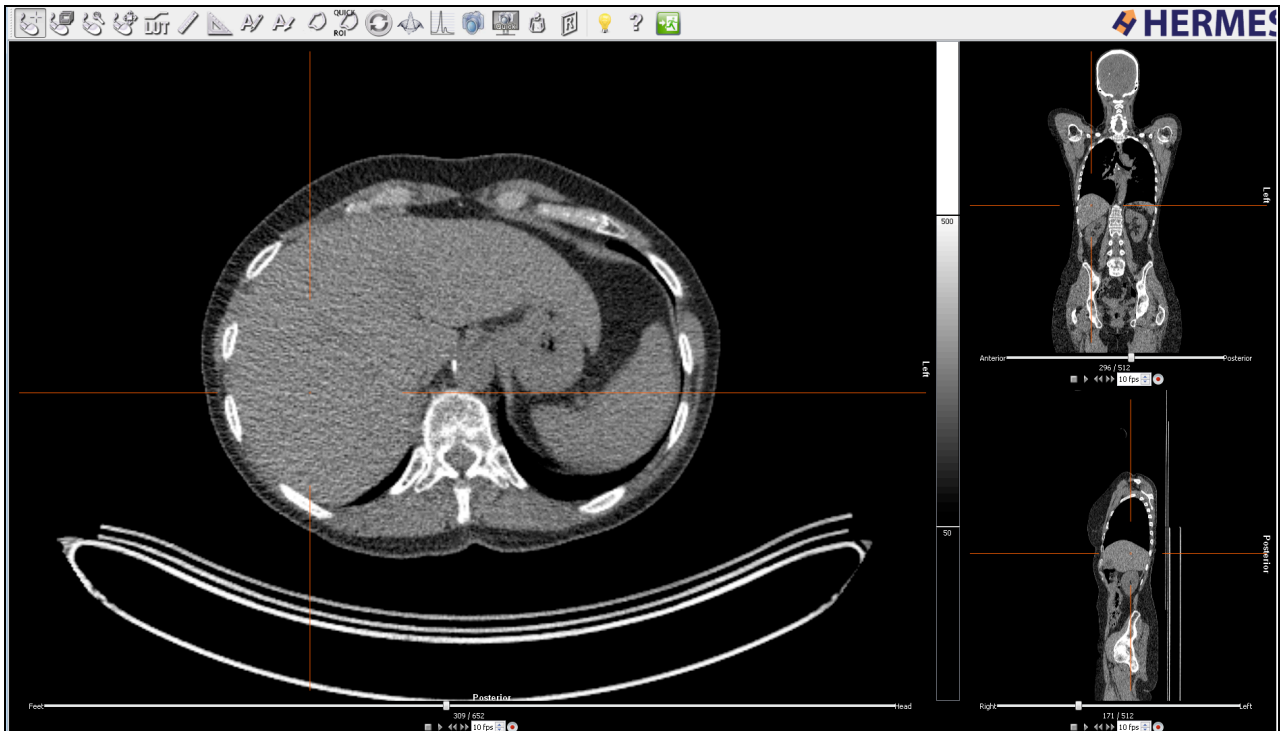
Acquisition:

- Predefined protocol;
 - Specials → PETCT_LD_WB_UMCN;
 - Specials → PETCT_LD_WB_XL_UMCN (including legs);

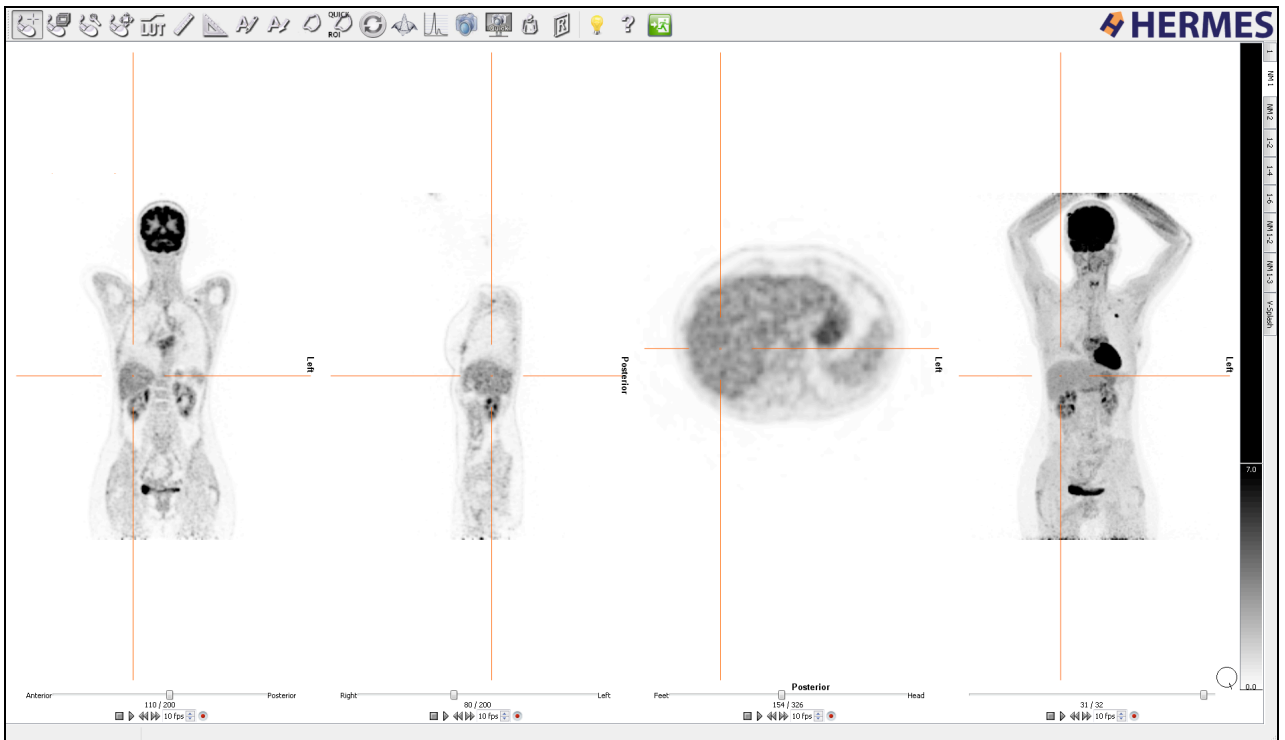
Processing

- Reconstruct PET/CT fused images using TrueD Siemens application;
- Go to the Local Database using the patient browser and select the correct patient;
- Send to "Hermes and Impax";
 - Patient Protocol;
 - PET WB;
 - PET WB UNCORRECTED;
 - PET WB NEDPAS;
 - Fused transaxial (only to IMPAX);
 - CT_3, 0_B31f;
- Put the following files offline;
 - AC_CT;
 - Low Dose CT 3.0 B31;
 - Topogram;
 - Select files in browser and direct off-line using Transfer → Export to offline
 - PET Raw Data, (= incl Normalisation);
 - Select files in browser, select all files under PET Raw Data than select off-line using Transfer → Export to offline.

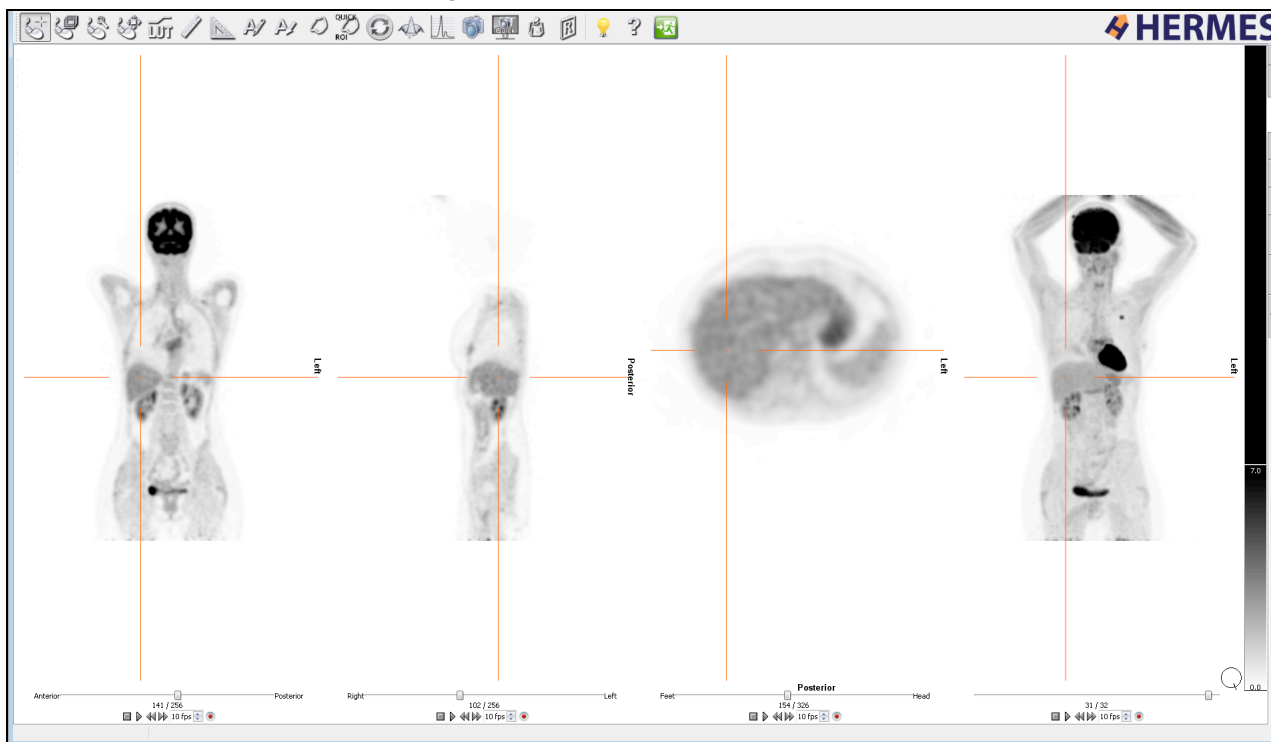
III. Positioning of the point in the CT scan



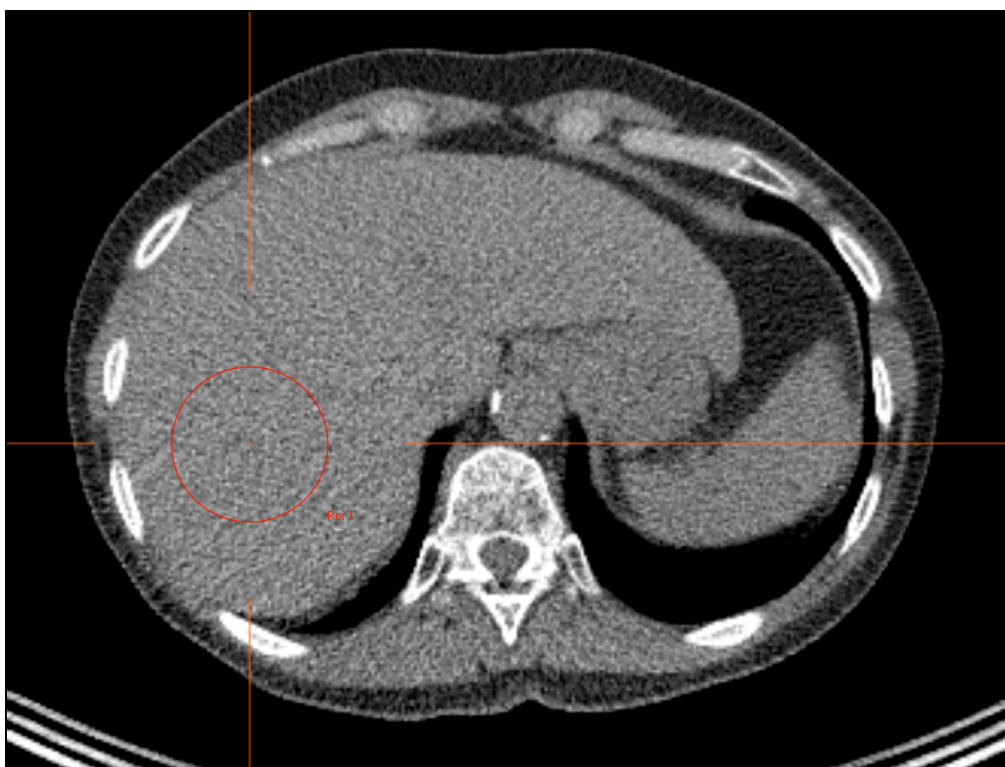
IV. Positioning of the point in the PET WB scan



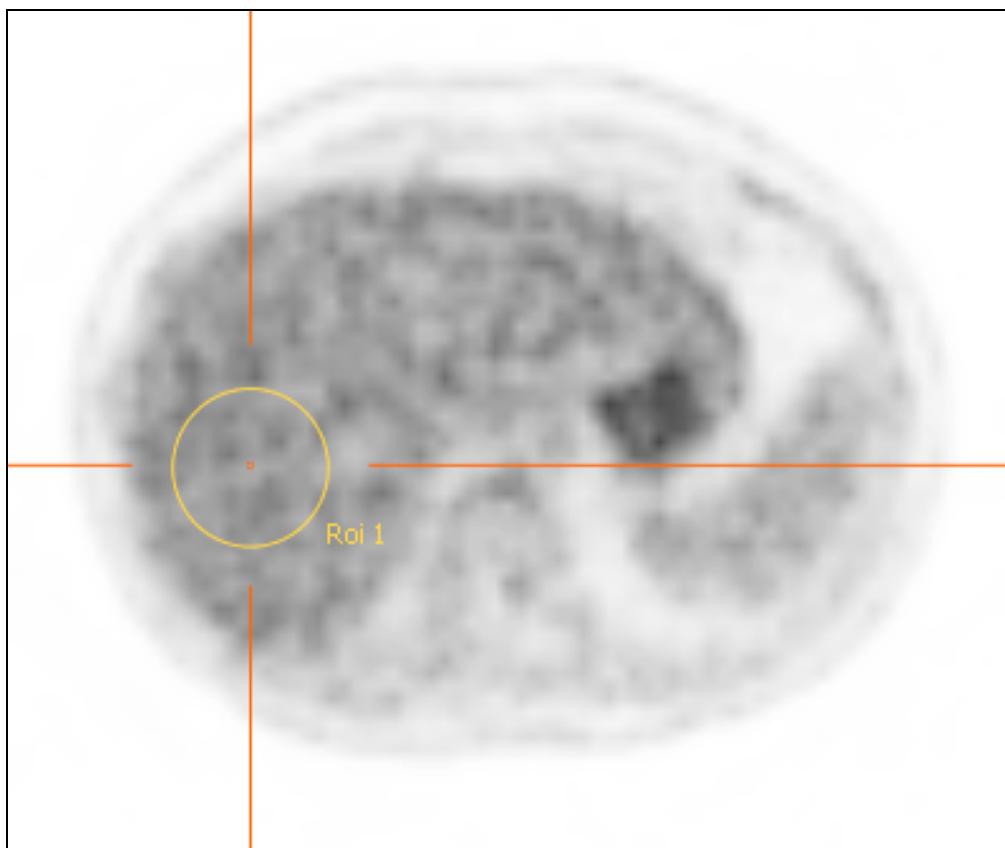
V. Positioning of the point in the PET WB EANM scan



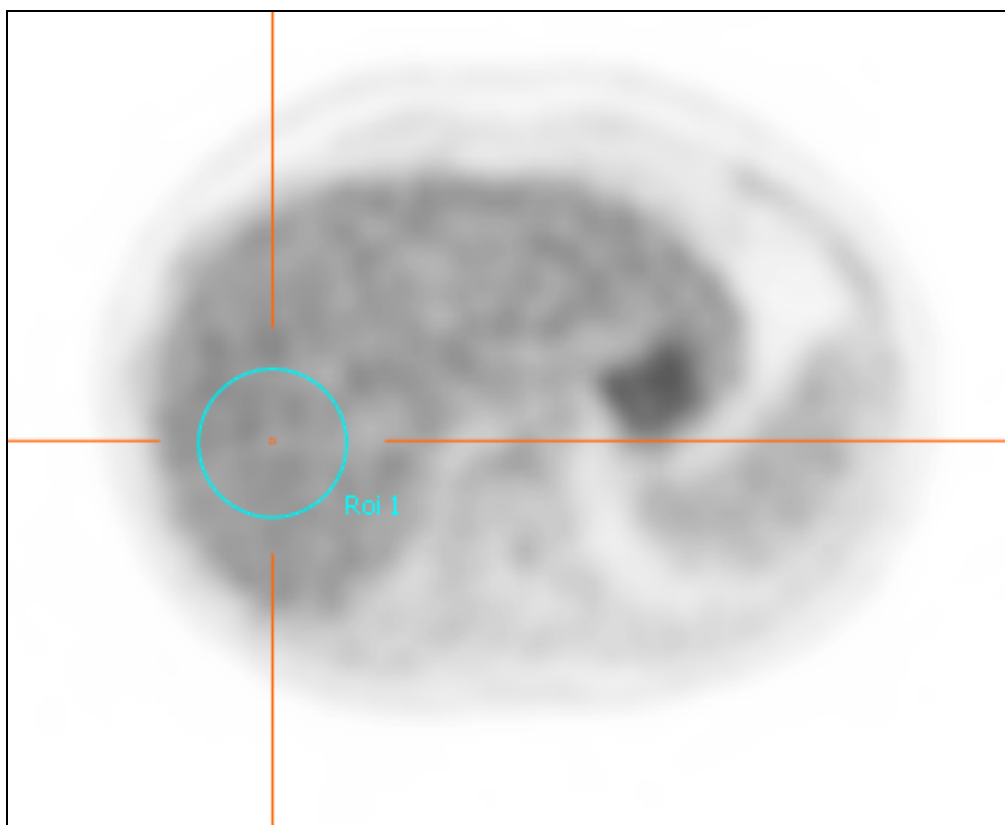
VI. First ROI on CT scan



VII. First ROI on PET WB scan



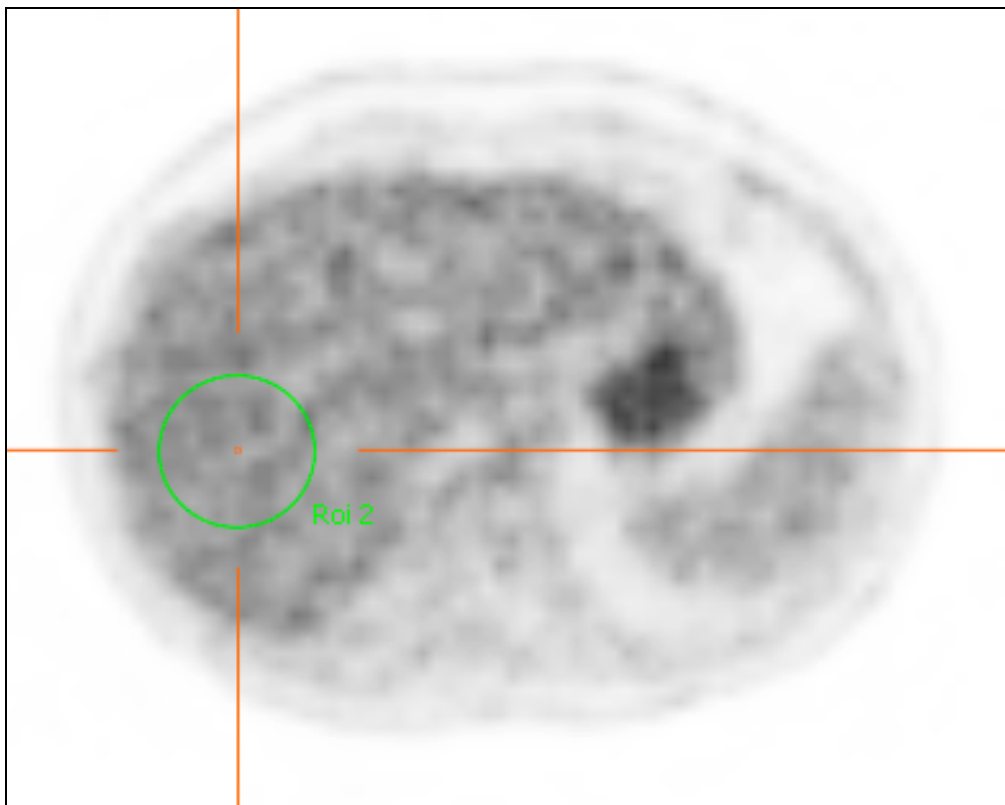
VIII. First ROI on PET WB EANM scan



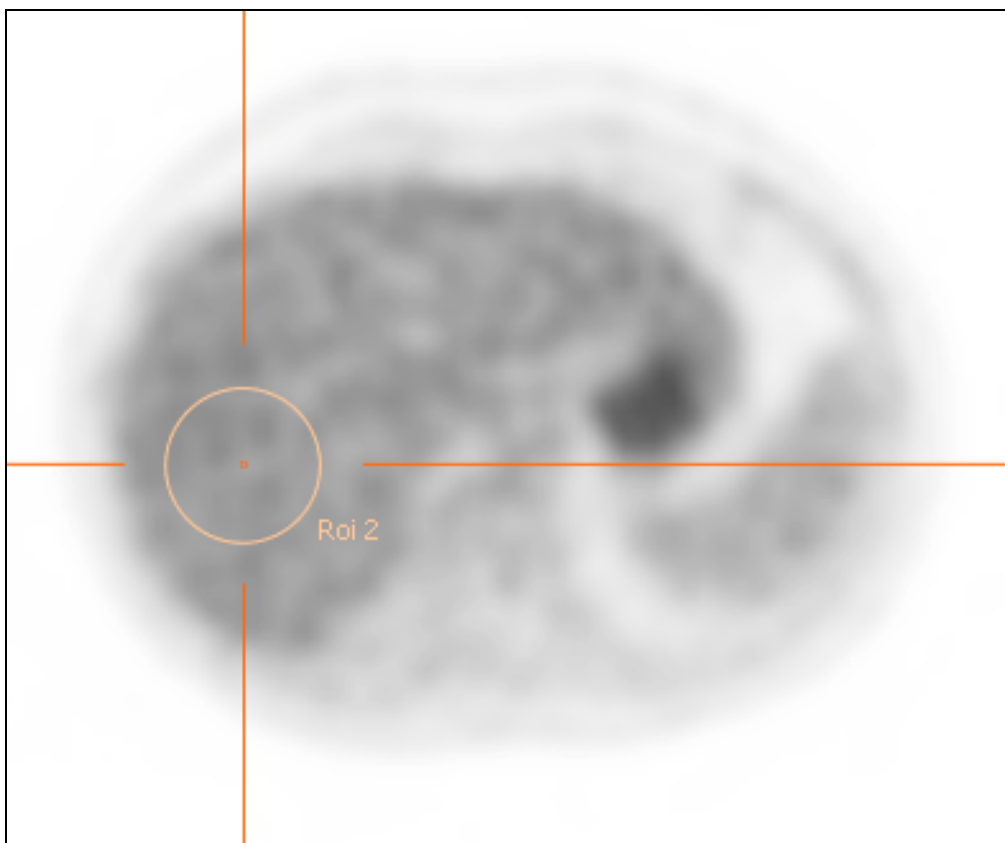
IX. Second ROI on CT scan



X. Second ROI on PET WB scan



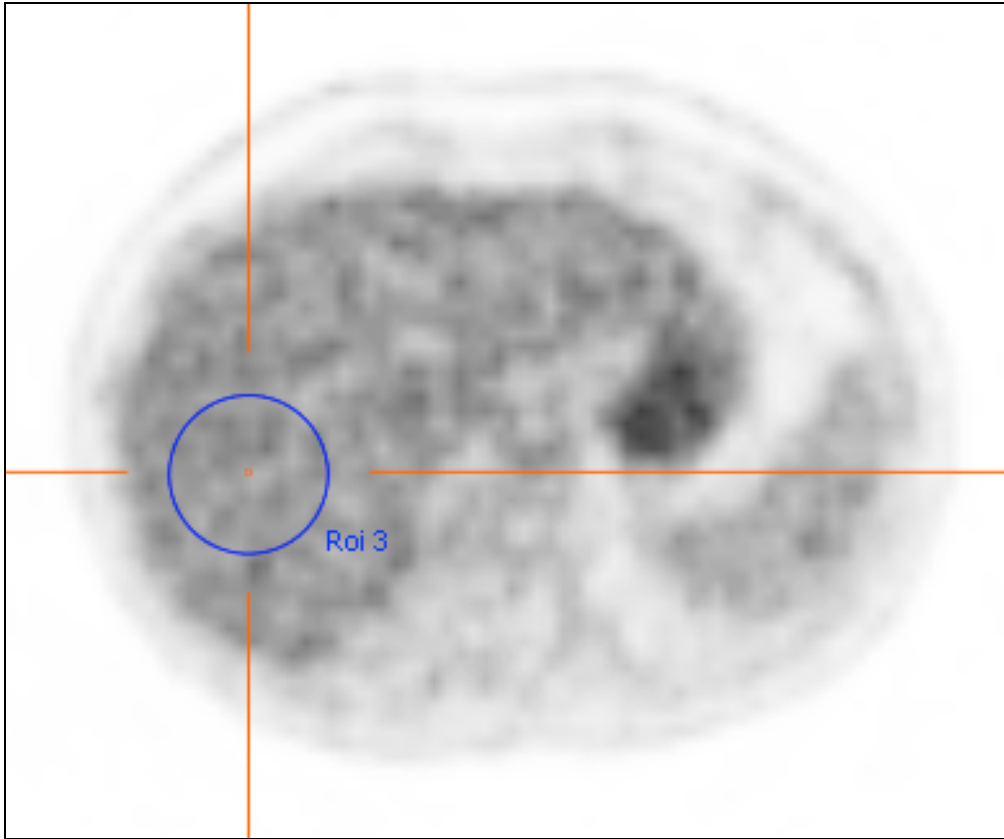
XI. Second ROI on PET WB EANM scan



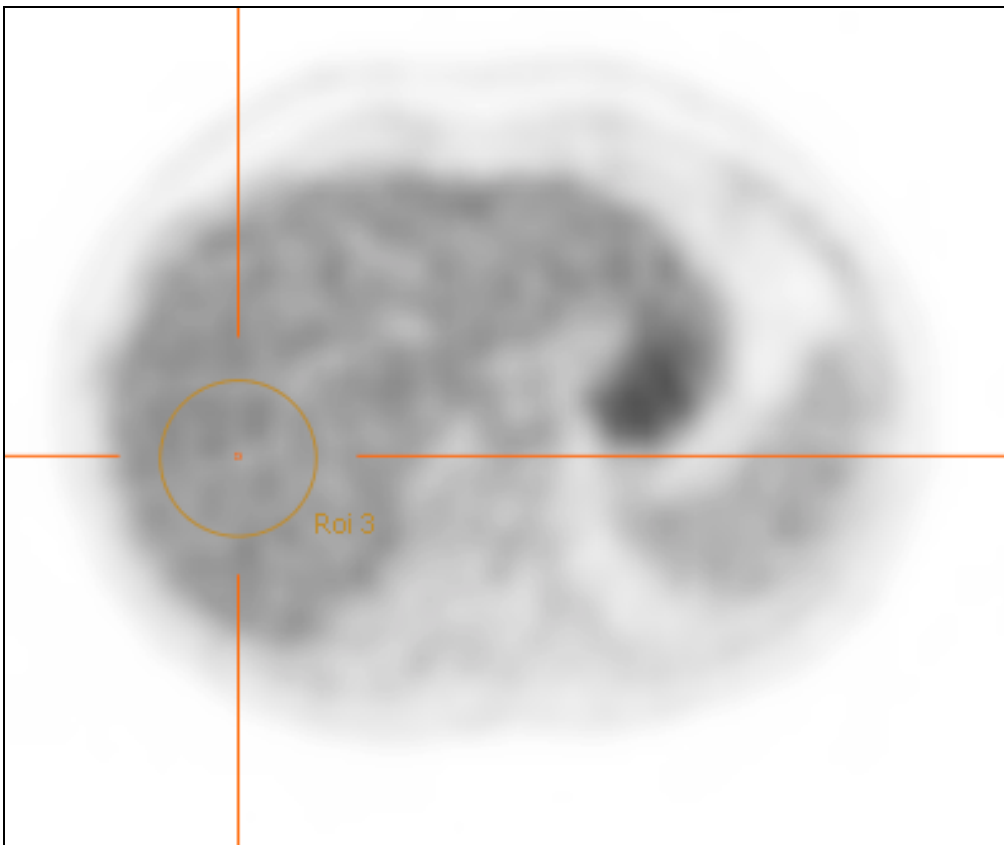
XII. Third ROI on CT scan



XIII. Third ROI on PET WB scan



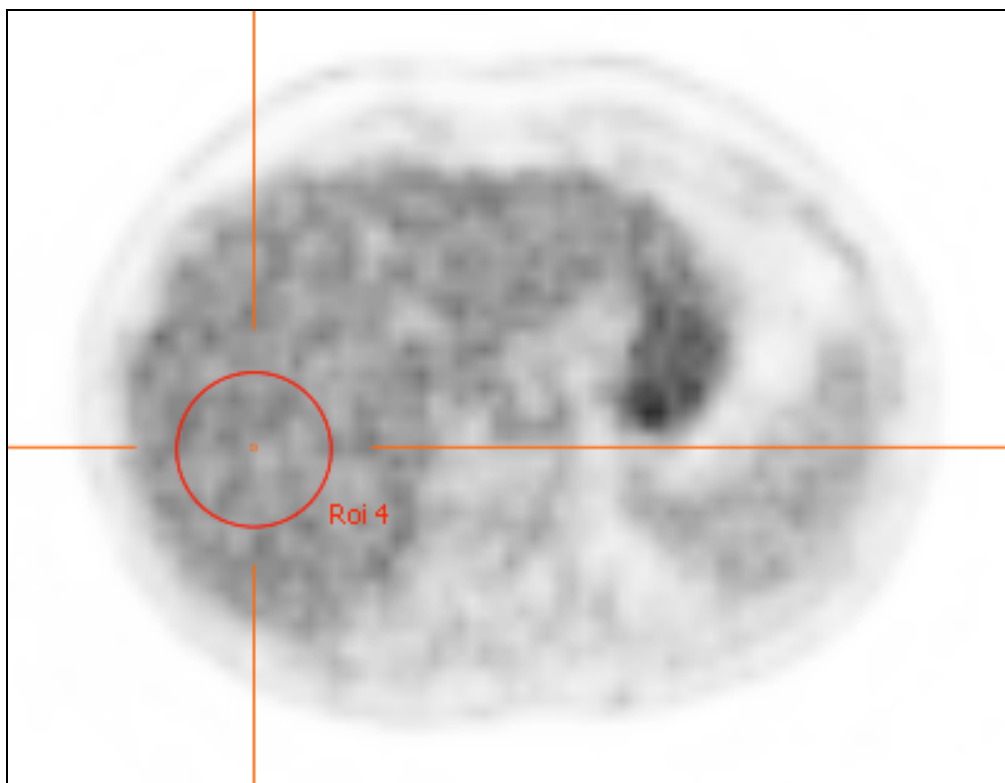
XIV. Third ROI on PET WB EANM scan



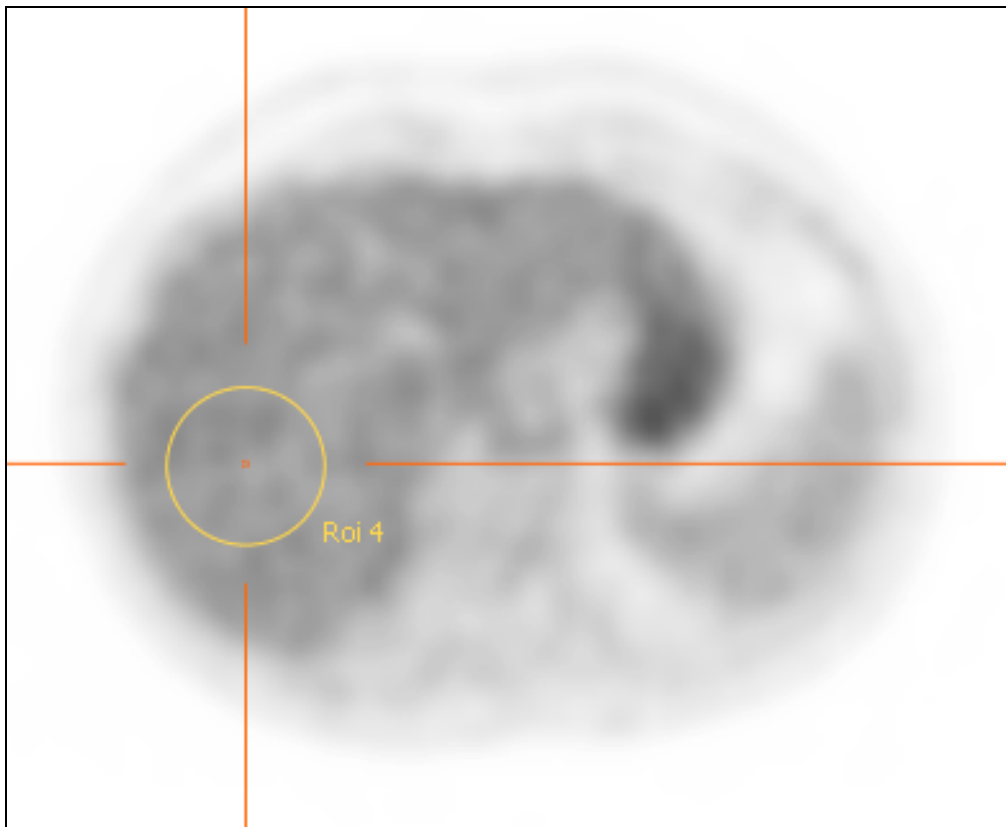
XV. Fourth ROI on CT scan



XVI. Fourth ROI on PET WB scan



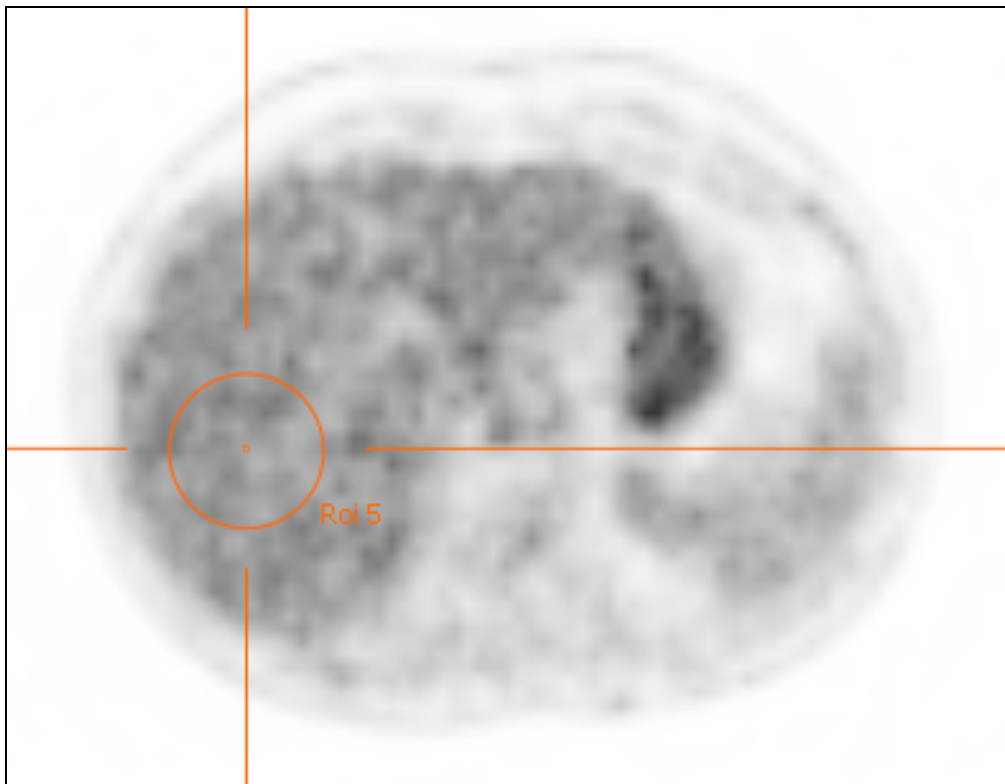
XVII. Fourth ROI on PET WB EANM scan



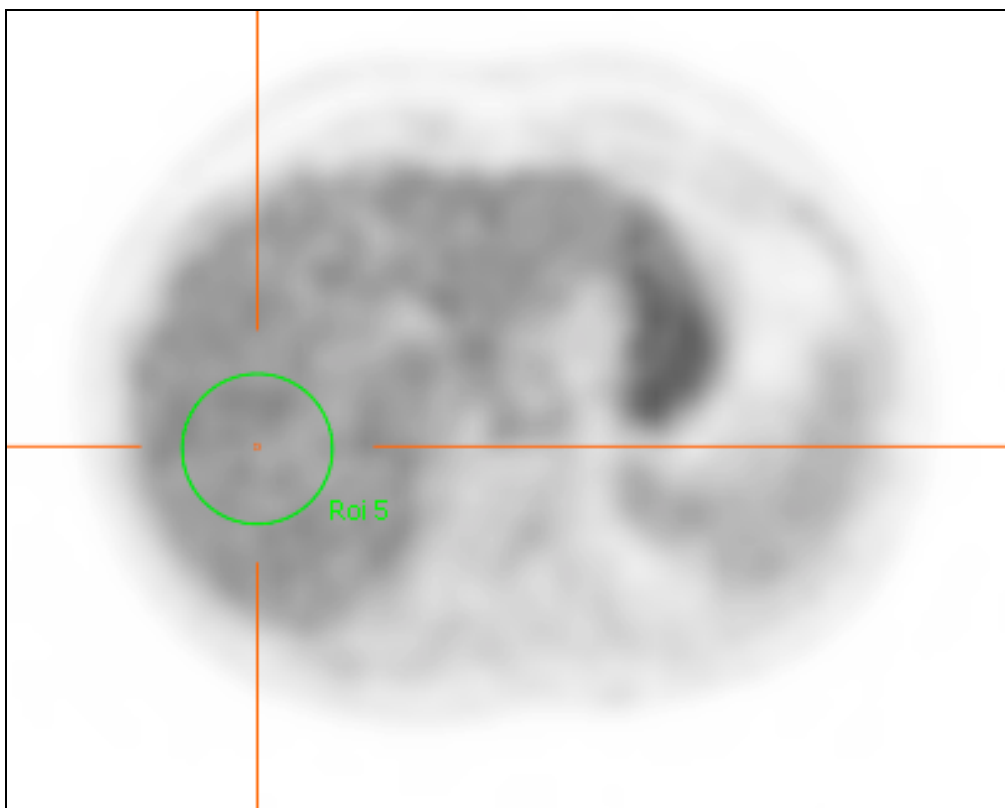
XVIII. Fifth ROI on CT scan



XIX. Fifth ROI on PET WB scan



XX. Fifth ROI on PET WB EANM scan



XXI. Values of the ROI's in the PET WB

Roi/Voi	Image Number	Cells	Total	Mean	Min	Max	Median	Deviation	Suv Peak	Diameter mm	Area cm ²	Volume cm ³
Roi												
Transverse												
Roi 1	156	118	330.55	2.78	2.05	3.62	2.78	0.32		50		19.57
Roi 2	155	114	321.42	2.82	2.13	3.66	2.83	0.34		50		18.91
Roi 3	154	118	329.76	2.77	2.02	3.68	2.74	0.33		50		19.57
Roi 4	153	118	328.40	2.76	1.95	3.62	2.77	0.36		50		19.57
Roi 5	152	112	313.22	2.75	1.98	3.67	2.73	0.39		50		18.58
Coronal												
Sagittal												
Voi												
Transverse												
Coronal												
Sagittal												

XXII. Values of the ROI's in the PET EANM WB

Roi/Voi	Image Number	Cells	Total	Mean	Min	Max	Median	Deviation	Suv Peak	Diameter mm	Area cm ²	Volume cm ³
Roi												
Transverse												
Roi 1	156	193	550.98	2.75	2.35	3.18	2.78	0.17		50		19.54
Roi 2	155	189	534.94	2.77	2.47	3.15	2.76	0.17		50		19.14
Roi 3	154	193	551.64	2.76	2.42	3.16	2.73	0.18		50		19.54
Roi 4	153	193	546.73	2.73	2.33	3.19	2.71	0.20		50		19.54
Roi 5	152	186	524.68	2.72	2.27	3.24	2.71	0.22		50		18.83
Coronal												
Sagittal												
Voi												
Transverse												
Coronal												
Sagittal												

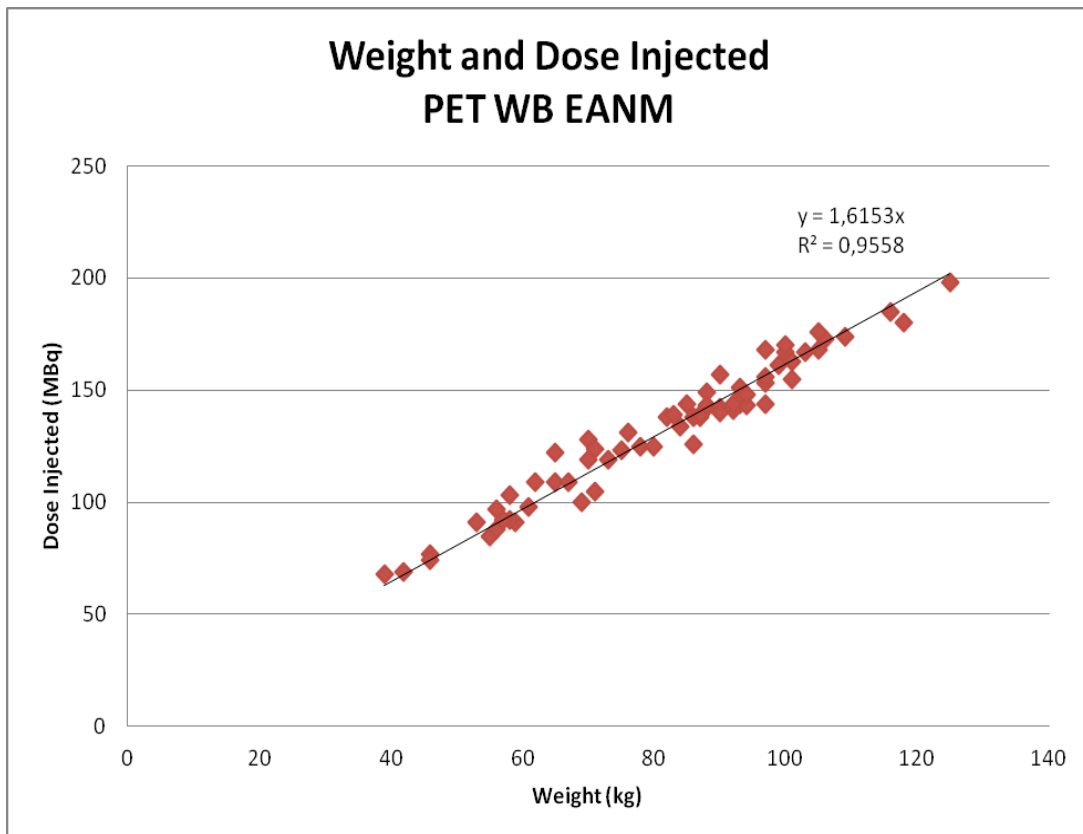
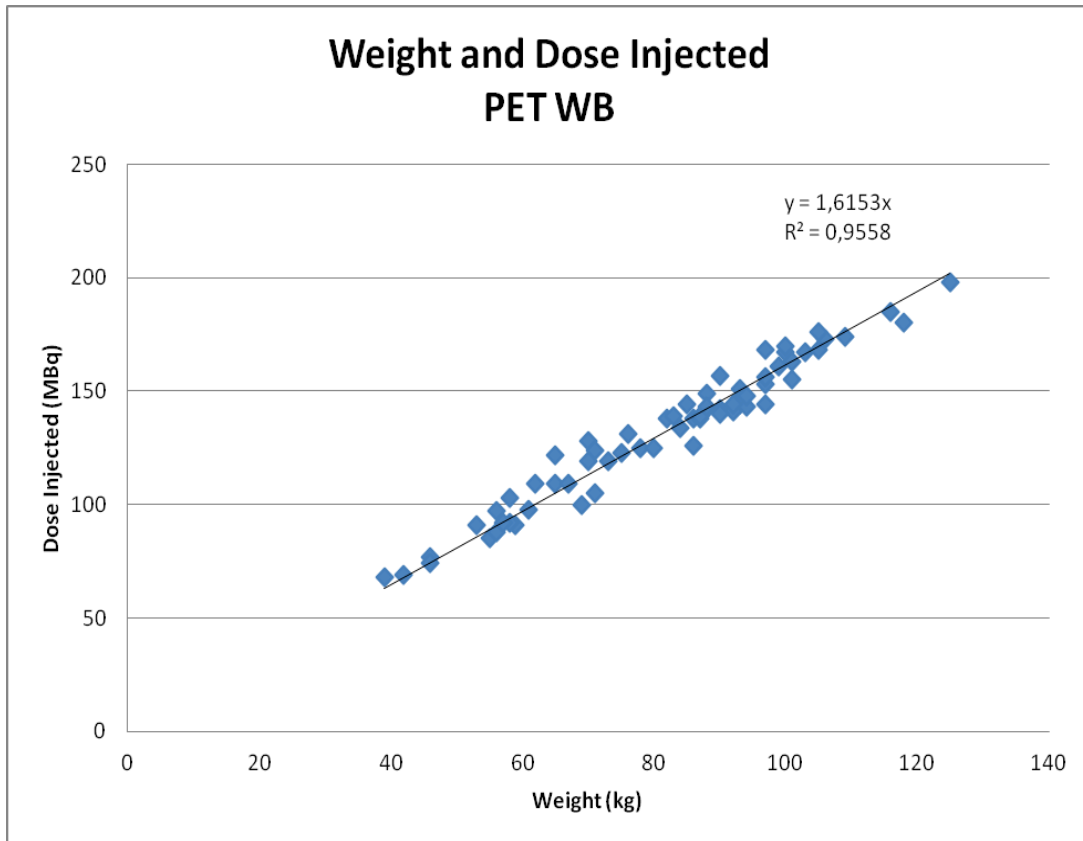
XXIII. Table of every value of every patient of PET WB

ROI 1		ROI 2		ROI 3		ROI 4		ROI 5		Total		Dose Injected (MBq)	Gender	Weight (Kg)	Height (cm)	BMI						
Mean	Deviation	SNR	Mean	Deviation	SNR	Mean	Deviation	SNR	Mean	Deviation	SNR											
2.74	0.4	6.85	2.8	0.59	4.745763	2.68	0.62	4.322581	2.64	0.46	5.73913	2.86	0.47	6.08506	2.744	0.508	5.401675	153	F	67	184	28.65
2.78	0.32	6.8875	2.82	0.34	8.29418	2.77	0.33	8.393393	2.76	0.36	7.666667	2.75	0.39	7.051282	2.776	0.348	7.977011	109	F	65	185	23.88
2.57	0.47	5.4680851	2.65	0.53	5	2.71	0.46	5.891504	2.59	0.4	6.475	2.58	0.45	5.733333	2.62	0.462	5.670396	126	M	68	182	25.96
1.53	0.89	9.5	1.53	0.22	6.904545	1.53	0.2	7.89	1.53	0.21	7.28574	1.53	0.21	7.28574	1.53	0.204	7.5	68	F	39	164	14.5
2.32	0.4	7.75	2.32	0.25	6.294206	2.36	0.28	7.714236	2.22	0.28	6.939462	2.27	0.28	6.907932	2.239	0.29	7.712941	99	F	61	170	21.1
3.58	0.44	8.1363636	3.62	0.5	7.24	3.65	0.53	6.886792	3.63	0.52	6.989769	3.53	0.42	8.404762	3.602	0.482	7.473029	123	F	75	174	24.77
2.32	0.4	5.8	2.48	0.42	5.904762	2.55	0.5	5.1	2.65	0.52	5.089154	2.7	0.49	5.930204	2.54	0.466	5.450644	144	M	97	178	30.61
2.87	0.46	6.239104	2.87	0.41	7	2.85	0.41	6.95122	2.83	0.41	6.902439	2.8	0.5	5.8	2.844	0.438	6.493051	144	F	85	167	30.48
2.23	0.34	5.5588235	2.3	0.3	7.666667	2.29	0.31	7.387097	2.32	0.36	6.444444	2.35	0.4	5.875	2.298	0.342	6.78298	105	F	71	161	27.29
2.21	0.37	5.972973	2.19	0.37	5.916919	2.19	0.37	5.916919	2.19	0.39	5.635395	2.19	0.47	4.959574	2.194	0.394	5.569528	100	F	69	165	20.85
2.52	0.45	6.16	2.52	0.43	6.16	2.52	0.43	6.16	2.52	0.43	6.16	2.52	0.43	6.16	2.52	0.43	6.16	100	F	69	165	20.85
2.89	0.43	6.720892	2.82	0.47	6.212766	2.86	0.5	5.32	2.89	0.48	5.020833	2.91	0.49	5.330776	2.914	0.474	6.147679	138	F	68	168	30.42
2.48	0.55	4.5080909	2.62	0.57	4.596491	2.81	0.68	4.132353	2.65	0.59	4.498255	2.6	0.56	4.642857	2.632	0.53	4.461071	212	M	100	191	27.41
2.15	0.37	6.808008	2.15	0.3	7.186867	2.14	0.31	6.903226	2.12	0.35	6.057143	2.06	0.34	6.058824	2.124	0.334	6.395201	165	F	78	163	28.36
2.25	0.5	4.49056	2.22	0.47	4.723404	2.16	0.39	5.538462	2.18	0.44	4.954545	2.28	0.44	5.189818	2.218	0.448	4.950893	162	F	67	160	22.27
3.33	0.41	6.101952	3.25	0.43	5.267247	3.23	0.43	5.47987	3.23	0.48	5.47987	3.23	0.52	5.057352	3.242	0.504	5.242893	142	M	70	173	23.39
2.03	0.39	5.209322	2.06	0.35	5.995714	2.14	0.33	6.694448	2.08	0.42	5.609474	2.11	0.37	7.027073	2.084	0.348	6.782628	119	M	78	176	25.18
2.08	0.36	5.777778	2	0.33	6.060606	2.08	0.39	5.333333	2.18	0.45	4.844444	2.15	0.4	5.375	2.098	0.388	5.435233	109	M	67	168	23.74
2.67	0.38	7.026395	2.71	0.44	6.159091	2.81	0.42	6.890476	2.83	0.36	7.861111	2.79	0.36	7.75	2.762	0.392	7.045918	109	F	62	154	26.14
2.84	0.59	4.819593	2.8	0.56	5	2.81	0.62	4.532258	2.81	0.62	5.403846	2.79	0.46	5.8125	2.81	0.554	5.072202	244	F	78	165	23.63
3.41	0.36	9.472222	3.43	0.38	9.026796	3.37	0.38	8.888421	3.31	0.43	7.895774	3.3	0.43	7.674419	3.364	0.396	8.494949	128	F	70	158	24.8
2.63	0.55	4.8809091	2.63	0.49	5.267247	2.63	0.49	5.267247	2.63	0.49	5.267247	2.63	0.49	5.267247	2.63	0.49	5.267247	100	F	69	165	20.85
2.45	0.54	4.577077	2.3	0.47	5.219149	2.43	0.44	5.522727	2.38	0.42	5.666667	2.4	0.35	6.857143	2.432	0.444	4.477477	134	M	94	177	26.81
1.92	0.34	5.6470588	1.93	0.3	6.433333	1.96	0.38	5.420503	1.93	0.39	5.461538	1.93	0.32	6.34375	1.914	0.346	5.820909	125	M	80	166	23.12
2.5	0.45	5.555556	2.51	0.44	5.704545	2.52	0.46	5.478261	2.5	0.46	5.434783	2.5	0.44	5.681818	2.506	0.45	5.568889	167	M	100	188	28.29
3.62	0.61	5.8344282	3.57	0.65	5.482308	3.64	0.73	4.986301	3.79	0.73	5.197811	3.73	0.66	5.65915	3.67	0.676	5.428394	241	F	105	157	46.86
2.38	0.53	4.49056	2.63	0.56	4.684429	2.85	0.52	5.096754	2.6	0.58	4.482769	2.73	0.54	5.059556	2.598	0.546	4.78242	190	M	118	186	34.11
1.57	0.21	7.476095	1.59	0.22	7.18995	1.53	0.18	6.95032	1.49	0.2	7.45	1.45	0.25	5.524	1.524	0.204	7.476095	161	F	85	162	20.86
2.88	0.51	5.6470588	2.84	0.51	5.666667	2.88	0.53	5.433982	2.95	0.59	5	2.89	0.54	5.573037	2.908	0.536	5.425073	164	M	104	175	37.22
3.21	0.38	6.4473684	3.22	0.38	6.473684	3.21	0.47	6.829707	3.15	0.46	6.847826	3.14	0.41	7.696837	3.186	0.42	7.58574	144	M	93	165	27.17
1.73	0.27	8.007474	1.87	0.34	4.91795	1.87	0.37	4.915914	1.73	0.33	5.242424	1.82	0.34	5.92941	1.724	0.33	5.224242	264	M	95	163	27.07
2.37	0.46	5.521379	2.4	0.45	5.333333	2.45	0.45	5.444444	2.48	0.47	5.276986	2.4	0.51	4.705882	2.42	0.468	5.07094	289	M	100	187	28.6
2	0.28	7.1428571	1.97	0.29	7.05714	1.93	0.27	7.148948	1.88	0.27	6.362962	1.93	0.27	7.148948	1.942	0.274	7.08799	168	M	81	166	19.51
2.59	0.21	6.3225926	2.59	0.22	6.3225926	2.59	0.24	7.487698	2.52	0.26	5.64974	2.55	0.29	6.796265	2.578	0.292	7.323886	142	M	80	175	23.9
1.96	0.23	8.507331	1.94	0.28	6.828971	1.94	0.26	7.461538	1.89	0.22	8.599095	1.87	0.21	8.904762	1.92	0.24	8.17	134	F	45	140	15.07
2.48	0.45	5.511111	2.47	0.43	5.744488	2.39	0.41	5.822608	2.3	0.38	6.056322	2.35	0.41	5.731707	2.388	0.418	5.764423	142	M	88	174	29.07
3.1	0.56	5.585743	3.03	0.58	5.224138	2.97	0.59	5.033886	3.01	0.52	5.788462	2.96	0.56	5.285714	3.014	0.562	5.362889	174	F	109	180	33.64
2.32	0.4	5.8	2.28	0.39	5.848454	2.31	0.37	6.243243	2.36	0.49	4.983227	2.34	0.47	4.978723	2.322	0.424	4.476415	295	F	92	170	31.83
2.2	0.29	7.5862662	2.21	0.3	7.366667	2.22	0.32	7.25	2.26	0.34	6.84176	2.23	0.32	7.8875	2.278	0.314	7.254777	85	F	95	165	20.2
2.12	0.31	6.359787	2.11	0.31	6.306452	2.05	0.26	7.894456	2.05	0.23	8.93043	2.06	0.27	7.52853	2.078	0.276	7.323886	142	M	80	175	23.9
2.41	0.53	4.547858	2.41	0.49	5.020503	2.39	0.45	5.311111	2.44	0.46	5.304346	2.51	0.49	5.122449	2.432	0.482	5.045543	368	F	110	175	35.32
2.27	0.38	5.9736842	2.24	0.4	5.8	2.33	0.41	5.882327	2.35	0.41	5.731707	2.22	0.4	5.5	2.278	0.4	5.695	119	M	73	169	25.56
2.26	0.47	4.809506	2.32	0.49	4.734684	2.39	0.53	4.509434	2.42	0.56	4.324249	2.42	0.38	6.473684	2.37	0.486	4.876543	198	M	125	197	32.21
2.82	0.44	6.4090909	2.82	0.48	5.875	2.84	0.37	7.675876	2.84	0.31	8.1623	2.82	0.33	8.545455	2.828	0.386	7.284245	124	F	71	158	28.44
2.49	0.3	8.3	2.56	0.32	8	2.57	0.31	8.290323	2.52	0.29	8.290323	2.52	0.29	7.194296	2.526	0.312	8.096964	122	M	85	180	20.86
2.67	0.34	7.859412	2.59	0.39	6.987939	2.54	0.37	6.884848	2.53	0.34	7.441676	2.52	0.33	7.757676	2.578	0.352	7.323886	243	M	75	164	22.15
2.33	0.33	7.0690861	2.37	0.32	7.40625	2.36	0.36	6.955556	2.32	0.31	7.463871	2.29	0.31	7.633333	2.334	0.324	7.203704	228	M	74	178	23.36
2.4	0.25	9.6	2.37	0.25	9.48	2.29	0.29	7.896552	2.32	0.31	7.463871	2.27	0.31	7.645891	2.35	0.282	8.333333	88	F	96	163	21.08
2.59	0.29	8.930345	2.59	0.3	8.633333	2.67	0.31	8.612903	2.71	0.31	8.741935	2.65	0.32	8.28125	2.642	0.306	8.633987	91	F	59	169	20.66
2.44	0.41	5.891295	2.36	0.37	6.378378	2.41	0.4	6.025	2.33	0.44	5.289459	2.26	0.43	5.255014	2.36	0.41	5.756088	269	M	83	180	25.62
2.67	0.49	5.957429	2.82	0.43	5.50591	2.83	0.44	6.438988	2.84	0.44	6.454545	2.84	0.38	7.473684	2.84	0.436	6.50761	147	M	93	178	25.95
2.35	0.31	7.9506452	2.35	0.32	7.24376	2.34	0.31	7.949267	2.35	0.34	6.91765	2.35	0.34	6.91765	2.348	0.324	7.246394	174	F	63	166	19.23

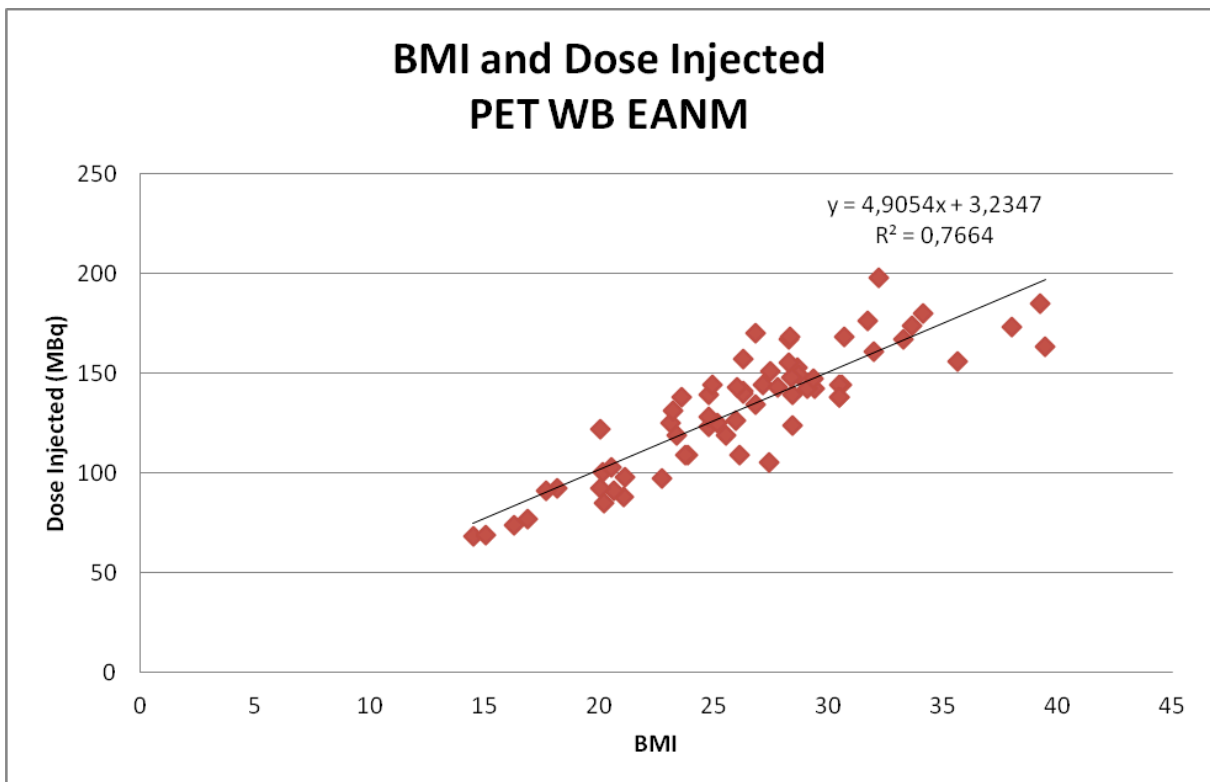
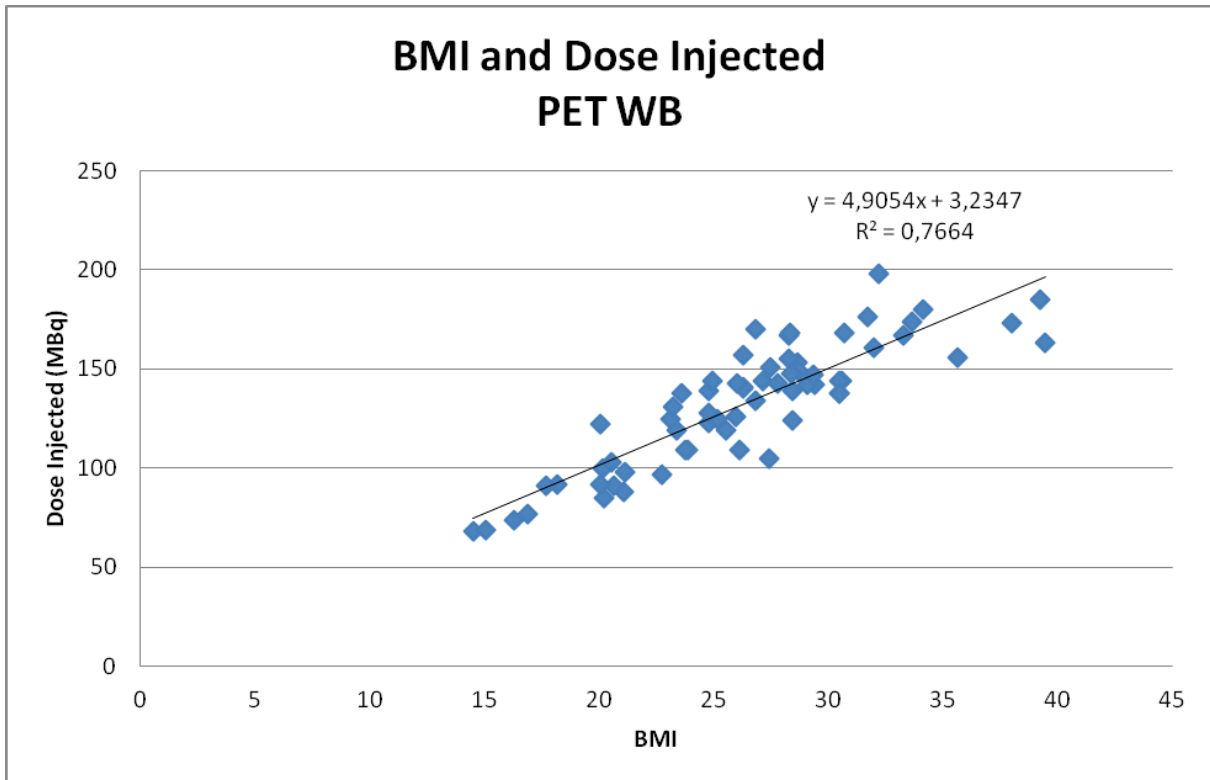
XXIV. Table of every value of every patient of PET EANM WB

ROI 1		ROI 2		ROI 3		ROI 4		ROI 5		Total		Dose Injected (MBq)	Gender	Weight (Kg)	Height (cm)
-------	--	-------	--	-------	--	-------	--	-------	--	-------	--	---------------------	--------	-------------	-------------

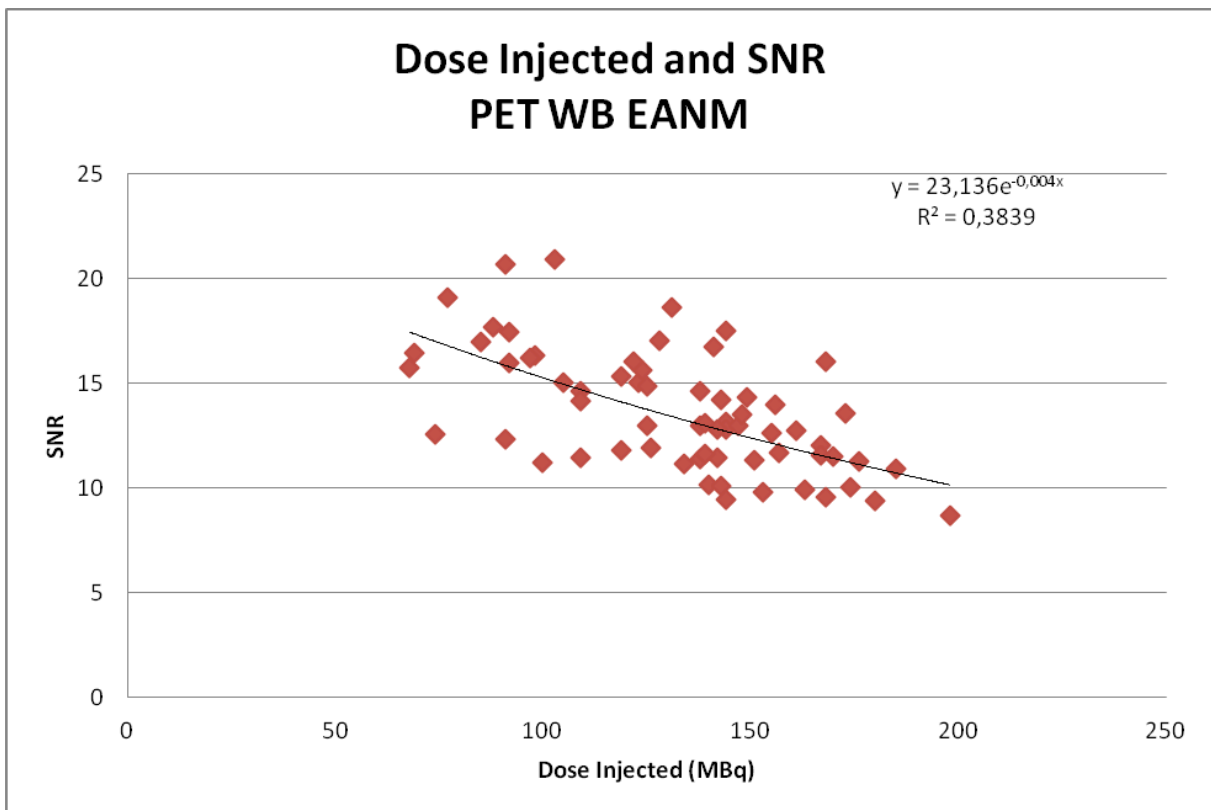
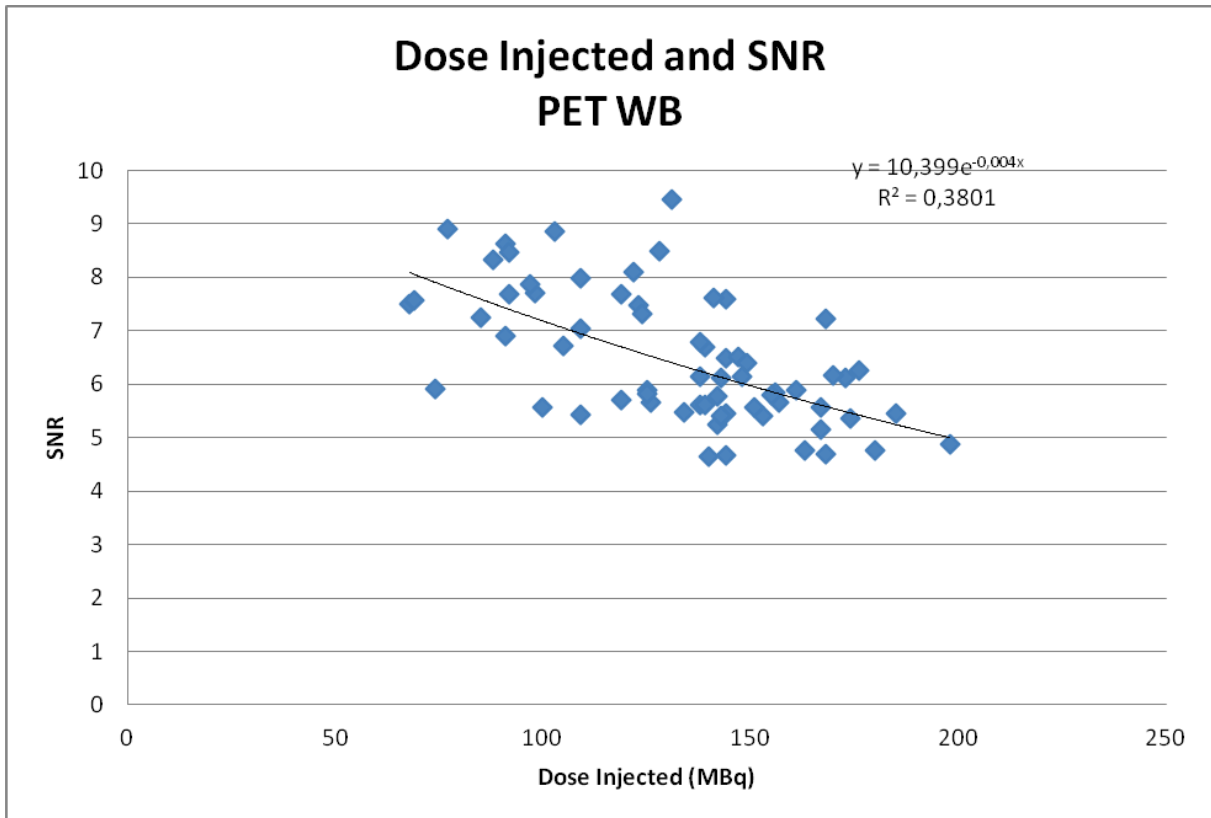
XXV. Relation between Weight and Dose Injected on the PET WB and PET WB EANM



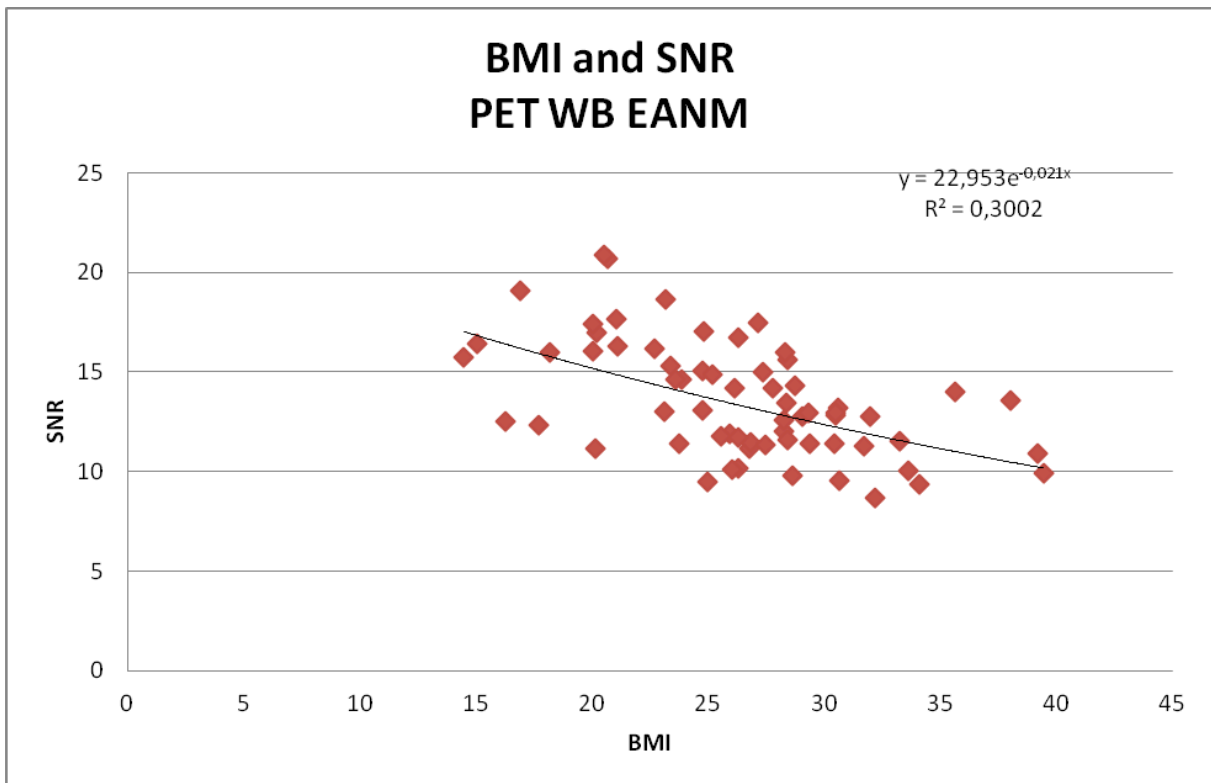
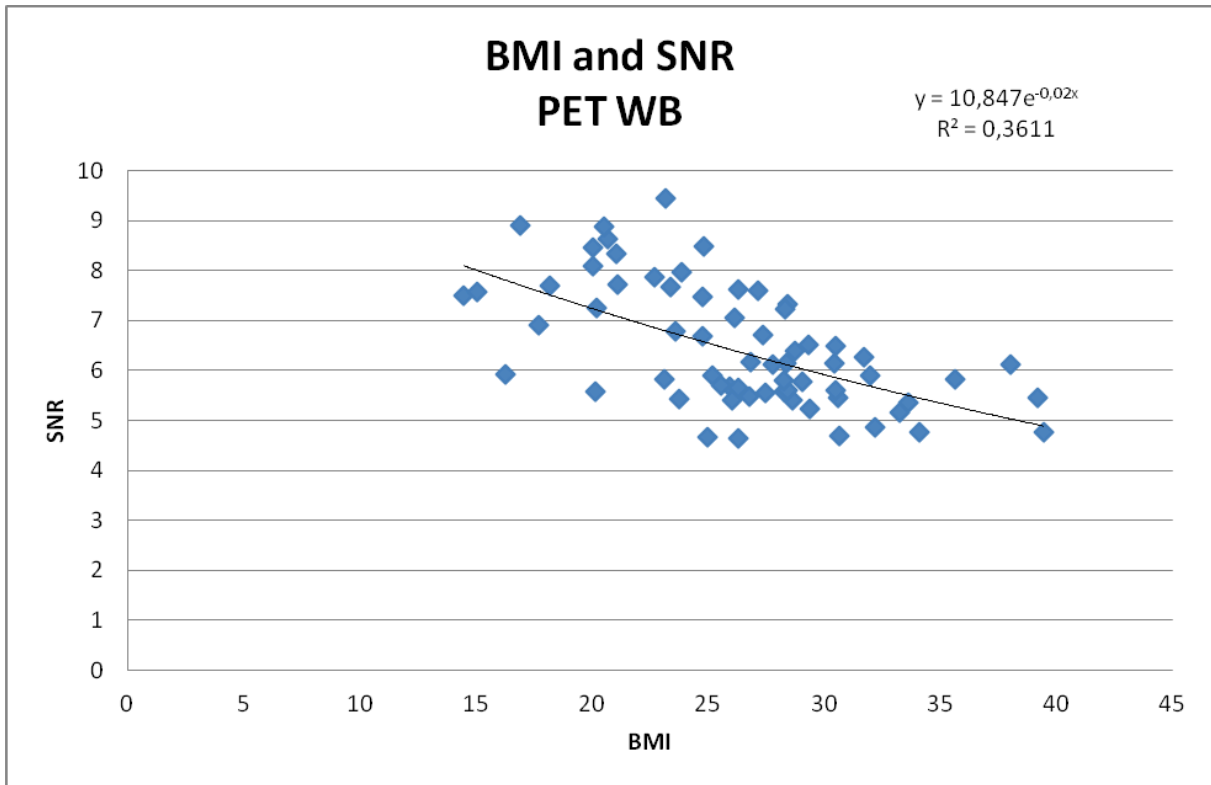
XXVI. Relation between BMI and Dose Injected on the PET WB and PET WB EANM



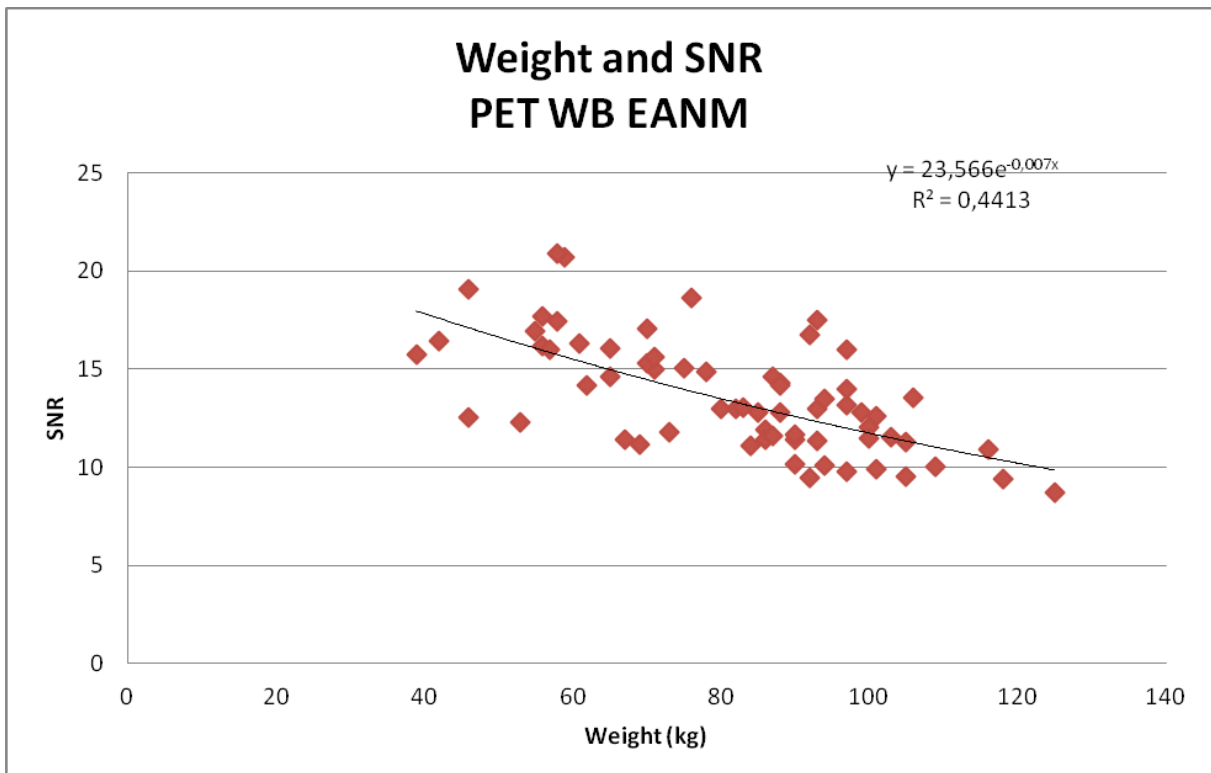
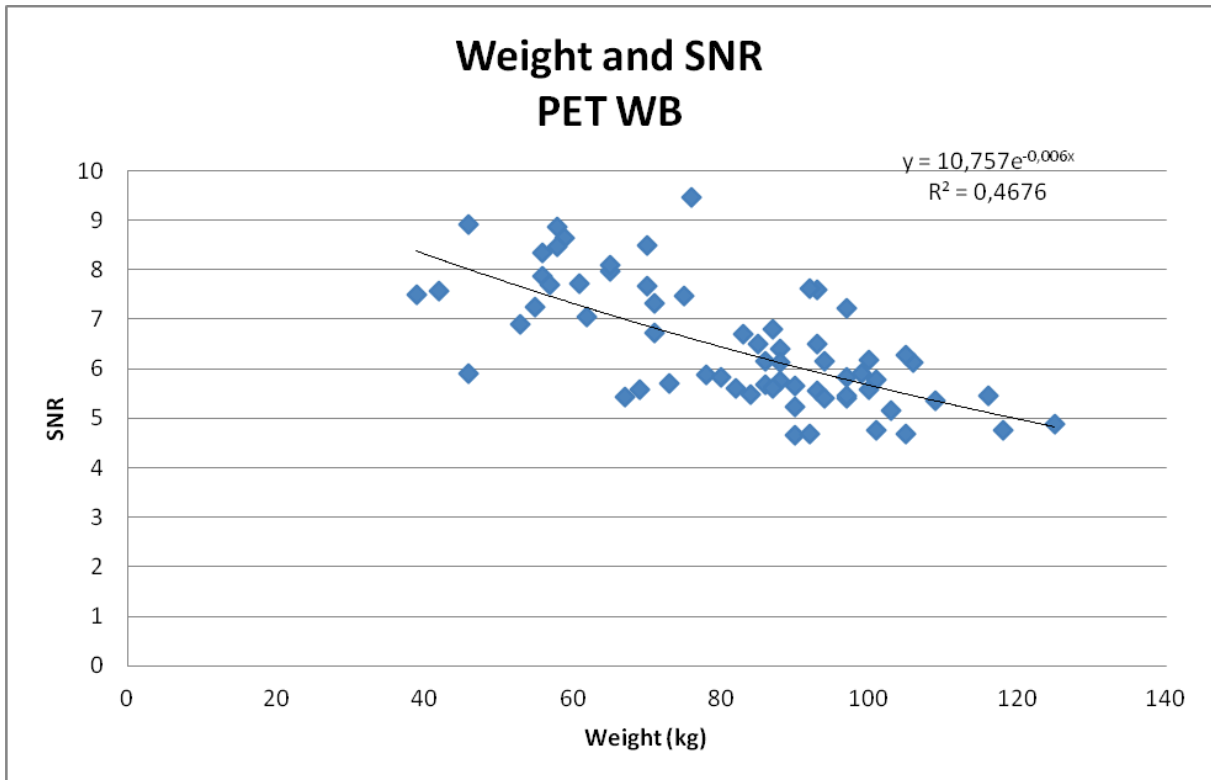
XXVII. Relation between Dose Injected and SNR on the PET WB and PET WB EANM



XXVIII. Relation between BMI and SNR on the PET WB and PET WB EANM



XXIX. Relation between Weight and SNR on the PET WB and PET WB EANM



XXX. Equations

$$D = a \times W$$

$$SNR_{liver} = \frac{\mu_{liver}}{\sigma_{liver}}$$

$$\mu_{liver} \propto T_{liver}$$

$$\sigma_{liver} \propto (T_{liver})^n$$

$$T_{liver} \propto D_A \times F(X)$$

$$\mu_{liver} \propto D_A \times F(X)$$

$$\sigma_{liver} \propto (D_A \times F(X))^n$$

$$SNR_{liver} \propto \frac{\mu_{liver}}{\sigma_{liver}} \propto (D_A)^{1-n} \times F(X)^{1-n}$$

$$SNR_{liver}^* \propto \frac{SNR_{liver}}{(D_A)^{1-n}}$$

$$SNR_{liver}^* = r_1 \times X \times r_2$$

$$SNR_{liver}^* = r_2 \times X^\eta$$

$$SNR_{liver}^* = r_2 \times e^{\eta \times X}$$

$$SNR_{liver}^* = \frac{SNR_{standard}}{(D'_T(X))^{1-n}}$$

$$D'_T(X) = \left(\frac{SNR_{standard}}{SNR_{liver}^*} \right)^{\frac{1}{1-n}}$$

$$SNR_{standard} = SNR_{liver}(X) = (D_A)^{1-n} \times F(X)^{1-n}$$

$$D'_T(X) = a \times b \times \left(\frac{r_{1,W} \times b + r_{2,W}}{r_{1,X} \times X + r_{2,X}} \right)^{\frac{1}{1-n}}$$

$$D'_T(X) = a \times b \times (r_{2,w})^{\frac{1}{1-n}} \times b^{\frac{r_1}{1-n}} \times (r_{2,X})^{\frac{1}{1-n}} \times X^{\frac{r_1}{1-n}}$$

$$D'_T(X) = a \times b \times (r_{2,w})^{\frac{1}{1-n}} \times e^{\frac{r_1 \times b}{1-n}} \times (r_{2,X})^{\frac{1}{1-n}} \times e^{\frac{r_1 \times X}{1-n}}$$

$$D'_T(X) = C_1 \times \left(\frac{C_2}{r_{1,X} \times X + r_{2,X}} \right)^{\frac{1}{1-n}}$$

$$D'_T(X) = C_3 \times X^{C_4}$$

$$D'_T(X) = C_5 \times e^{C_6 \times X}$$

$$D'_T(X) = C_3 \times W^{C_4}$$

$$D'_T(X) = C_5 \times e^{C_6 \times W}$$

$$D'_T(W)[MBq] = 0,0305 \times W[kg]^{1,889}$$

$$SNR_{liver}^* = 0,537$$

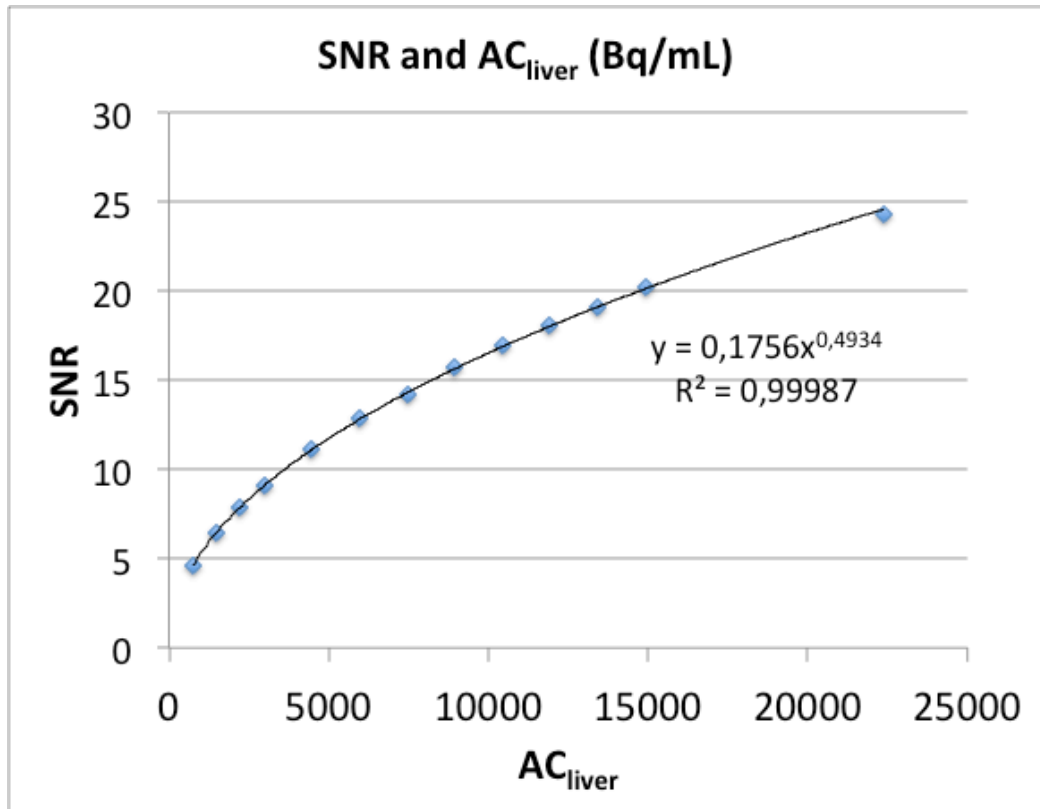
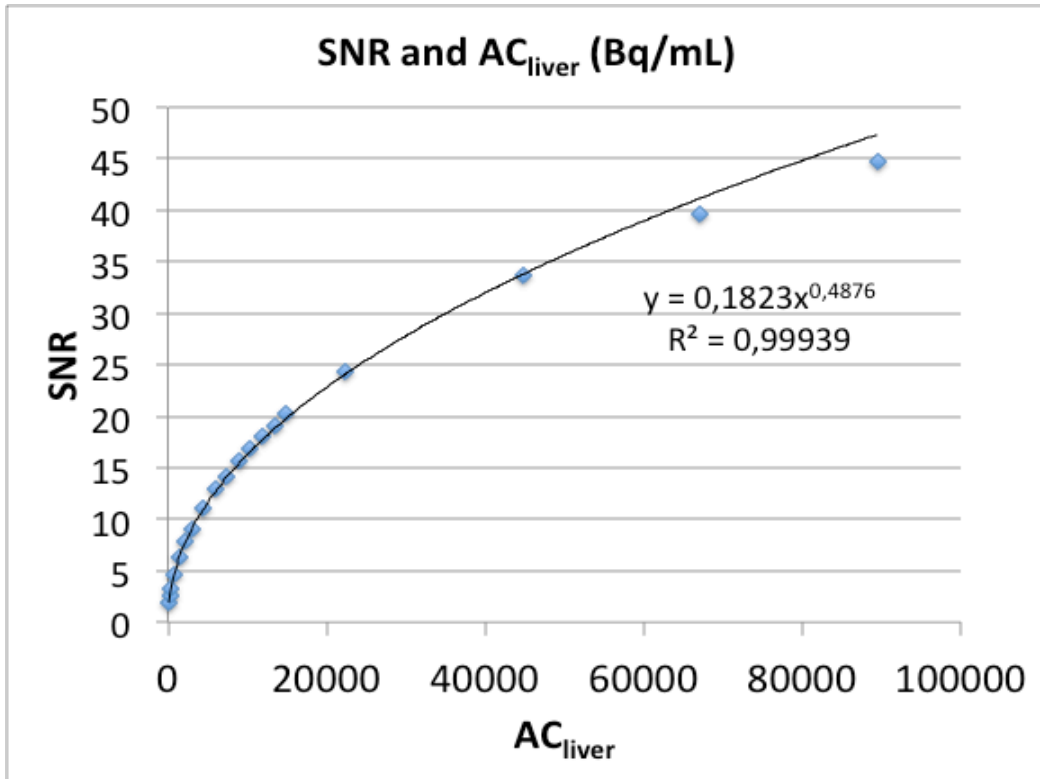
$$SNR_{standard} = 6,1$$

$$D'_T(W)[MBq] = 15,41 \times e^{0,02546 \times W[kg]}$$

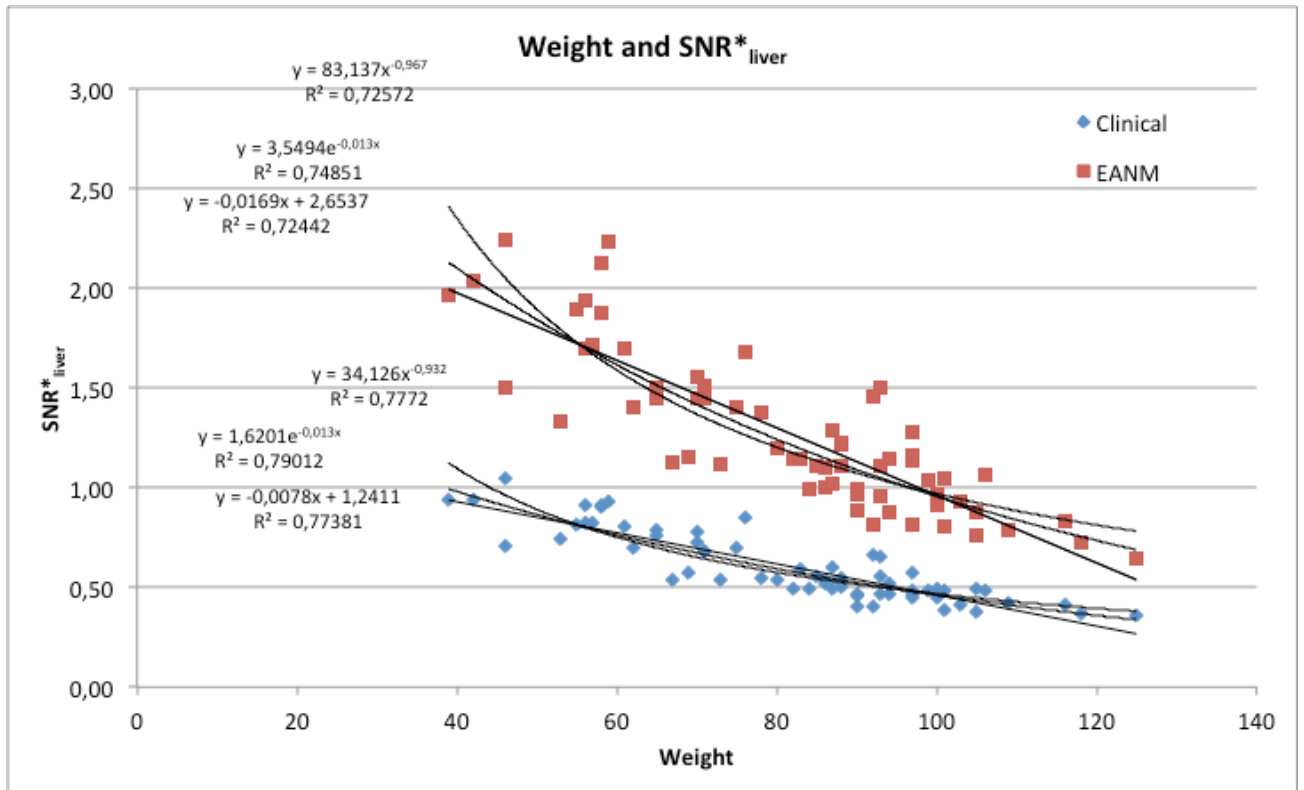
$$SNR_{liver}^* = 0,550$$

$$SNR_{standard} = 6,2$$

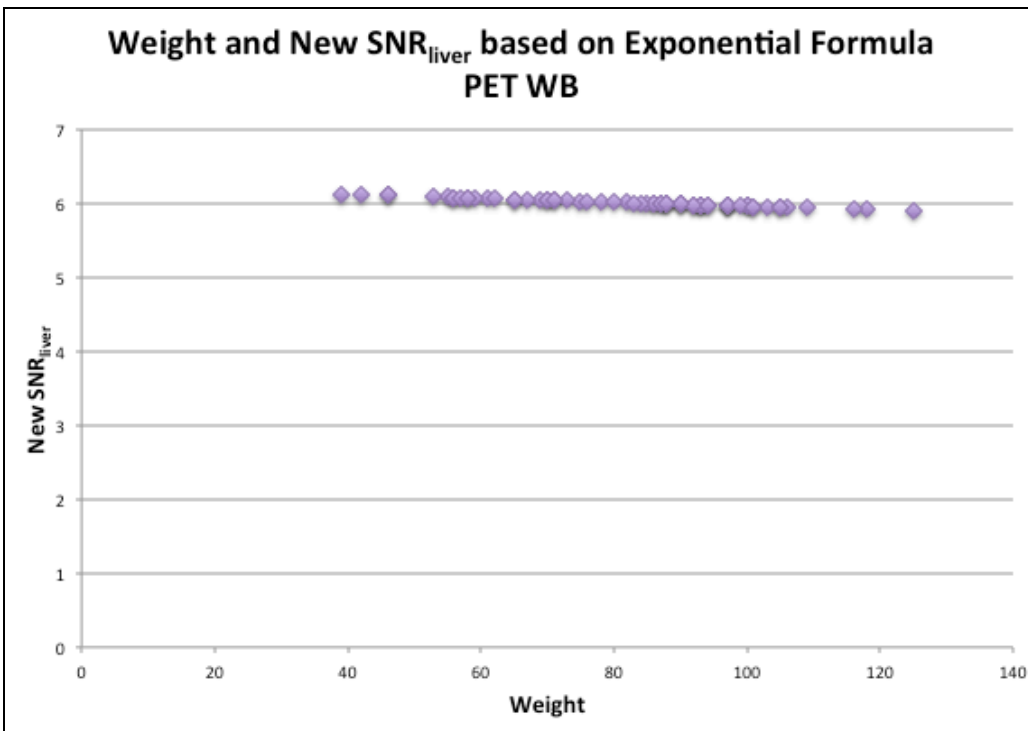
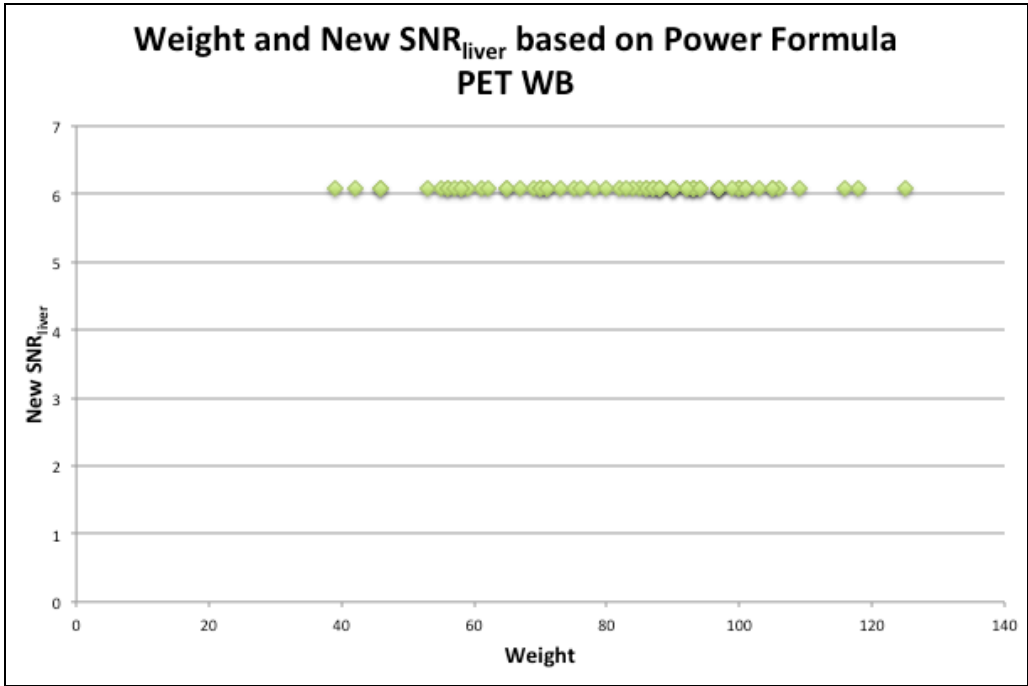
XXXI. Relation between SNR and AC_{liver} from 5 to 3600s and 30 to 900s respectively



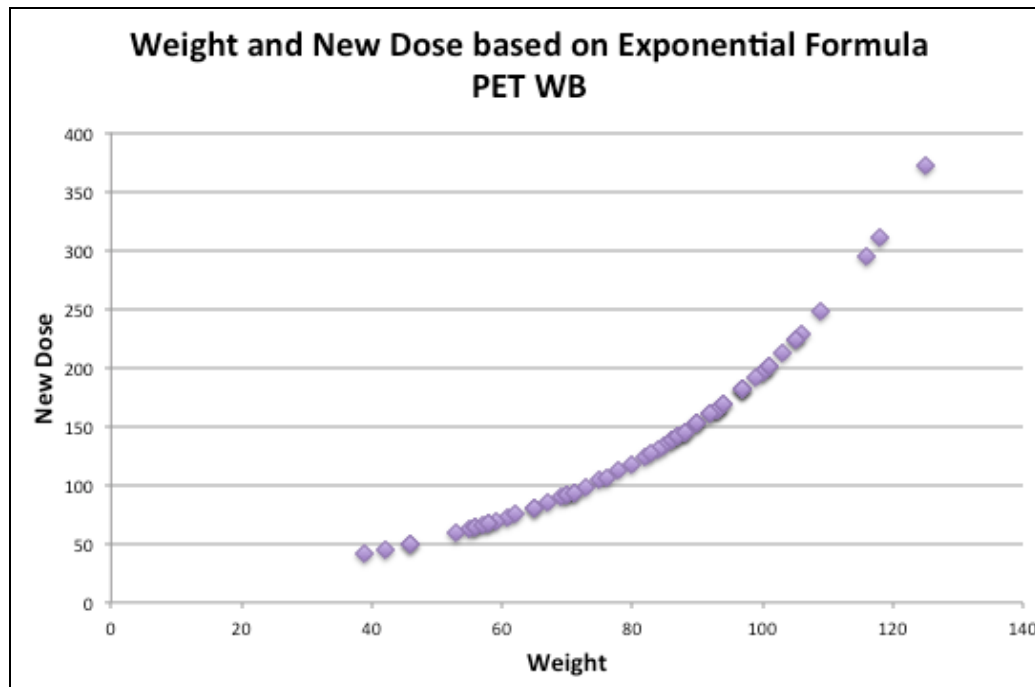
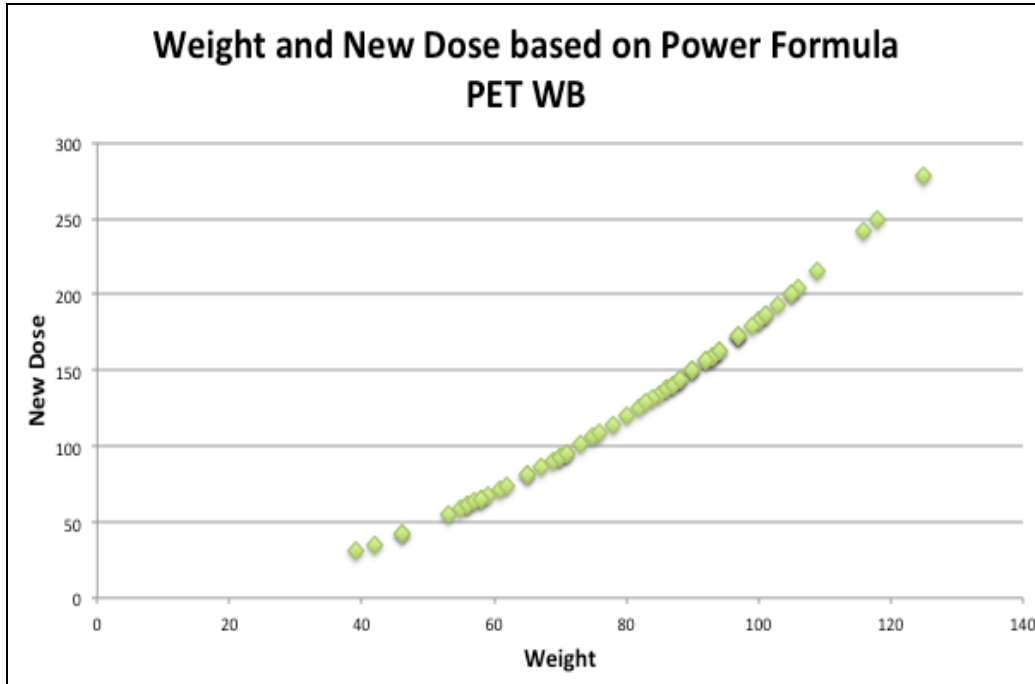
XXXII. Relation between Weight and SNR*_{liver} in Clinical and EANM reconstructions



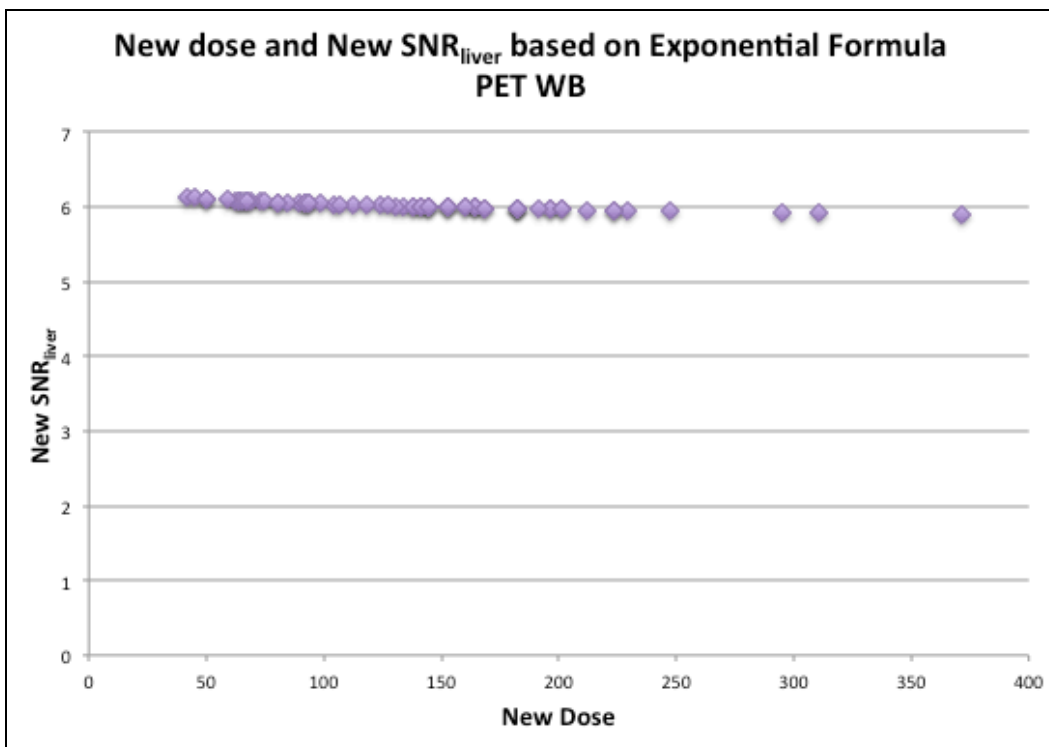
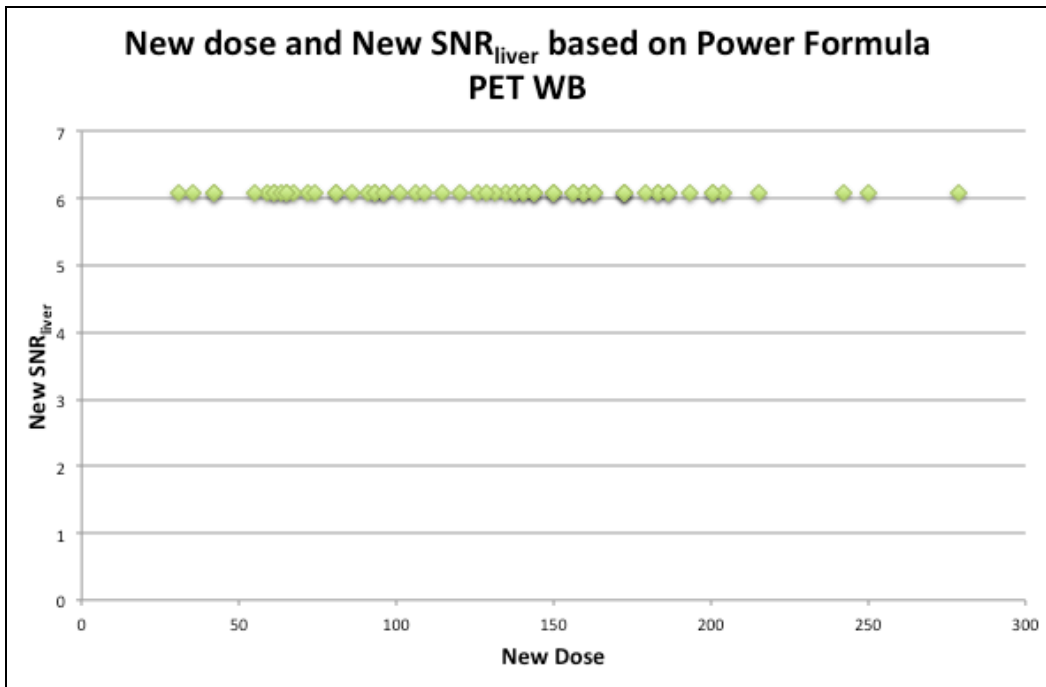
XXXIII. Relation between Weight and New SNR_{liver} based on Power and Exponential Formulas



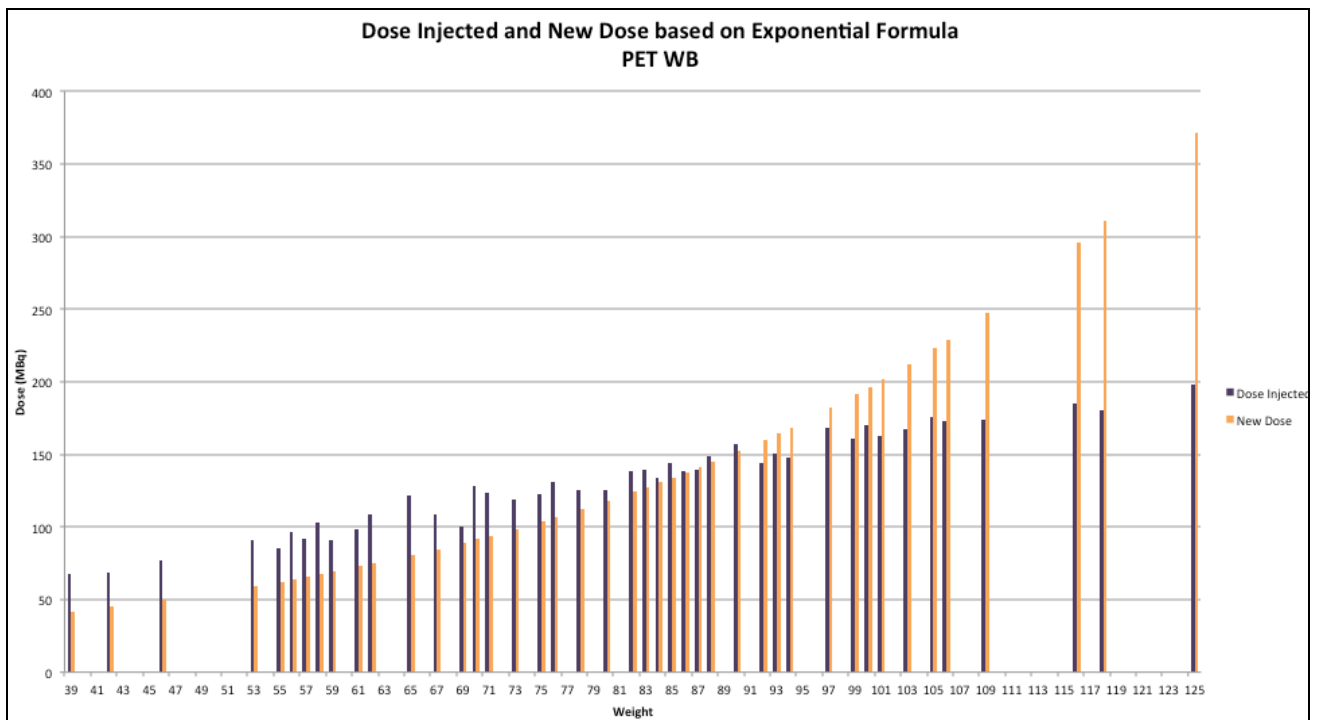
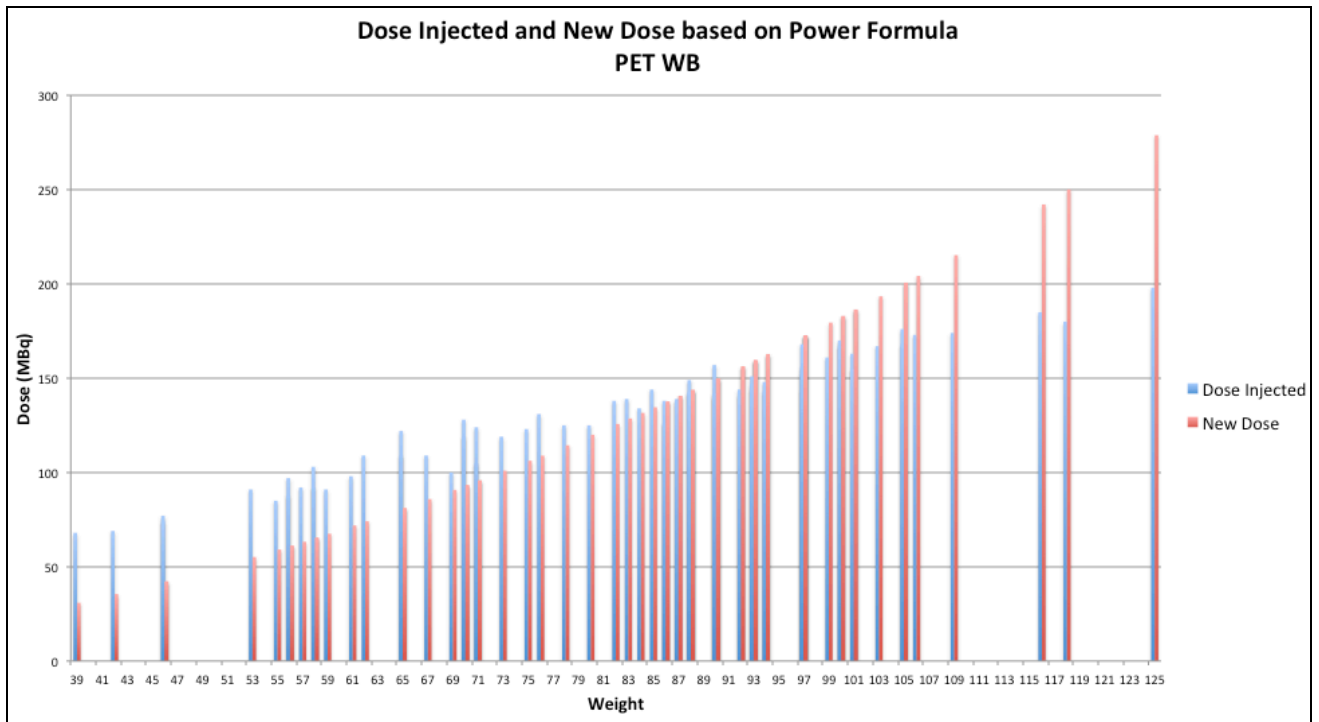
XXXIV. Relation between Weight and New dose based on Power and Exponential Formulas



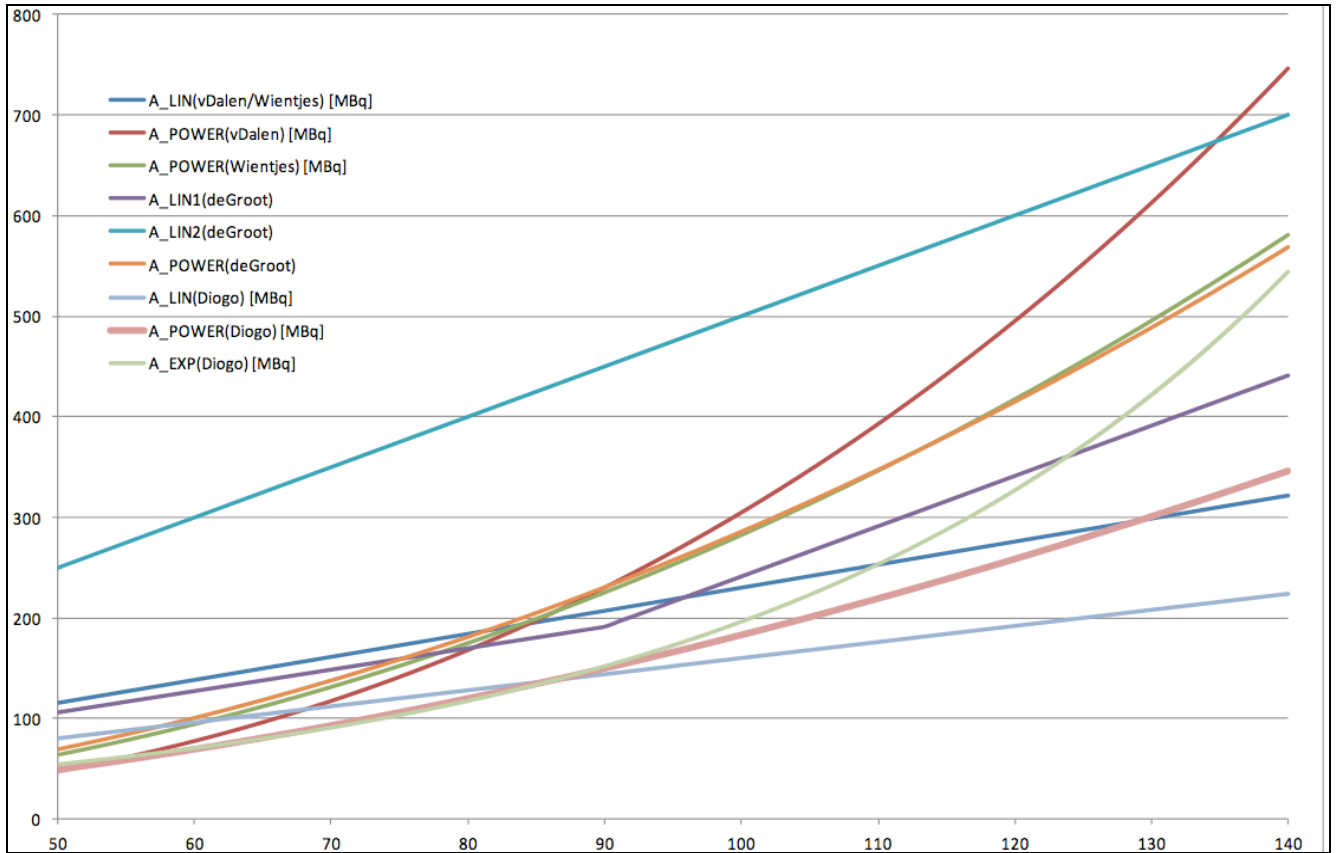
XXXV. Relation between New Dose and New SNR_{liver} based on Power and Exponential Formulas



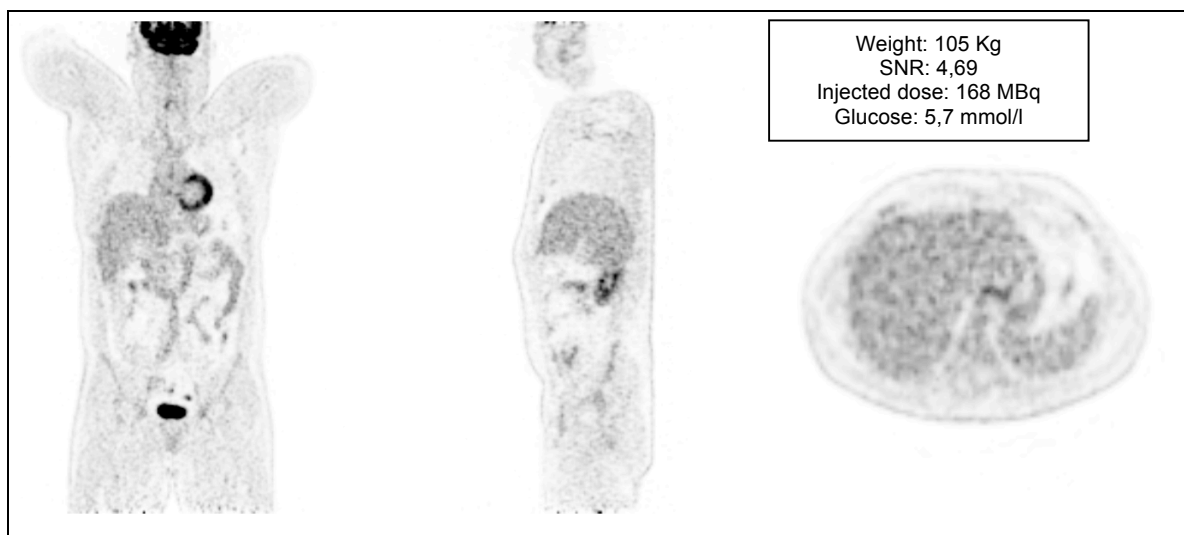
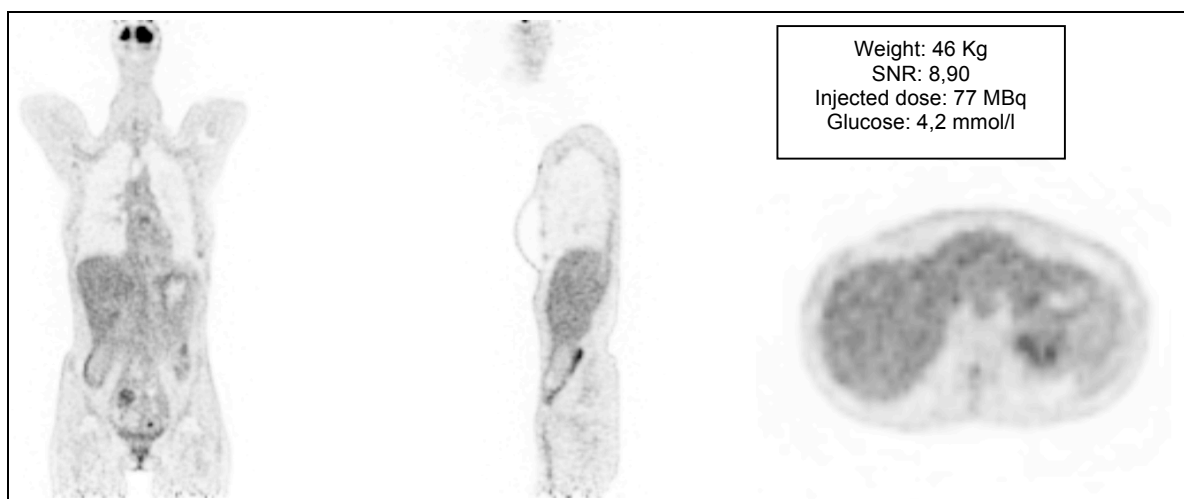
XXXVI. Relation between the dose injected and the new dose based on Power and Exponential Formula



XXXVII. Equations for dosing schemes according to different references



XXXVIII. Different SNRs in different patients



The effects of weight and injected dose in the liver's Signal-to-Noise Ratio in patients submitted to PET/CT scans

